INVESTIGATION OF LAYOUT OPTIMIZATION FOR OFFSHORE WIND FARMS AND A CASE STUDY FOR A REGION IN TURKEY

A THESIS SUBMITTED TO
THE GRADUATE SCHOOL OF NATURAL AND APPLIED SCIENCES
OF
MIDDLE EAST TECHNICAL UNIVERSITY

BY

BARAN KAYA

IN PARTIAL FULFILLMENT OF THE REQUIREMENTS
FOR
THE DEGREE OF MASTER OF SCIENCE
IN
CIVIL ENGINEERING

FEBRUARY 2022

Approval of the thesis:

INVESTIGATION OF LAYOUT OPTIMIZATION FOR OFFSHORE WIND FARMS AND A CASE STUDY FOR A REGION IN TURKEY

submitted by **BARAN KAYA** in partial fulfillment of the requirements for the degree of **Master of Science** in **Civil Engineering, Middle East Technical University** by,

Prof. Dr. Halil Kalıpçılar
Dean, Graduate School of **Natural and Applied Sciences** _____

Prof. Dr. Erdem Canbay
Head of the Department, **Civil Engineering** _____

Assoc. Prof. Dr. Elif Oğuz
Supervisor, **Civil Engineering, METU** _____

Examining Committee Members:

Prof. Dr. A. Burcu Altan-Sakarya
Civil Engineering, METU _____

Assoc. Prof. Dr. Elif Oğuz
Civil Engineering, METU _____

Assoc. Prof. Dr. Nilay Sezer-Uzol
Aerospace Engineering, METU _____

Assoc. Prof. Dr. Nejan Huvaj-Sarıhan
Civil Engineering, METU _____

Asst. Prof. Dr. Mehmet Adil Akgül
Civil Engineering, Yeditepe University _____

Date: 09.02.2022

I hereby declare that all information in this document has been obtained and presented in accordance with academic rules and ethical conduct. I also declare that, as required by these rules and conduct, I have fully cited and referenced all material and results that are not original to this work.

Name, Last name : Baran, Kaya

Signature :

ABSTRACT

INVESTIGATION OF LAYOUT OPTIMIZATION FOR OFFSHORE WIND FARMS AND A CASE STUDY FOR A REGION IN TURKEY

Kaya, Baran
Master of Science, Civil Engineering
Supervisor : Assoc. Prof. Dr. Elif Oğuz

February 2022, 125 pages

In this thesis, the focus was to develop an optimization tool by using mathematical layout optimization methods aiming to increase the energy capacity or reduce the cost of an offshore wind farm. For this purpose, two wind farm layout optimization (WFLO) models were developed using genetic algorithm (GA): model (a) minimizing the cost of power for variable turbine number, model (b) maximizing the power generation for fixed turbine number. Wind speed and wind direction were assumed constant. Therefore, unlike previous studies, smaller grid sizes were used in the models developed in this thesis, and better-performing layouts were obtained than in the literature. Continuous approach to WFLO problem (WFLOP) guarantees the best result since it evaluates unlimited number of possibilities. However, it complicates the problem as well as brings high computational costs. Therefore, discrete approach was used in this thesis, and the performance of using finer grids was investigated. As a result, it was observed that the optimum layout may be improved as the grid size decreases. Following this, developed models within the scope of this thesis were applied to a high offshore wind potential area in Turkey, and a preliminary wind farm layout design was proposed for this area.

Keywords: Wind Energy, Offshore Wind Farm, Layout Optimization, Genetic Algorithm

ÖZ

DENİZ ÜSTÜ RÜZGAR SANTRALLERİ İÇİN YERLEŞİM DÜZENİ OPTİMİZASYONUNUN İNCELENMESİ VE TÜRKİYE'DE BİR BÖLGE İÇİN BİR VAKA ÇALIŞMASI

Kaya, Baran
Yüksek Lisans, İnşaat Mühendisliği
Tez Yöneticisi: Doç. Dr. Elif Oğuz

Şubat 2022, 125 sayfa

Bu tezde, bir deniz üstü rüzgâr santralinin enerji üretim kapasitesini artırmak veya enerji üretim maliyetini azaltmak için matematiksel yerleşim düzeni optimizasyon yöntemlerini kullanarak bir optimizasyon aracı geliştirmeye odaklanılmıştır. Bu amaçla, genetik algoritma (GA) kullanılarak iki farklı rüzgâr santrali yerleşim düzeni optimizasyonu (RSYDO) modeli geliştirilmiştir: model (a) değişken türbin sayısı için enerji üretim maliyetini minimize eden, model (b) sabit türbin sayısı için enerji üretimi kapasitesini maksimize eden. Bu tezde, rüzgâr hızı ve rüzgâr yönü sabit kabul edilmiştir. Bu nedenle, önceki çalışmalardan farklı olarak, bu tezde geliştirilen modellerde daha küçük karelaj boyutları kullanılmış ve daha önceki çalışmalara kıyasla aynı alan için daha iyi performans gösteren yerleşim düzenleri elde edilmiştir. RSYDO problemine (RSYDOP) sürekli yaklaşım, değerlendirdiği olasılık sayısı limitsiz olduğu için en iyi sonucu garanti eder, ancak problemi karmaşıklaştırmasının yanında yüksek hesaplama maliyetlerini de beraberinde getirir. Bu nedenle, bu tezde diskrit yaklaşım kullanılmış ve farklı karelaj boyutları kullanılmasının performansı incelenmiştir. Sonuç olarak karelaj boyutu küçüldükçe optimum yerleşim düzeninin gelişim gösterebileceği gözlenmiştir. Bunu takiben, bu tez kapsamında geliştirilen modeller Türkiye'de yüksek rüzgâr potansiyeli olan bir

deniz üstü rüzgâr santrali alanı için uygulanmıştır ve bu alan için ön tasarımlı bir yerleşim düzeni önerilmiştir.

Anahtar Kelimeler: Rüzgâr Enerjisi, Deniz Üstü Rüzgâr Santrali, Yerleşim Düzeni Optimizasyonu, Genetik Algoritma

To my family…

ACKNOWLEDGMENTS

I would like to express my deepest gratitude to my advisor Assoc. Prof. Dr. Elif Oğuz for her always kind attitude, tolerance, encouragement, and motivating advice. It was a great honor to work with such a wonderful advisor.

I would like to thank my parents Dilek Kaya and H. Bayram Kaya, whose support and love I have always felt, and my younger brother Sercan Kaya, who is just at the beginning of the road but whose success I believe in. I would also like to thank Sezen Bostan-Yılmaz and Olgun Yılmaz, whom have always been a part of my family, for always being there for me.

I am grateful to Yasin Kaya for both his technical support and friendship, I am glad you were just a phone call away.

Last but not least, I would like to thank my dear wife Nihan Kaya for being my future.

TABLE OF CONTENTS

LIST OF TABLES

TABLES

LIST OF FIGURES

FIGURES

LIST OF ABBREVIATIONS

ABBREVIATIONS

ACSA	Ant Colony Search Algorithm
AEP	Annual Energy Production
AFAD	Disaster and Emergency Management Presidency
AGA	Adaptive Genetic Algorithm
BPA	Bastankah and Porté-Agel
BERR	Department of Business, Enterprise and Regulatory Reform
BPSO	Binary Particle Swarm Optimization
CfD	Contracts for Difference
CFD-MIP	Computational Fluid Dynamics with Mixed-integer Programming
COE	Cost of Energy
CR	Crossover Rate
CRO	Coral Reefs Optimization
DIUS	Department of Innovation, Universities and Skills
DOE	Department of Energy
DPS	Definite Point Selection
DTI	Department of Trade and Industry
EEA	European Environment Agency
EML	Electricity Market Law
EMST	Euclidean Minimum Spanning Tree
EPS	Extended Pattern Search
ER	Elitism Rate
EU	European Union
FIT	Feed-in tariff
GA	Genetic Algorithm
GBO	Gradient-based Optimization

GGA	Global Greedy Algorithm
GHA	Greedy Heuristic Algorithm
GHG	Greenhouse Gas
GPSO	Gaussian Particle Swarm Optimization
GSA	Gradient Search Algorithm
HM	Heuristic Method
HSA	Harmony Search Algorithm
IBA	Improved Basic Approach
IEA	International Energy Agency
ICPS	Initial Candidate Points Selection
JEDI	Jobs and Economic Development Impact
LCOE	Levelized Cost of Energy
LDC	Least Developed Countries
MAS	Multi-Agent System
MARS	Multi Adaptive Regression Splines
MCS	Monte Carlo Simulation
MDPSO	Mixed Discrete Particle Swarm Optimization
MENR	Ministry of Energy and Natural Resources
MILQO	Mixed Integer Linear and Quadratic Optimization
MILP	Mixed Integer Linear Programming
MOEA	Multi-objective Evolutionary Strategy Algorithm
MOGA	Multi-objective Genetic Algorithm
MPGA	Multi-population Genetic Algorithm
MR	Mutation Rate
MST	Minimum Spanning Tree
NDRC	National Development and Reform Commission
NEA	National Energy Administration
NPV	Net Present Value
NREL	National Renewable Energy Laboratory
NSGA-II	Non-domination Sorting Genetic Algorithm-II

OWF	Offshore Wind Farm
PGA	Peak Ground Acceleration
PSA	Pattern Search Algorithm
PSO	Particle Swarm Optimization
PSO-MAM	Particle Swarm Optimization with Multiple Adaptive Methods
RS	Random Search
RSYDO	Rüzgâr Santrali Yerleşim Düzeni Optimizasyonu
RSYDOP	Rüzgâr Santrali Yerleşim Düzeni Optimizasyonu Problemi
R&D	Research and Development
QAP	Quadratic Assignment Problem
QI	Quadratic Interpolation
SAA	Simulated Annealing Algorithm
SCP	Sequential Convex Programming
SEA	Seeded Evolutionary Algorithm
SIGA	Self-Informed Genetic Algorithm
SOA	State Ocean Administration
SOM	Self-Organizing Map
SS	Spread Sheet
TLP	Tension Leg Platform
TVAC	Time Varying Acceleration Coefficients
TWEA	Turkish Wind Energy Association
UK	United Kingdom
UNFCCC	United Nations Framework Convention on Climate Change
VAT	Value Added Tax
WFLO	Wind Farm Layout Optimization
WFLOP	Wind Farm Layout Optimization Problem
XA	Xie and Archer

LIST OF SYMBOLS

SYMBOLS

a	Axial induction factor
A	Rotor area (m^2)
C_P	Power coefficient
C_T	Thrust coefficient
D	Rotor diameter (m)
e	Euler's number
eff	Efficiency of a wind farm
k	Entrainment constant
N	Turbine number
V	Wind speed (m/s)
V_{avg}	Average wind speed (m/s)
V_{ci}	Cut-in wind speed (m/s)
V_{co}	Cut-out wind speed (m/s)
V_0	Free-stream wind speed (m/s)
V_r	Rated wind speed (m/s)
V'	Wind speed on downstream turbine (m/s)
P	Power (W)
r	Rotor radius (m)
r_0	Upstream turbine rotor radius (m)
x	Distance behind an upstream turbine (m)
y	Distance in prevailing wind direction (m)
z	Hub height (m)
z_0	Surface roughness (m)
ρ	Air density (kg/m^3)

CHAPTER 1

INTRODUCTION

Generating energy from fossil fuels causes an increase in production of carbon dioxide and other gases that are harmful for nature (Higgins & Foley, 2013). The Kyoto Protocol, adopted on 11 December 1997 in Kyoto, Japan, which entered into force on 16 February 2005, is an international agreement of the United Nations Framework Convention on Climate Change (UNFCCC). The United Nations agreed to the Kyoto Protocol in order to reduce emissions of harmful gases into the environment and reduce the effects of global warming. As the major cause of harmful gases present in the atmosphere, fulfilling the objectives of the protocol is substantially the responsibility of developed countries under the "common but differentiated" principle (United Nations Climate Change, 2019). The European Union (EU) planned to generate some of its energy needs from renewable sources following the Kyoto Protocol. Renewable energy is essential for dealing with challenges such as reducing carbon emission, improving energy security and struggling with climate changes which are considered as crucial issues by many European countries (Higgins & Foley, 2013).

The UNFCCC secretariat, known as UN Climate Change, was established in 1992 as part of the UN with the adoption of UN Convention on Climate Change, and is active in issues threatening the present and the future of humanity. According to their commitments, the countries were divided into four main groups as Annex-I, Annex-II, Non-Annex-I and least developed countries (LDC) under the convention (UNFCCC, 2022). After the establishment of the secretariat and the adoption of the UNFCCC which aims to prevent rising Greenhouse Gases (GHGs), the community has taken many steps to achieve its purpose. Despite the Kyoto Protocol, the content of GHG in the atmosphere has continued to increase rapidly. The factors like non-adjustable emission reduction targets, conflicts due to difficult fair share-burden

arising from legal bindings and disagreements between Annex-I and non-Annex I countries have made the Kyoto Protocol no longer useful. Therefore, a conference has been held in Copenhagen in 2009 which aimed to create a successor agreement to the Kyoto. The outcome; however, has not met with the expectations mainly due to the disregard of countries for the threatening changes in the global climate. This conference, which was considered as a failure in that time, prepared the basis for the Paris Agreement. In contrast to the Kyoto Protocol, the Paris Agreement, signed in 2015 with the participation of 196 parties, has long-term targets such as achieving zero GHG by the second half of this century. The Paris Agreement was not intended to solve the global climate problem; however, this agreement has shown the global warming fact to the world and the need to turn to low-carbon strategies is crucial (Falkner R., 2016).

1.1 Renewables: Wind energy

While the world population is rapidly increasing, energy consumption is also increasing and expected to increase by 56% between 2010-2040 (Kumar et al., 2016). Fossil fuels such as oil, natural gas and coal are the largest energy production sources in the rapidly developing industry sector (Timmons et al., 2014). Economic developments, increasing demands and global climate concerns on the other hand require transition from fossil fuel dependency to other energy sources. Nuclear energy uses non-fossil sources as fuel, so GHG emission is much less compared to fossil fuel sources. However, it does not fully meet the desired solution due to the negative effects of radioactive waste and high radiation it releases on human health and nature (Kumar et al., 2016). On the other hand, the use of renewable and sustainable energy production sources such as wind, wave, tidal, solar, biomass and geothermal has become widespread in the last few decades, considering that it will be an effective solution to the problems created by increasing GHG emissions (Chen, 2011; Da et al., 2011; Vis & Ursavas, 2016). With its high energy potential, wind is one of the renewable energy resources that can be utilized to meet the energy

consumption in the world. In addition to not emitting GHG, it is an important advantage that a modest area is sufficient for installation of wind turbines, which are the most commonly used wind energy conversion systems. Although these systems are well-developed over last few decades, there is still a need to increase their efficiency and performance and to reduce their cost (Kumar et al., 2016).

1.1.1 Onshore vs. offshore

In the 1990s, onshore wind energy, which had a remarkable growth with onshore wind farms especially installed in northwest Europe, dominated the energy sector (Henderson et al., 2003). While this growth has positive effects in reducing GHG emissions, some problems have become critical, such as the inconvenience of transporting large components of a wind turbine (i.e., blades and hub) and the limitations imposed by the negative visual and auditory effects. Technological improvements in recent years and increasing awareness of negative impacts in onshore have increased the investments in offshore wind industry due to its significant advantages such as higher wind speed and more consistent wind field. Also, deploying offshore wind turbines helps to eliminate some of the negative impacts of onshore wind farms such as visual pollution and noise. On the other hand, offshore wind turbines have some difficulties such as extreme weather conditions, larger loads, complexity of the design of the support structure (Henderson et al., 2003; O'Kelly & Arshad, 2016). Furthermore, offshore wind turbines require larger support structures and thicker underwater cables. In addition, special vessels are required to transport, install, and maintain the large components of the offshore wind turbines. Therefore, offshore costs are approximately 2.5-3 times that of onshore (Bilgili et al., 2011).

1.1.2 Offshore wind turbines: support structures

Support structures used for offshore wind turbines are divided into two main groups, fixed and floating. Bottom-fixed type structures consist of monopile, gravity, suction caisson, jacket, tripod, etc., and floating type structures consist of tension leg platform (TLP), barge, spar-buoy, etc. (Lefebvre & Collu, 2012). Various types of supporting structures with applicable depths can be seen in Figure 1.1.

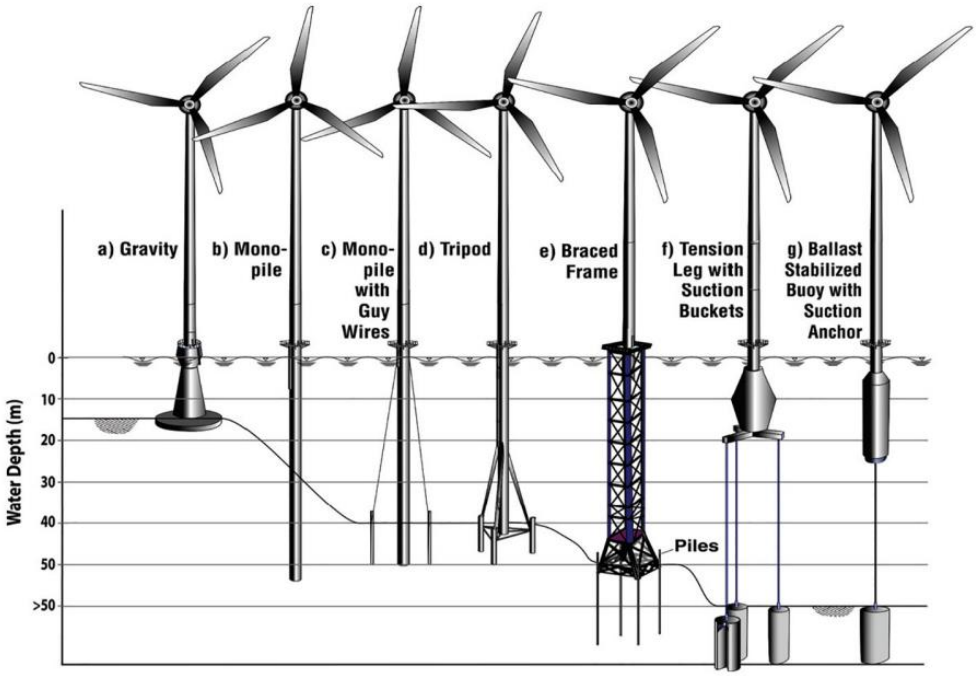

Figure 1.1 Various types of support structures and their applicable water depths (Malhotra, 2011)

1.1.2.1 Monopiles

For most of the offshore wind turbines installed near the shore, bottom-fixed types (see Figure 1.2) have been used as support structures, and the technology has developed in this direction. On the other hand, for reasons such as greater wind potential and abundance of suitable areas, installations are increasingly moving away from the shore. However, as moving away from the shore, the water depth varies

depending on the continental shelf. In waters deeper than 50 m, excessively large bottom-fixed support structures are required; hence, using bottom-fixed types are no longer feasible after that depth since manufacturing and installation costs will increase excessively. As an alternative, floating types are preferred as in the offshore oil and gas industry (Lefebvre & Collu, 2012).

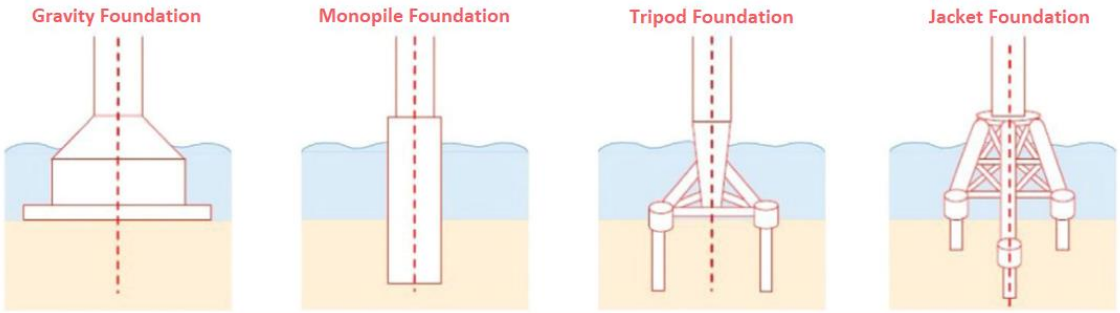

Figure 1.2 Illustration of bottom-fixed offshore wind turbine foundations (Micelli, 2012; X. Wu et al., 2019)

The most commonly preferred support structure for currently operating offshore wind turbines are monopile foundations since they are simple to install, have relatively low fabrication costs and have proven success in the field, as could be seen in supporting offshore oil and gas infrastructures (Lombardi et al., 2013). Monopiles are offshore wind turbines supported by a single large diameter pile made of cylindrical steel tubes, penetrated into the seabed by using piling or vibrating hammer (Byrne et al., 2015). If the seabed is very stiff, the monopile is positioned after the sea bed has been drilled to a certain depth with diameter slightly more than the diameter of the pile (Nikolaos, 2004). Main components of an offshore monopile wind turbine system is shown in Figure 1.3.

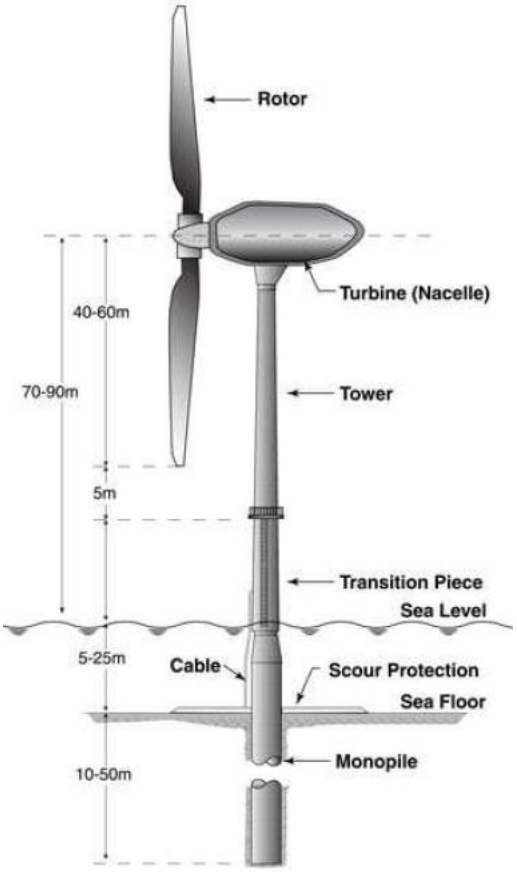

Figure 1.3 Offshore monopile wind turbine system components (Malhotra, 2011)

The number of offshore wind farms installed deeper than 30 m was almost negligible until 2010, and the support structures of the majority of the installed turbines were monopiles (Higgins & Foley, 2013). In general, monopiles are used in shallow water depths (20-40 m) (Wu et al., 2019). As the length of the monopile increases with increasing water depth, the natural frequency of the monopile decreases and becomes very sensitive to the dynamics of the turbine components after a certain depth. Therefore, extended monopile length and larger monopile diameters are required to provide the necessary stiffness. This elevates the cost of fabrication and makes installation more challenging. In other words, after a certain water depth, selection of monopile as a support structure for offshore wind turbines was neither practical nor feasible in those years (Higgins & Foley, 2013). In recent years however,

monopiles supported laterally with steel wires or different foundation types, such as tripods and jackets, have been developed as economically viable solutions to provide the required stiffness values to the structures built in water depths of 30-40 m (O'Kelly & Arshad, 2016). Commonly, piles with diameters of 5-6 m are used (Byrne et al., 2015), however, it is claimed that monopiles with diameters up to 10 m are viable up to 60 m water depth (Kallehave et al., 2015). Monopiles with diameters of more than 6 m have been produced in Europe and applied in waters deeper than 30 m with the technological improvements since 2010 (Kaya & Oğuz, 2019).

1.2 Offshore wind developments in Europe

Offshore wind energy technologies are well-developed in some countries, especially in the UK, Germany and Denmark, which constitute the vast majority of all installed offshore wind power capacity in Europe and even in the world. Moreover, these world leading countries in offshore wind industry improved their policies and regulations over time to reach their renewable energy goals. Therefore, it is critical to be able to enhance knowledge and prepare necessary legislation by taking advantage of their experience before developing an offshore wind turbine for newcomers. Turkey is one of the countries which is expected to enter into the offshore wind energy industry over the next years. In order to make feasible and successful investments, it is important to investigate the experiences of leading countries. Therefore, there is a significant need for a clear long-term-plan for offshore wind in Turkey in terms of availability of technological knowledge, technical expertise, and skilled workforce (Satir et al., 2018).

1.2.1 Offshore wind resources

In order to overcome the negative consequences of globally increasing energy demand, especially global climate change, some of the agreements adopted in

Europe have set some targets for the use of renewable energy sources (Hattam et al., 2017). For instance, due to the requirements of the Kyoto Protocol, the EU aimed to reduce GHG emissions by 8% in 2010 compared to 1990. In 1997, the European Commission published a paper on renewable energy with the aim of achieving an installed wind power capacity of 40 GW in 2010. However, since onshore wind developments alone are not predicted to be sufficient for achieving these targets, major steps have been taken to accelerate offshore wind energy developments towards the end of 1990s (Barthelmie, 1998).

The European Environment Agency (EEA) (2009) reported that the technical offshore wind energy capacity in Europe is 5,800 GW without any regulations or policy restrictions (EEA, 2009). According to the studies carried out by Lloyd & Hassan (1994), most of Europe's energy needs can be supplied from offshore wind sources in case all the large offshore wind power capacity of Europe is used.

1.2.2 Regulations and policies for offshore wind energy

Denmark has pioneered the first offshore wind energy applications by undertaking projects proving the success of offshore wind energy installations and launching the first full-scale offshore wind farm. The UK, however, is currently considered as the world leader in offshore wind energy sector with its transparent and ambitious procedures, long-term planning, and numerous projects contributing significantly to the reduction of GHGs. Germany, similarly, demonstrates its support for the development of the offshore wind energy industry in the country and its willingness to develop cost-effective technologies for this purpose. According to EU's Renewable Energy Directive (2009/28/EC), 2020 targets of these three countries for share of renewable energy sources in gross final energy consumption were as follows:

- Denmark – 30% (17% in 2005),
- UK – 15% (1.3% in 2005),
- Germany – 18% (5.8% in 2005)

Considering all their experiences in offshore wind industry, in this study, it is aimed to review the regulations and policies developed over the years in Denmark, the UK and Germany.

1.2.2.1 Denmark

In Denmark, which established the first commercial offshore wind farm in 1991, wind energy has played an important role in the country's energy policy in the last few decades (Ladenburg & Dubgaard, 2007). Denmark is the first country in Europe to make major investments in the wind energy sector (Sawyer et al., 2013) and is an important pioneer of the offshore wind energy market (Breton & Moe, 2009). Therefore, Denmark has unique experience compared to other countries working on offshore wind energy (Ladenburg & Dubgaard, 2007). However, offshore wind energy development in Denmark entered a period of stagnation due to the reduction in government support in the early 2000s (Zaaijer & Henderson, 2004) after the government stopped providing feed-in tariff (FIT**)** in 1999, aiming to create competition in the sector for development. During this period in which the interest to offshore was significantly decreased, no offshore wind energy installation took place between 2004-2008. After the targets set at the United Nations Climate Change Conference in Copenhagen in 2009, the interest in offshore wind energy increased again, and following this, installation of large wind farms has started with the financial support provided by the government (Sawyer et al., 2013). After 2010, large-scale offshore wind farms were implemented (Kaya & Oğuz, 2019) with increased support and investments, and Denmark reached an installed capacity of 1,703 MW at the end of 2020 (O'Sullivan, 2021).

1.2.2.2 The United Kingdom

With "the dash for gas" trend coming to an end in the early 2000s, which led to a decline in carbon emissions and electricity prices in the UK, the government has

started a new search for a similar effect. As a result, the development of offshore wind energy, which has received almost no support from the government until that date, has accelerated. In 2001, the Crown Estate, which holds the right to use the territorial waters of the UK, received an unexpected interest with 18 project applications. The Crown Estate, however, has taken a cautious approach, considering previous planning difficulties on land, and has offered rental for all projects (Zaaijer & Henderson, 2004). In 2002, UK Department of Trade and Industry (DTI), which was replaced by Department for Innovation, Universities and Skills (DIUS) and Department for Business, Enterprise and Regulatory Reform (BERR) (GOV.UK, 2022), published a report suggesting that the focus should be on three strategically important regions, the North-West, between the Welsh and Scottish coasts, the Greater Wash and the Thames Estuary, planned to be implemented in 2005-2015. In those years, developments in offshore wind energy have progressed rapidly and successfully thanks to the harmony between government and industry (Zaaijer & Henderson, 2004).

In the early 2000s, the research and development (R&D) studies and projects progressed rapidly, especially with considerable financial support from the UK government and some institutions. At the end of 2008, the UK reached an installed offshore wind power capacity of 590 MW, leaving Denmark behind as a leader in this field. Until that time, wind farms were installed in relatively preferable locations, close to the shore and not deeper than 20 m. Further offshore areas, however, were more suitable for implementation of larger projects even though they have more challenging conditions with greater water depths. Therefore, towards the end of this decade, large-scale projects under these challenging conditions began to be implemented (Higgins & Foley, 2013).

In the UK, offshore wind energy developments take place in three rounds defined by the Crown Estate. In the early 2010s, with the completion of the Crown Estate's round 1 projects and the implementation of most of the round 2 projects, the UK reached 3,641 MW (Higgins & Foley, 2014) and continued to maintain leadership in front of Denmark (Higgins & Foley, 2013). Also, after completion of round 1

projects, offshore wind energy sector has had some inferences such as average cost of energy (£69 per MWh) and minimum wind speeds (7-14 m/s) needed to meet economic targets (Feng et al., 2010). At the end of 2020, the UK reached total installed offshore wind capacity of 10,428 MW (O'Sullivan, 2021), which corresponds to 29% of the total installed offshore wind energy capacity in the whole world. However, this ratio was 33% at the end of previous year. The cause of this decrease is the slowdown of new offshore installations in 2020 compared to previous years due to the gap between the implementation of the Contracts for Difference (CfD) 1 and CfD 2 projects (Lee & Zhao, 2021). The CfD is a long-term plan which is the UK government's main mechanism to reduce carbon emissions in electricity generation. CfDs are signed between renewable energy producers and the Low Carbon Contracts Company (LCCC), which is a government company. In addition to encouraging the producer to invest in renewable energy by protecting from variable electricity prices, it also protects the consumer from the high costs of supporting renewable energy reflected in their bills (GOV.UK, 2021). Moreover, the Crown Estate was planning to reach its targeted capacity for the coming years with completion of round 3 projects with 25 GW power capacity (Higgins & Foley, 2013).

1.2.2.3 Germany

In 2002, Germany planned to implement large-scale installations by entering the offshore wind energy industry in its policies. The coasts of Germany have a large potential for offshore wind energy installations. However, most of the west and north coasts of Germany are under environmental protection, and Baltic Sea coasts are being widely used for shipping. These are the limiting factors restricting areas with high wind potential (Barthelmie, 1998; Sawyer et al., 2013). The fact that suitable areas for offshore wind energy installations were relatively far from the shore and therefore deep waters required the production of turbines and support structures that were more demanding than those day's technology. Therefore, the German government has focused on R&D studies. Offshore wind capacity has not expanded

as expected in 2000s due to some economic and technological challenges. Even, the first offshore installation in Germany, the Alpha Ventus wind farm, has commissioned in 2010. However, the German government, which imitates the concept of FIT in Denmark, has shown its support in this area by increasing tariffs in order to reach its renewable energy capacity targets (Sawyer et al., 2013).

After the Fukushima disaster in 2011, Germany decided to phase out the use of nuclear energy. However, this situation combined with the lack of natural gas resources in the country meant increasing dependence on foreign countries for their energy supply. The German government, which does not want to be dependent on foreign countries, aimed to close the energy deficit by increasing its investment and financial support for developing offshore wind energy (Hines & White, 2014). From 2015 to 2019, Germany has installed large-scale wind farms as can be seen in (Kaya & Oğuz, 2019) and is now one of the world's leading countries in offshore wind industry with an installed capacity of 7,689 MW (O'Sullivan, 2021). However, there occurred a slowdown in 2020 due to unfavourable conditions and restricted offshore wind project pipeline in Germany. As a result of this slowdown, China, which was in the 3rd place behind Germany until the previous year, moved ahead of Germany with new offshore wind energy installation in 2020 and took the 2nd place (Lee & Zhao, 2021).

As a summary of the results of these political developments in European leading countries, they set targets and determine policies related with these targets prior to entering in offshore wind energy industry. Government support on this issue is also crucial for development. In order to accelerate the licensing process by simplifying the procedure for offshore wind energy projects, the trend in European countries in recent years is to monopolize management and control structure by reducing the number of relevant agencies and required licenses (deCastro et al., 2019).

1.2.3 Offshore wind power potential and installed capacity

At the end of 2020, total offshore wind energy installations in Europe accounted for a large majority of all installations with an approximate ratio of 72% (Lee & Zhao, 2021), while this ratio was 76% at the end of previous year (Lee & Zhao, 2020). The share of European countries has been in a decreasing trend due to large-scale installations in China as can be seen in Figure 1.4 (Lee & Zhao, 2021). Economic support mechanisms, three of main are the FIT system, the feed-in premium system and the quota system, contributing to the development of the sector by providing financial convenience to offshore wind energy investors in Europe are one of the factors leading Europe by far in terms of installed offshore wind power capacity (deCastro et al., 2019).

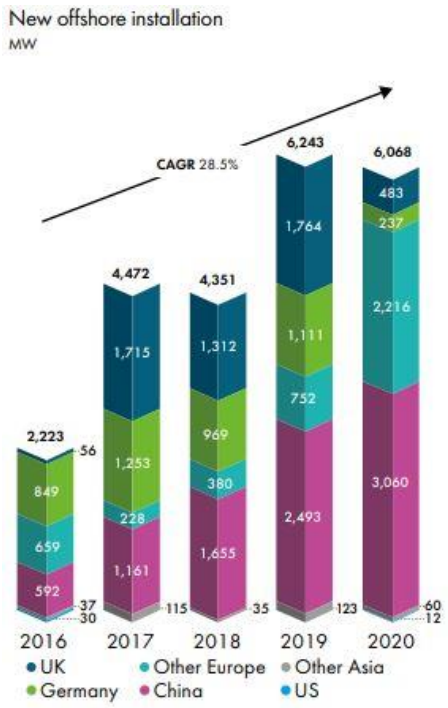

Figure 1.4 New installations of leading countries since 2016 (Lee & Zhao, 2021)

Among support structure types, monopiles are the most common type particularly in Europe (Oh et al., 2018), as can be seen in Figure 1.5, with a ratio of 81% of all installed foundations at the end of 2020 (O'Sullivan, 2021). Due to the European

continental shelf, it is possible to install wind farms in shallow water depths. The monopile systems are the most commonly preferred systems in Europe due to its economic advantages in shallow water depths. Also, it is relatively easier to install monopiles because of easier drilling in the European seabed, which is mainly composed of sand and gravel. These factors make monopile structures more economical in Europe (Oh et al., 2018). This section aimed to review monopile systems in the Europe since Europe dominated the offshore wind industry and most of offshore wind energy installations are located in Europe.

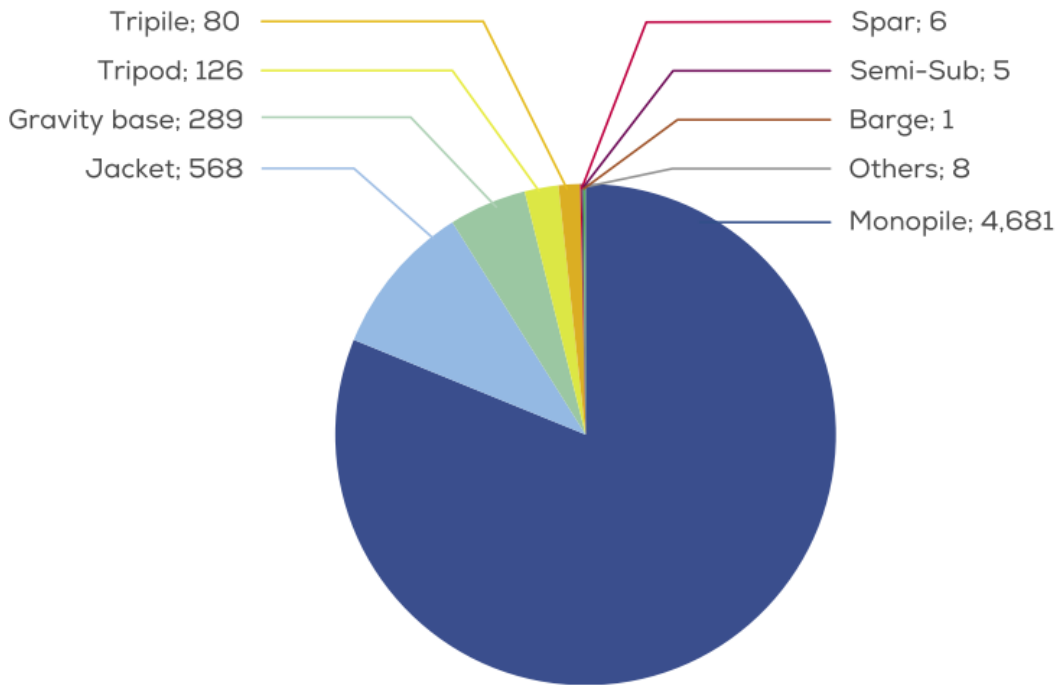

Figure 1.5 Total foundation numbers at the end of 2020 in Europe (O'Sullivan, 2021)

By the end of 2020, the cumulative installed offshore wind energy in Europe reached 25,014 MW, with a total number of 5,402 wind turbines. This amount of offshore wind capacity was installed in just 12 countries. The UK has the largest capacity in Europe with the total number of 2,294 turbines, reaching 10,428 MW, which represents 42% of all installations in Europe. Germany follows the UK by 31%, followed by the Netherlands, Belgium, and Denmark (O'Sullivan, 2021).

Cumulative percentage installed capacity and the number of wind turbines by country in Europe at the end of 2020 are shown in Figure 1.6.

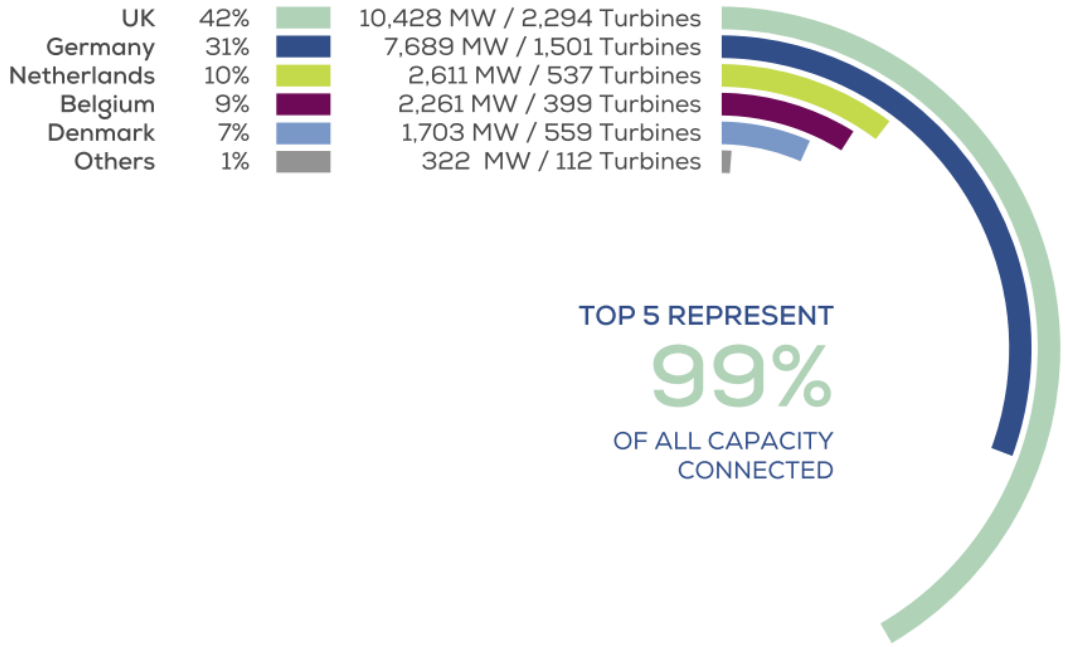

Figure 1.6 Cumulative installed capacity and number of turbines by country in Europe at the end of 2020 (O'Sullivan, 2021)

These developments in Europe and the demonstration of the applicability of the offshore have encouraged industrialized countries such as China and the United States to move towards offshore wind energy (Zaaijer & Henderson, 2004).

1.3 Wind energy in Turkey

The main energy sources of Turkey were coal (lignite) together with hydropower, and energy production from renewable energy sources was not in practice in Turkey until the 2000s. To benefit from renewable sources and decrease energy dependency to fuels, Electricity Market Law (EML) came into force in 2001. The private sector participation and projects on electricity efficiency increased with the aid of EML. So new legislation and laws on electricity production are continued to be put in place. A new law came into force to raise the share of renewable energy sources, among

other sources of electricity production, in 2005. Electricity Market and Security of Supply Strategy, which was announced in 2009, became an important step for the improvement of renewable energy sources. The strategy aimed at the renewable share of electricity production for the country might be 30% at the end of 2023 (Bölük, 2013).

1.3.1 Situation in Turkey

Turkey is an energy-dependent country with a ratio of 75% imported power and stays behind the EU, which has a rate of 54% of energy dependency (Uğurlu & Gokcol, 2017). The country aims to increase projects on renewables, especially wind power, to reduce energy dependency. According to Figure 1.7, which shows wind potential map of Turkey at 100 m height, west of the country has a high potential for wind power. Turkish Wind Energy Association (TWEA) states that the Aegean Region is the greatest with 38.46% installed wind turbine capacity, and the Marmara Region follows it with 34.71% capacity. Turkey is one of the developing countries, and its increasing population requires an average of 8% more energy annually, which may be generated by the offshore wind (Ilkiliç & Aydin, 2015). Today, Turkey has 198 fully commissioned onshore wind farms and 25 wind energy farms under construction. The total number of wind turbines installed in Turkey is 3,155 at the end of July 2019 (TWEA, 2020). After the first deployment of a wind turbine in 1998, currently, energy generation from wind in Turkey reached to 9.22% of all energy generation (TWEA, 2021). However, Turkey, which has renewable targets like European countries, does not have any offshore wind projects yet. High wind speeds, measured at the seas covering the coasts of Turkey, indicate the high offshore wind potential in Turkey. According to Malkoc (2007), offshore wind potential in Turkey is 10,463 MW (Malkoc, 2007). However, before developing an offshore wind turbine for Turkey, it is critical to be able to enhance knowledge and prepare necessary legislation. Since each renewable energy system needs to be designed for a specific location, a great number of feasibility studies carried out by researchers in

order to determine the most suitable regions for offshore wind turbine deployment in Turkey.

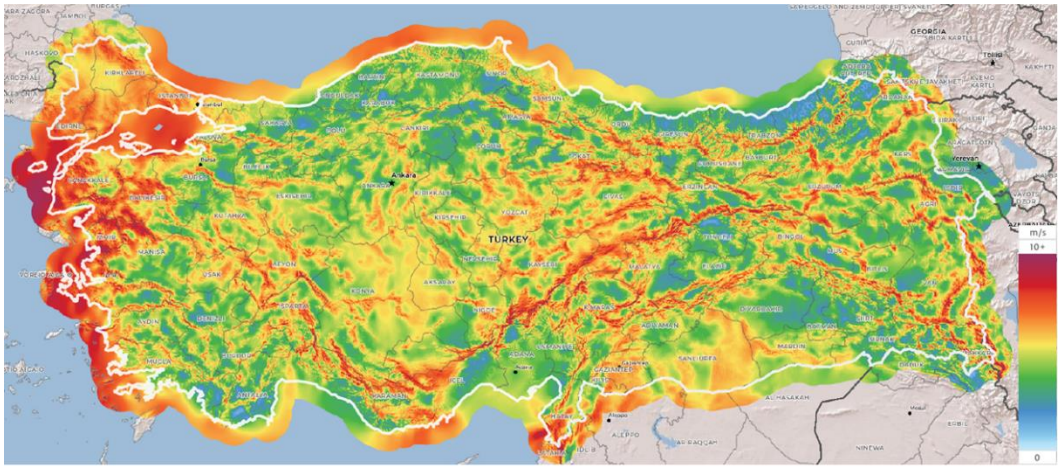

Figure 1.7 Wind speed map of Turkey at 100 m height (Global Wind Atlas, 2021)

According to feasibility studies carried out for Turkey by the Ministry of Energy and Natural Resources (MENR), nine regions, namely, Igneada, Gokceada, Bozcaada, Bababurnu, Alanya, Anamur, Iskenderun, Akıncı Burnu and Saros (see Figure 1.8) are identified as the most feasible locations for offshore deployment (Ilhan & Bilgili, 2016; Satir et al., 2018). For being competent in developing an offshore wind farm, recently, Turkey has started to be involved in several projects with European countries such as Denmark, Germany, and the UK within the Strategic Cooperation Programme. Denmark, which provides approximately 40% of its energy production from wind and is one of the world's leaders in the offshore wind industry, has ongoing bilateral projects with Turkey within the scope of the Strategic Sector Cooperation Programme. The first meeting was held in March 2019 in Ankara to discuss the offshore wind projects, which are expected to strengthen this cooperation. During this meeting, Denmark, which has gained many experiences particularly in the areas of planning and project development throughout the years in the field of offshore wind energy, shared their knowledge and experience in the development of relevant policies, strategies, and solutions (Şengül, 2019).

Figure 1.8 Map of high offshore wind potential regions in Turkey (Google Earth, 2022)

1.3.2 Site selection criteria for offshore wind farm installations

Considering the Aegean Sea coasts of Turkey, Bozcaada and Gokceada are selected as one of the feasible locations to deploy an offshore wind farm. The bottom-fixed type of supporting structures seem suitable for the water depths of around 20-30 m at this location (Satir et al., 2018); however, the water depth of a region is not a unique criterion while selecting a suitable region. Territorial waters and military zones, wind condition, distance to shore, electricity transmission from turbines to interconnect system, submarine conditions, marine environment, civil aviation, fishery, marine traffic, underground cables, pipelines are another factors which affect the site selection for offshore wind farms (Argin et al., 2019; Köroğlu & Ülgen, 2018).

Territorial water is defined as adjacent waters to the shore of a country with a width of nearly 22 km; however, the Aegean coasts of Turkey are very close to Greek Islands; therefore, the boundary of territorial water for both Turkey and Greece are around 11 km. During suitable site selection for offshore technology, the territorial water limitation should be considered not to create territorial water and continental

shelf problems between the two countries. In contrast to the Aegean coasts, other coasts of the country (i.e., the Black Sea and the Mediterranean Sea coasts) have a long distance to neighbour countries; thus, territorial water limitation is not a critical criterion for these coasts. Among the selected locations, Saros, Bababurnu, Gokceada, and Bozcaada are in the Aegean Sea; however, none of those regions are critical in terms of limitation on territorial water; therefore, all the selected locations are suitable for installing offshore wind turbines. The other criterion for offshore site selection is *military zones.* Especially, Black Sea has a lot of military zones where military training and shooting is conducted. Among the selected locations, Igneada is the only place located in the Black Sea; however, Igneada is not critical in terms of existence of the military zone. The Aegean Sea also has some military zones and unexploded mined terrains, which was remained from the Gallipoli Campaign. Bababurnu, Gokceada, and Bozcaada are critical locations since they are located close to military regions; however, the criticality of Bababurnu is more important than Bozcaada and Gokceada. While Bababurnu is surrounded by critical military zones, Gokceada and Bozcaada have partial military zones, hence there exist suitable locations at the appropriate depth for offshore wind turbines at Bozcaada and Gokceada. *Civil aviation* is another factor that affects site selection for offshore wind farms since existance of civil aviation activity can create safety problems for both offshore turbines and aircraft. The noise of the turbines also creates confusion for the radar system. All selected locations for offshore wind projects are far from the airport or small aircraft landing areas; therefore, civil aviation is not a problematic criterion for selected regions. *Marine traffic* is also important while selecting a suitable site for an offshore project since offshore turbines cannot be installed in places where marine traffic is heavy. In addition to today's marine traffic situation, the future situation is also important. Before choosing a suitable site, the future economic development of regions that are close to the offshore project site should be considered since shipping routes may change with economic developments. Among the selected regions, Iskenderun is on critical shipping routes since the region has the advanced iron-steel ports of Turkey; therefore, the selection of Iskenderun for

installation of an offshore wind project might not be favorable. In addition to Iskenderun, Bababurnu also has heavy marine traffic since it is on the trajectory of Turkey's busiest ports; therefore, Bababurnu and Iskenderun are not suitable for the installation of offshore wind farm. The distance between existing *pipelines or underground cables* and the project field is another important challenge because cables and pipelines can be damaged during the construction of wind turbines. At least 500 m distance is required between pipelines or cables and project locations to avoid possible damage. Today, there exists no pipeline system for selected regions except for Bababurnu, which is close to capacity for pipelines and underground cables. In addition to Bababurnu, Igneada is also critical since there exists a natural gas pipeline project from Russia to Turkey on Igneada coasts (Argin et al., 2019). Additionally, seismic properties for potential site for offshore wind farm installation is also important since seismicity affects both turbine tower and foundation. According to Figure 1.9 which is showing seismic properties of the countries in terms of Peak Ground Accelerations (PGAs) 10% probability of exceedance in 50 years, Turkey has high seismicity and close to subduction zone where severe earthquakes can occur (De Risi et al., 2018). Therefore, earthquake risks of the candidate regions for offshore wind turbines are critical. For the selected regions, PGA values for 43 years return period (68% in 50 years) prepared by the Disaster and Emergency Management Presidency (AFAD) are given in Table 1.1.

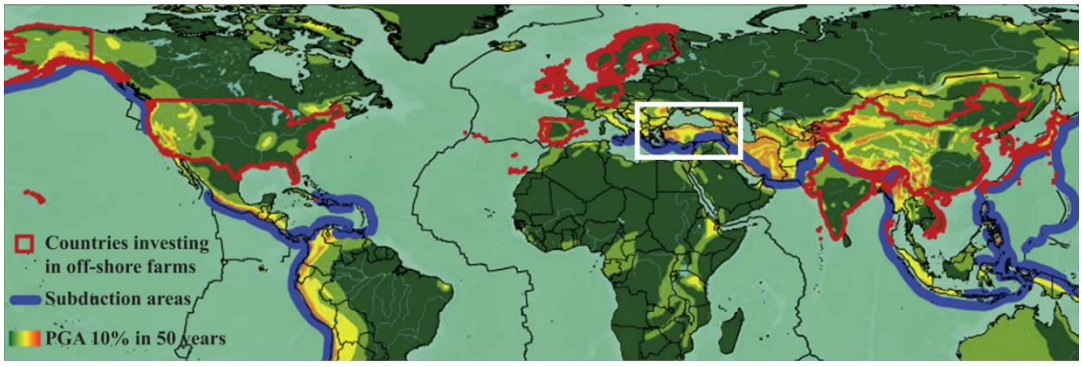

Figure 1.9 Map of countries investing in offshore wind farms (red boundaries), subduction trenches (blue lines), and global seismic hazard map, modified from (De Risi et al., 2018)

According to AFAD Online Earthquake Catalog (2021), the most critical region in terms of seismic activity is seen as Saros with 0.137 by considering PGA 68% in 50 years. In addition to high seismicity, the region also has high turbulence from the land; therefore, the operation and installation of offshore wind turbines to Saros will be difficult in terms of foundation and tower design (Bingöl, n.d.). One of the most important criteria for appropriate site selection for offshore wind turbines is wind velocity, which directly affects wind power efficiency, and for Bozcaada and Gokceada, the mean wind speeds at 100 m height are 8.55 m/s and 8.4 m/s, respectively. Therefore, the installation of offshore wind turbines to these high wind potential regions provide higher energy efficiency than other regions. In conclusion, Akıncı Burnu, Anamur, Alanya, Bozcaada, and Gokceada are suitable locations for the installation of offshore wind turbines by considering stated factors; however, to obtain higher efficiency from wind power, Bozcaada and Gokceada come into prominence in terms of high wind speed. All site selection criteria for high wind potential sites are presented in Table 1.1.

A more detailed study has been carried out by Yıldız (2021), and she determined that the most suitable region for installing an offshore wind farm in Turkey is Bozcaada, considering both environmental and restrictive conditions.

Table 1.1 Properties of selected locations in Turkey

Location	Territorial Waters (Argin et al., 2019)	Military Zone (Argin et al., 2019)	Civil Aviation (Argin et al., 2019)	Marine Traffic (Argin et al., 2019)	Pipeline (Argin et al., 2019)	PGA 68 % in 50 years (AFAD Online Earthquake Catalog, 2021)	Mean Wind Speed at 50 m (m/s) (Global Wind Atlas, 2021)	Mean Wind Speed at 100 m (m/s) (Global Wind Atlas, 2021)
Akıncı Burnu	√	√	√	√	√	0.073	6.40	6.61
Alanya	√	√	√	√	√	0.060	3.83	3.93
Anamur	√	√	√	√	√	0.048	5.74	6.00
Bababurnu	x	x	√	x	x	0.129	7.70	8.17
Bozcaada	√	~	√	√	√	0.091	8.16	8.55
Saros	√	√	√	√	√	0.137	7.17	7.87
Gokceada	√	~	√	√	√	0.130	7.92	8.40
Igneada	√	√	√	√	x	0.044	5.82	6.25
Iskenderun	√	√	√	x	√	0.089	5.27	5.65

√ not critical ~ partially critical x critical

1.4 Summary

Considering high offshore wind energy potential in Turkey, it is important to learn the developments and the technology of leading countries in offshore wind industry. Although there are many installations of offshore wind farms especially in Europe, there is no substantial attempt to take advantage of this high offshore wind potential in Turkey. In Chapter 1, after describing the importance of renewable energy systems, the developments in renewable energy and the use of resources, the industrial developments in offshore wind energy, the use of offshore wind energy potential and resources, regulations and policies, and installed power capacities in leading countries are reviewed in detail and summarized.

1.5 Motivation of this study

Increasing investments in offshore wind industry due to the increasing trend to renewable energy around the world makes offshore wind farms a popular research topic. It is known that environmental conditions directly affect the amount of electricity yielded from offshore wind farms. Also, due to the shading created by the turbines on each other, the variable wind speeds in the wind farm area reduce the production capacity. This shading situation should be minimized by positioning the turbines in an optimum layout to increase the effective use of offshore wind potential significantly, which is known as wind farm layout optimization problem (WFLOP). There are many methods proposed so far for solving WFLOP; however, the performance of different grid sizes has not been investigated. It is also critical to be able to propose a method considering different wind conditions and wind turbines to determine grid size since grid size determination is still unclear and important in WFLOPs.

Although there is no offshore wind farm design for Turkey nowadays, in case of a possible design, the existing optimization methods will need to be adapted for

suitable areas in Turkey. So, proposing a pre-designed optimum layout might be beneficial for a potential installation in a country that has not entered the offshore industry yet (i.e., Turkey). For this purpose, developing two models considering variable and fixed turbine numbers, in other words, a single two-staged model was developed for different cases, and application of this model was carried out for a region in Turkey having high offshore wind energy potential.

The rest of this thesis is organized as follows: previous studies in the literature related to optimization of wind farm layout is reviewed and presented in Chapter 2; Chapter 3 defines the methodology proposed for WFLOP using genetic algorithm (GA). Chapter 4 presents the formulations used in power generation of a wind turbine, cost and wake calculations for application of GA in this thesis; Chapter 5 presents and discusses the results obtained by running the codes for different cases. Chapter 6 provides conclusion of this thesis.

CHAPTER 2

LITERATURE REVIEW

In this chapter, what is WFLOP is described, and the methods, techniques and algorithms used in previous studies on both onshore and offshore WFLOP are examined in order to determine an appropriate methodology for our problem. Also, significant improvements and novelties in the literature are described in this chapter.

2.1 Wind farm layout optimization problem (WFLOP)

Because of the economic considerations, it is desired to install wind turbines clustered in large wind farms as close as possible. However, this brings about the trade-offs that depend on the distance from the shore and the distance between the turbines. While the distance to the shore increases, the cable cost increases as the distance of electricity transmission increases. Moreover, the support structure cost will also increase as the water depth will probably increase. On the other hand, as the wind speed generally increases the further away from the coast, the energy production potential will also increase. Furthermore, increasing the distance between the turbines will again increase the cable cost, but will reduce wake losses (Lackner & Elkinton, 2007). That's why the WFLOP getting more and more attraction and take so much attention of wind farm developers. The rapidly developing offshore wind energy technology is gradually reducing costs, but offshore is still more expensive compared to onshore (Hevia-Koch & Klinge Jacobsen, 2019). In a wind farm, it is possible to increase the energy production capacity or to reduce the costs by using wind farm layout optimization (WFLO) methods, thereby reducing the levelized cost of energy (LCOE) (Lackner & Elkinton, 2007). In addition, since the areas suitable for offshore installation is limited, it is important to use offshore efficiently by placing the turbines in the optimum layout when installing a wind farm

(Ozturk & Norman, 2004). Although this problem is generally tried to be solved by creating a regular rectangular layout with turbines lined up in rows at certain intervals, some research have shown that it is possible to further reduce energy losses by creating irregular layouts using optimization methods (Grady et al., 2005; Huang, 2007; Kusiak & Song, 2010; Mosetti et al., 1994; Ozturk & Norman, 2004; Rivas et al., 2009; Şişbot et al., 2010).

2.2 Previous WFLO applications

As a rule of thumb, a ratio of 10 ha/MW was considered to meet the land requirement for wind farms, including infrastructure (Bansal et al., 2002). However, this ratio is not sufficient to determine turbine spacing because there are many factors that vary such as site conditions, wind speed, wind direction and turbine size. Patel (1999) proposed 8-12 rotor diameters (D) spacing in prevailing wind direction and 1.5-3D spacing in crosswind direction, see Figure 2.1, for optimum turbine spacing. On the other hand, it was claimed that Patel's (1999) proposal uses the wind energy potential of the field inefficiently, and an alternative method that uses the field more efficiently by creating a denser layout was proposed Ammara et al. (2002). After all, any of these basic and intuitional approaches did not treat the situation as an optimization problem.

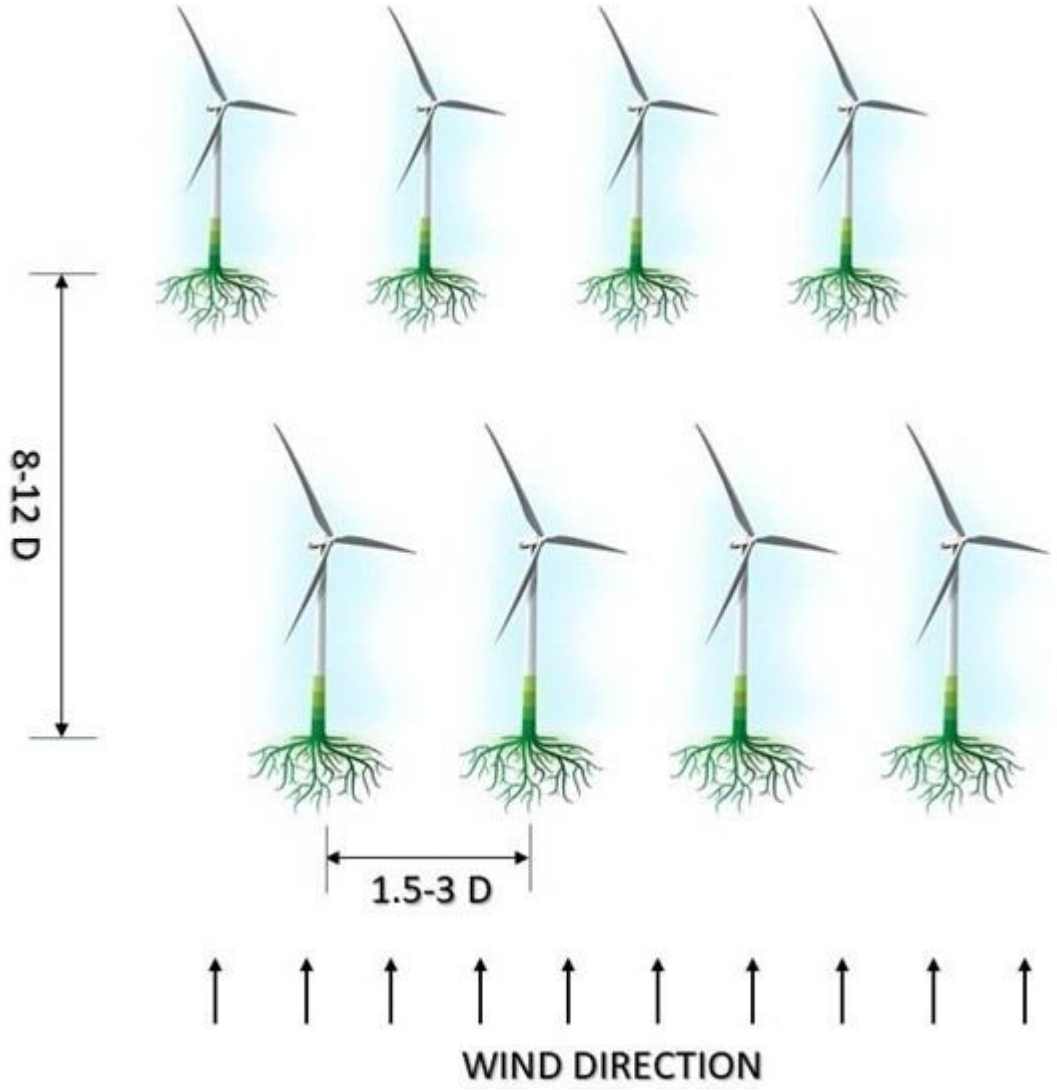

Figure 2.1 Optimum turbine spacing in accordance with rule of thumb, modified from (Emami & Noghreh, 2010)

The first study to consider placing turbines in a wind farm as an optimization problem was carried out by Mosetti et al. (1994). They used a square land with dimensions of 2.0 km by 2.0 km and divided the land into the square grids with side length of five turbine diameters. To be sure about that the turbines provide the minimum separation distance, only placement in the middle of grid cells was allowed. The main purpose of their study was to prove that GA is applicable and feasible by performing a layout optimization study aiming to obtain maximum power

with minimum installation cost in a wind farm. In their study, optimization studies were carried out for 3 wind conditions: constant wind speed and direction, constant wind speed and variable wind direction, variable wind speed and direction.

Ozturk and Norman (2004) discussed and tried to solve WFLOP using heuristic approaches for the first time. In their study, it was asserted that the wind farm area is evaluated as a continuous solution space. However, since the move operator of greedy heuristic algorithm (GHA) places the turbines in predetermined positions, this predetermination makes the approach partial continuous. Moreover, GHA was not preferred in further studies due to its negative aspects such as the possibility of achieving local optimum results and the difficulty of determining the initial solution.

Grady et al. (2005) considered same cases for same conditions used by Mosetti et al. (1994) by allowing much more individuals and generations. A single column was optimized, and the optimum layout was obtained by copying the optimum column to the other columns. The results obtained at the end of the optimization were compared with the results of Mosetti et al. (1994). The reason for the difference in the resulting optimum layout (see Figure 2.2) was probably that the number of individuals and generations used by Mosetti et al. (1994) does not allow to converge the global optimum layout. Nevertheless, Mosetti et al. (1994) and Grady et al. (2005) proved that using GA is an effective method for WFLO.

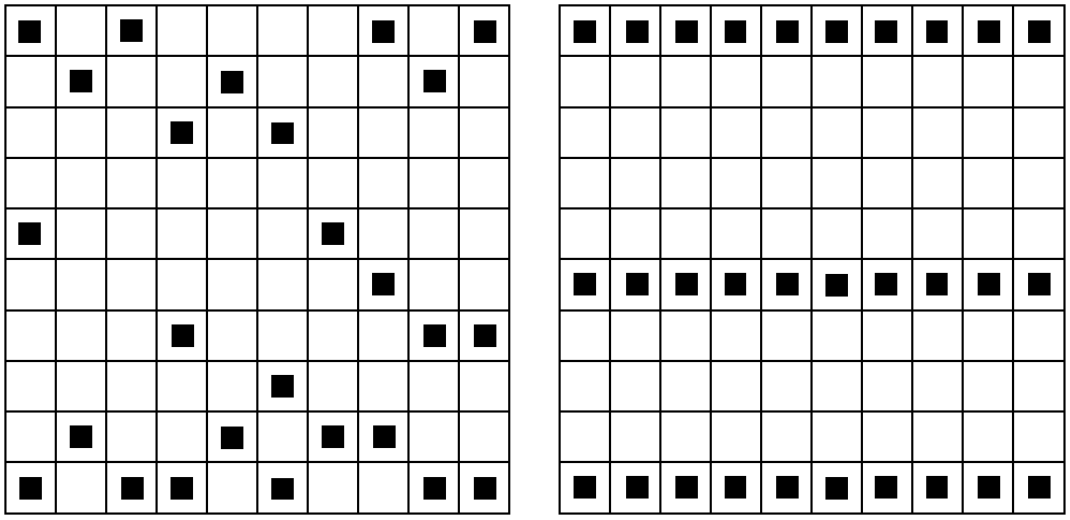

(a) (b)

Figure 2.2 Optimum wind farm layout proposed by: (a) (Mosetti et al., 1994) and (b) (Grady et al., 2005)

Lackner and Elkinton (2007) developed a method that minimize the LCOE for offshore wind farms. They run the method using gradient search algorithm (GSA) for two-turbine wind farm; however, one year later, Elkinton et al. (2008) argued that GSA does not contain randomness. Therefore, GSA is less suitable for such problems than others because lack of randomness creates a tendency to local solutions rather than global solutions.

Castro Mora et al. (2007) proposed a GA which is able to choose the best turbine for a specific location in the wind farm to maximize the net present value of a wind farm by taking into account the investment costs. The results showed that, unlike traditional mathematical methods, evolutionary algorithms (EAs) are efficient for layout optimization problems. However, they did not make any recommendation regarding the placement of turbines.

Marmidis et al. (2008) proposed Monte Carlo simulation method which is based on the use of random numbers and tested the method for constant wind speed and direction, as in the study of Mosetti et al. (1994) and Grady et al. (2005), Marmidis et al. (2008) obtained better results than Mosetti et al. (1994) and Grady et al. (2005)

using the Monte Carlo simulation method. However, this method has a disadvantage of long computation time.

Herbert-Acero et al. (2009) carried out an optimization study using simulated annealing algorithm (SAA) and GA. They used varying parameters such as wind speed, wind direction, turbine number, turbine spacing, and hub height. The results obtained from these two algorithms showed that SAA gave slightly better results and took less computation time than GA. Moreover, it was demonstrated once again that such EAs are well suited for WFLOPs.

Ma et al. (2009) used quadratic interpolation (QI) method to optimize the layout of wind farm; however, the feasibility and reasonability of this method was not verified.

Following Mosetti et al. (1994) and Grady et al. (2005), Wan, Wang, Yang, Li, et al. (2009) also treated WFLOP in the same way and developed a similar model. The optimized layout and related results were compared with Grady et al.'s (2005). Although half of the number of individuals were allowed, they advanced the performance of GA using the model they developed, according to Grady et al.'s (2005) results.

Emami and Noghreh (2010) introduced a more comprehensive objective function compared to previous studies (Grady et al., 2005; Mosetti et al., 1994), which also controls the cost for layout optimization, taking into account the limited financial resources in real conditions. Their findings showed higher energy production than previous studies for two cases they considered: (i) constant wind speed and variable wind direction, (ii) variable wind speed and variable wind direction.

In his thesis, Mittal (2010) repeated the previous studies (Grady et al., 2005; Marmidis et al., 2008; Mosetti et al., 1994) and compared his results with the previous ones. In all these studies, he revealed that there were inconsistencies and incompatibilities. In other words, the optimal result obtained in these studies did not represent the accurate solution.

Rahmani et al. (2010) compared the optimal wind farm layout obtained using the particle swarm optimization (PSO) method with those in previous studies (Grady et al., 2005; Marmidis et al., 2008; Mosetti et al., 1994). He concluded that PSO gives better results than GA, which is also an EA, is suitable for implementation for WFLOP and needs further improvements.

Şişbot et al. (2010) aimed to obtain a layout that produces maximum energy with a limited budget in the appropriate area they determined for the installation of onshore wind farm, near Gokceada in the Aegean Sea. In previous studies, layout was optimized by collecting all objectives in a single objective function. However, in their study, arguing that WFLOP is a multi-objective problem, power and cost were evaluated in separate objective functions. The wind speed and direction were assumed to be constant, with reference to the average wind speed and the prevailing wind direction calculated using historical data. This assumption allowed the grid area to be rectangular in accordance with the minimum spacing distance (Patel, 1999), thus allowing the wind farm area to be used more effectively.

Kusiak and Song (2010) extended the method developed by Lackner and Elkinton (2007), but this time a multi-objective evolutionary strategy algorithm (MOEA) was used instead of GSA which was found not appropriate for WFLOP (Elkinton et al., 2008). Also, some additional constraints and assumptions were added to the optimization methodology for facilitating WFLOP solving. Kusiak and Song (2010) worked using a more complete objective function than previous studies due to the comprehensiveness of the cost function considering different costs such as operation and maintenance costs.

Saavedra-Moreno et al. (2011) proposed a novel approach to implement traditional GA using GHA instead of randomly determining the initial solution, and named it Seeded EA (SEA). The results indicated that using SEA performed much better than using GA or GHA alone.

Chen and MacDonald (2012) claimed that in the optimum wind farm layout of onshore wind farms, the most critical locations have to be given priority to negotiate

with the land owners to save money and time. Their motivation for carrying out their study is that not every landowner may be willing to have wind turbines installed on their land. As a result, for an area consisting of nine adjacent parcels, each of which has a different owner, optimum layouts obtained using the assumption that some landowners might have negative approach.

Kwong et al. (2012) conducted a work for the multi-objective WFLOP that considers two objectives that are maximum energy generation and minimum noise level at the boundaries of the wind farm. They used Non-domination Sorting GA (NSGA-II) that is variant of traditional GA. The main difference of NSGA-II from traditional GA is sorting individuals and selecting parents, detailed in (Deb et al., 2002).

Gonzalez et al. (2013) proposed a new method to optimize large offshore wind farm layout. The aim was to maximize the profit, so they developed a complete model estimating the costs considering both initial investment costs in the construction phase and operational costs during its lifespan. The model was also estimating the income considering the main factors having negative effects on the profit such as wake losses, energy prices, etc. They used GA as optimization method; however, the crossover and mutation operators were slightly different from the previous applications. The crossover operator was identifying the positions of turbines relative to each other and adding or removing turbines to satisfy the minimum spacing distance. The mutation operator was specifying the feasible turbine positions and placing the turbine in a random feasible position. Due to these modifications in crossover and mutation allowed shorter computation time by avoiding unfeasible solutions. Different from previous GA applications, they divided the computational space into zones for reducing complexity of WFLOP solution.

Couto et al. (2013) developed a code in MATLAB that calculates wind energy production, taking into account the wake effect and different wind turbine characteristics. After that, an optimization model maximizing the energy developed in modeFRONTIER software using GA and the results were compared with the commercial software WindFarmer and previous studies (Grady et al., 2005;

Marmidis et al., 2008; Mosetti et al., 1994) for verification. The results of their study showed that the model developed by Couto et al. (2013) gave better results then previous studies.

Mosetti's cost model is the most widely used model for WFLO, but since it is dimensionless, it is not suitable for use in real wind farm cost calculations. In addition, previous studies have tried to simplify wind conditions, but real data should be used in layout optimization for a commercial wind farm. Chen (2013) argued in his thesis that cost and wind models used in previous studies were not sufficient to reflect the reality to establish a commercial wind farm. For this reason, he used a more comprehensive cost model, Jobs and Economic Development Impact (JEDI) that was developed by the U.S. Department of Energy/National Renewable Energy Laboratory (DOE/NREL). JEDI considers economic multipliers for land usage costs, costs in labour market, income, and output (Goldberg et al., 2004; Wang, Cholette, Zhou, et al., 2018). He calculated the cost by using the rated power and turbine number data obtained from 50 wind farms in Texas. In addition, real wind data from a region in Texas were used in his study. Moreover, there were 2 objectives; one is to maximize efficiency and the other is to minimize cost of power, by using turbines of different types with different hub heights.

Y. Chen et al. (2013) proposed a method to solve WFLOP using different hub heights and applied their method for both theoretical and realistic conditions. First, they validated the GA parameters by comparing them with previous studies (Grady et al., 2005; Mosetti et al., 1994). They then compared the results by applying the method they developed to wind farms at different hub heights and same hub heights. Their findings demonstrated that different hub heights resulted in more power output. In their approach, they used two-stage GA; in the first stage, they optimized the location of the turbines while in the second stage, they optimized the hub heights for optimized layout. Unlike previous studies, they preferred to place the turbines in the corners of the cells, not in the middle. However, while the previous ones had n x n possible location, this time there was (n-1) x (n-1) possible location because at the

boundaries of the wind farm, it was not allowed to locate a turbine. Therefore, this placement method reduces the effective use of the wind farm area.

Duan et al. (2014) developed a model using GA and tested their model for two types of wind turbines: (i) 2 MW, 100 m, (ii) 335 kW, 37 m, rated power and hub heights respectively. The aim of using multi-type wind turbines was to reduce the wake losses and take full advantage of the energy potential of the field. They tested the model for three different cases as in the study of Mosetti et al. (1994). The results showed that using multi-types of wind turbines might allow full usage of wind resources by reducing wake effects.

Rahbari et al. (2014) proposed a new approach to optimize layout design of wind farms for maximum efficiency. They applied Quadratic Assignment Problem (QAP) and GA methods together with Initial Candidate Points Selection (ICPS) by considering additional criteria such as seabed soil conditions and prohibited areas which had not been accounted for previous approaches. The aim of considering this problem in a wider context was to increase the applicability of the solution in real conditions. Moreover, unlike the usual in application of GA, tournament selection-based elimination was used to create diversity in next generations. Also, they applied their model not only for one type of turbine but also for two different turbine types.

Gao et al. (2014) studied on the optimum spacing distance of wind turbines for a hypothetical offshore wind farm area in Hong Kong. They investigated the results of three different layout pattern: aligned, staggered, and scattered. The aim of their study was to obtain an optimal layout with minimum LCOE for fixed number of turbines. First, they determined the optimum number of turbines according to the varying spacing distances in prevailing wind direction and crosswind direction for aligned and staggered patterns. Then, the optimum layout for scattered layout was obtained using Multi-population GA. For same number of turbines, among these three patterns, the scattered layout gave the best results with the lowest LCOE and the highest annual energy production (AEP).

Shakoor et al. (2015) proposed a new approach to obtain an optimum layout for same wind farm area, 2 km x 2 km, had been widely used in literature. Unlike the studies in the literature, they positioned the wind farm area according to the wind direction differently. They positioned the wind turbines using the widest measure of the land, which is its diagonal, is perpendicular to the prevailing wind direction (see Figure 2.3). In this case, it was possible to fill the two sides in the direction of the wind with turbines. Therefore, the area could be used more effectively. The layout proposed by Shakoor et al. (2015) was about 7% more efficient than that of Mosetti et al. (1994), using the same number of turbines. They also compared the results of their approach with similar studies in the literature, and it was proven that the new approach gives better results.

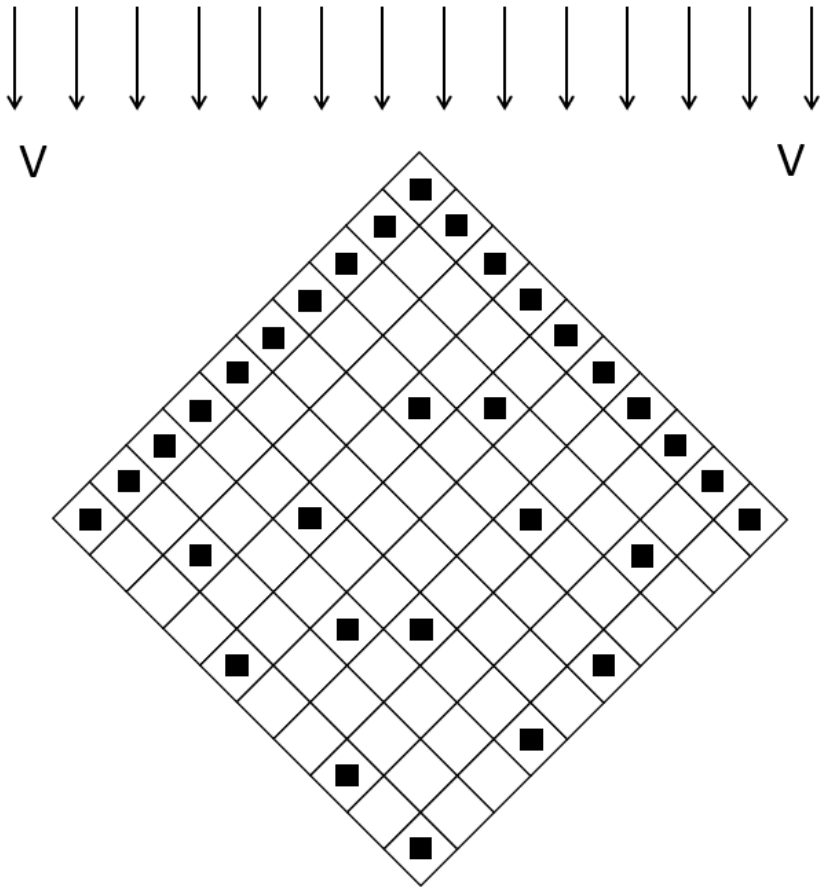

Figure 2.3 Wind farm layout proposed by Shakoor et al. (2015), modified from (Shakoor et al., 2015)

Wang et al. (2015) divided the wind farm area into 20x20 grids unlike the previous studies that widely prefer to divide the wind farm area into 10x10 grids. Also, they optimized the wind farm area by using continuous approach. One of the aims was to compare the results from these two grids and the continuous approach and to observe if there was any improvement. Another aim of Wang et al. (2015) was to compare two cost models which are named as Mosetti's and Chen's in the literature. This comparative study showed that 20x20 grids should be preferred instead of 10x10 grids since 20x20 grids gave better results, worth the increase in the computational cost. However, the same cannot be said for the continuous approach since the improvement was so small and not worth the increase in the computational cost. Another result of their study was that Mosetti's cost model gives more accurate results than Chen's for a large number of turbines.

Abdulrahman and Wood (2017) performed an optimization for onshore and offshore using GA. They included 61 different commercial wind turbines covering a ranges of 66-115 m rotor diameter and 11-17 m/s rated speed. However, using different turbines and hub heights brought along the trade-off between power and cost. The results of their study showed that the turbines having lower rated speed and larger rotor diameter should be preferred primarily. Therefore, Abdulrahman and Wood (2017) strongly suggested that a wind farm should be designed using different wind turbines with different hub heights in order to reduce the wake effects. In the comparison of onshore and offshore, it was observed that optimization of wind farms for offshore is more effective since the lower entrainment constant in offshore delays free stream wind speed recovery.

Tang et al. (2017) applied the same method as Mosetti et al. (1994) for a different case study. Instead of identical turbines, four different types of turbines with higher power generation capacity, various hub heights and rotor diameters were used, named as mixed installation, in accordance with the needs of the industry. In addition, in their study, 4D was chosen instead of 5D as the safe distance to reduce computational cost. The wind farm layout was optimized using eight wind turbines with four different types of turbines, for both identical installation and mixed

installation. The results showed that mixed installation reduces wake deficit and thus enables more efficient use of the wind farm area.

Tang et al. (2018) furthered the study carried out by Tang et al. (2017). They used combination of GA and PSO instead of only GA for simultaneous optimization of turbine type selection and wind farm layout. Also, there was an additional objective which was to minimize the distance between turbines. They handled the WFLOP using continuous approach, not grid-based approach. It can be said that it is a much more comprehensive and complex study than the previous one. For validation, it was compared to the results of three wind scenarios, 8, 12 and 17 m/s. In addition to the previous one, the results also showed that the optimization for mixed installation is more effective for higher wind speeds.

Wang et al. (2018) studied WFLOP using continuous approach, aiming to minimize the cost of energy (COE). They performed two case studies, one for a two-dimensional flat area and the other for a three-dimensional (real) space also considering terrain altitude variations. For the selected wind farm area, variable turbine number was used in the optimum range specified in the literature. In their study, hub height, like the number of turbines, varied within a predefined range (10, 20, and 40 m). The wind farm layout was optimized for both constant and varying hub heights using varying number of turbines. The results showed that the hub height difference provides an improvement, but the larger the hub height difference, the more remarkable the improvement. Despite varying hub heights in 2D case, wake loss was inevitable for small range of hub height difference. However, even if the hub height was constant for 3D case, wake loss could be prevented up to a certain number of turbines by taking advantage of the terrain altitude variations. That is, it was easier to prevent or reduce wake loss in 3D case than in 2D case.

One of the widely used methods to control the minimum distance between turbines is Omnidirectional Restriction (see Figure 2.4) which prevents some excessive restriction compared to restriction using the method which divides the wind farm area into circular or rectangular grids. However, in the crosswind direction, these

two methods still excessively restrict the effective use of the wind farm area. As an alternative method, Sun et al. (2019) proposed a new spacing method called Directional Restriction (see Figure 2.5). In this method, the restrained area is determined according to the crosswind direction and the waste of space is prevented. Moreover, in case of mixed installation, the restrained area is determined according to the diameter of each turbine. Sun et al. (2019) applied the WFLO method, which they developed by controlling the minimum distance between turbines using the Directional Restriction method, for four different cases: (a) aligned layout with uniform wind turbines, (b) optimized layout with uniform wind turbines, (c) optimized layout with nonuniform wind turbines and (d) a commercial nonuniform offshore wind farm. The results showed that the nonuniform layout with nonuniform wind turbines gave the best results in terms of efficient use of space with the same number of turbines. Lastly, they designed the layout of a potential wind farm, and the results demonstrated that the method proposed by Sun et al. (2019) is suitable to solve WFLOP.

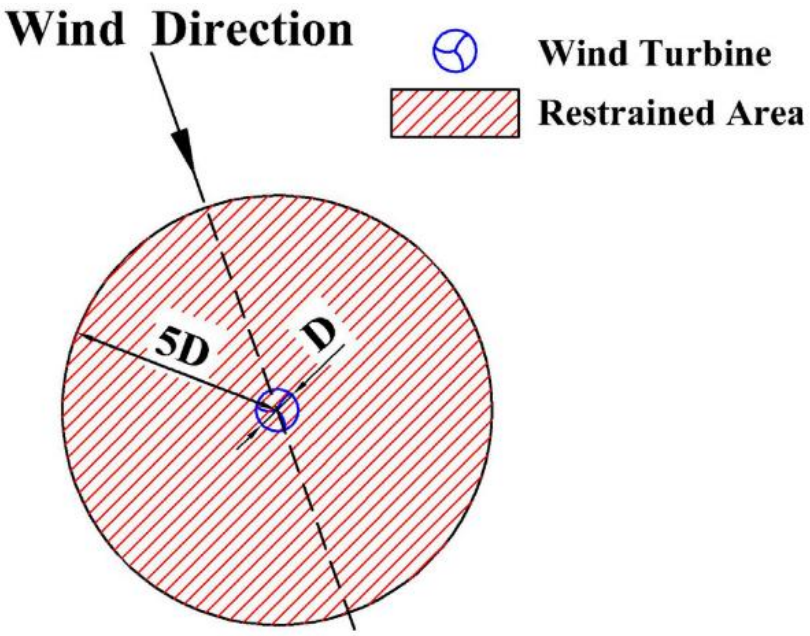

Figure 2.4 Restrained area for Omnidirectional Restriction method (Sun et al., 2019)

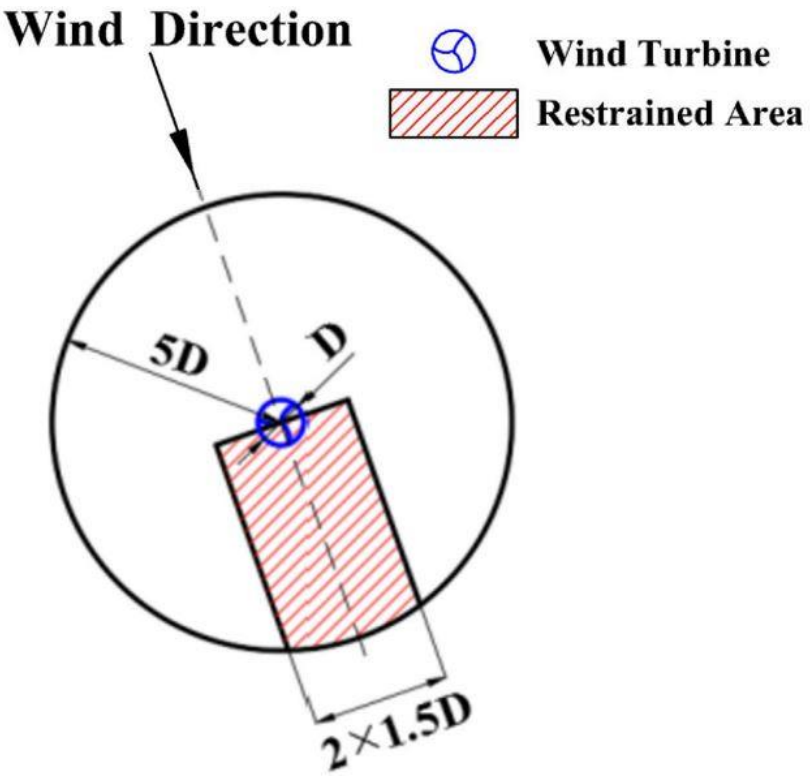

Figure 2.5 Restrained area for Directional Restriction method (Sun et al., 2019)

Ju and Liu (2019) performed GA's crossover and mutation operators differently, inspired by the survival of the best part of individuals in nature. While each step is random in traditional GA, they have proposed two new algorithms, Adaptive GA (AGA) and Self-Informed GA (SIGA), based on GA that work by placing the worst-positioned turbine in a better position in terms of power generation. In AGA, the worst turbine was placed at a random lox, whereas in SIGA, Multivariate Adaptive Regression Splines (MARS) regression based on Monte Carlo Simulation was used for the relocation. As a result, their results in different wind conditions and different wind farm sizes concluded that AGA and SIGA reach the optimum result faster than traditional GA.

Park et al. (2019) proposed a method that consists of two steps, batch optimization and post-optimization. To summarize briefly, the grids having a turbine in the optimum layout which are obtained in batch optimization are divided into grids again

within themselves, and re-optimization is performed for the new grids, which is post-optimization. Looking at their results, it can be said that the layout with post-optimization provides about 2% more efficiency than that of the batch optimization.

Unlike previous studies, Wu et al. (2020) focused on wind turbine layout together with cable route, using GA for turbine layout and GeoSteiner algorithm (Winter & Zachariasen, 1997) for cable layout. To the best knowledge of Wu et al. (2020), there are very few studies in the literature that consider optimizing cable routing, and these studies have generally considered the cable routing optimization problem as a minimum spanning tree (MST) problem. However, Wu et al. (2020) thought that considering the problem as an Euclidean minimum Steiner tree (EMST) problem and solving the problem using the GeoSteiner algorithm could yield better results. The reason for using the GeoSteiner algorithm was that it is the fastest solving algorithm for EMST problems. The results of their study showed that EMST could give better results than that of MST. The novelties and the main contributions of their study were to consider wind turbine layout and cable routing at the same time and to consider cable routing problem as an EMST, using GeoSteiner algorithm, instead of MST.

2.2.1 Optimization methods and comparison of algorithms

WFLOP is a combinatorial optimization problem (Eroğlu & Ulusam Seçkiner, 2013). Although there are many optimization algorithms available to be used in WFLOP, the dynamics within this problem bring some algorithms to the forefront for reasons such as applicability and giving compatible results. Elkinton et al. (2008) discussed five optimization algorithms, GA, GSA, GHA, pattern search algorithm (PSA), and SAA, and examined their applicability for WFLO. They argued that GSA does not contain randomness. Therefore, GSA is less suitable for such problems than others because lack of randomness creates a tendency to local solutions rather than global solutions. PSA has some randomness but still requires a long calculation time similar to GSA. Considering the randomness and accounting time in the SAA, it

seems appropriate for WFLOP. However, Elkinton et al. (2008) focused on GA and GHA because they are more suitable for solving WFLO compared to other algorithms due to its simplicity and comparability in application. Yet, Ozturk and Norman (2004) stated that GHA is not preferable due to its negative aspects such as the possibility of achieving local optimum results and the difficulty of determining the initial solution. As time passes and knowledge progresses, new algorithms and methods such as MCS, PSO, QI were proposed. However, as investigations and discussions in the literature have shown, there is a widespread view that GA is the most widely used, proven and convenient method in terms of reliability in linear and non-linear problems, applicability, and adaptability, etc. (Yildiz et al., 2014). All previous methods and algorithms used to solve WFLOP are summarized in Table 2.1. As can be seen from Table 2.1, GA is the most commonly used algorithm for solving WFLOP, so GA was used to solve the WFLOP in this study.

2.2.2 Wake models

The sum of energy generated from identical stand-alone turbines as many as the number of turbines in a wind farm would likely be more than the energy generation of the wind farm (Sørensen et al., 2006). The reason behind this is the loss of energy due to the wake effect caused by the fact that the turbines shade each other (Chowdhury et al., 2013). The modelling of wind turbine wakes can be considerably complex and should be considered in three-dimensional space (Sezer-Uzol & Uzol, 2013). However, in this thesis, the wake is considered in two-dimensional to solve WFLOP.

Archer et al. (2018) reviewed the six most common wake loss models; Jensen, Larsen, Frandsen, Gaussian (Bastankah and Porté-Agel (BPA), Xie and Archer (XA)), and Geometric Model and evaluated their performance by comparing some issues such as absolute error, bias, correlation coefficient, and ability to predict power production for Lillgrund (offshore) in Sweden, Anholt (offshore) and Nørrekær (onshore) in Denmark. These three major wind farms were selected for

comparison since they vary in terms of distinctive aspects such as located on sea or land, layout, and spacing distances. Consequently, Jensen and XA models were recommended due to their good overall performance. All these six models can be used for wake calculations; however, Jensen model is the most commonly used model in the WFLO studies (see Table 2.1). As Pérez et al. (2013) demonstrated, the Jensen wake model provides shorter computation time and performs better compared to other models, Larsen and Ainslie. For all these reasons, Jensen model was used for wake calculations in this thesis and details are presented in Section 4.3.

2.2.3 Discrete vs. continuous approach

Computational domain (searching approach) of an WFLOP can be selected as: (i) continuous (unrestricted coordinate) approach and (ii) discrete (grid-based) approach. In the continuous approach, number of possible turbine locations is unlimited so it considers the whole wind farm area (Shakoor, Hassan, Raheem, & Wu, 2016). By doing this, continuous approach guarantees the global optimum if sufficient number of generations is allowed. The second approach is known as discrete approach which divides the wind farm area into small cells and considers a limited number of possible turbine locations. Due to requiring long computation time and complexity of continuous approach, it was decided to use discrete approach in this thesis. As can be seen in Table 2.1, almost all studies where GA was used, discrete approach was followed as well. Examples of layouts are shown in Figure 2.6 and Figure 2.7.

Figure 2.6 Vineyard Wind 1 wind farm layout (POWER TECHNOLOGY, 2021)

Figure 2.7 Gemini wind farm layout (Van Oord, 2022)

Table 2.1 Previous studies on WFLOP

Reference	Optimization method	Computational domain	Wake model	Grid size
(Mosetti et al., 1994)	GA	Discrete	Jensen	5Dx5D
(Ozturk & Norman, 2004)	GHA	Continuous	Jensen	-
(Grady et al., 2005)	GA	Discrete	Jensen	5Dx5D
(Lackner & Elkinton, 2007)	GSA	Continuous	Jensen	-
(Castro Mora et al., 2007)	GA	Discrete	Jensen	Unspecified
(Marmidis et al., 2008)	MCS	Discrete	Jensen	5Dx5D
(Ma et al., 2009)	QI	Discrete	Jensen	5Dx5D
(Herbert-Acero et al., 2009)	SAA, GA	Unspecified	Jensen	Unspecified
(Wan, Wang, Yang, Li, et al., 2009)	GA	Discrete	Jensen	5Dx5D
(Wan, Wang, Yang, & Zhang, 2009)	GA	Continuous	Unspecified	-
(Rivas et al., 2009)	SAA	Continuous	Jensen	-
(Emami & Noghreh, 2010)	GA	Discrete	Jensen	5Dx5D
(Mittal, 2010)	GA	Discrete	Jensen	5Dx5D
(Rahmani et al., 2010)	PSO	Continuous	Jensen	5Dx5D
(Şişbot et al., 2010)	MOGA	Discrete	Jensen	8Dx2D

Table 2.1 (continued)

(Kusiak & Song, 2010)	MOESA	Continuous	Unspecified	-
(Fagerfjäll, 2010)	MILP	Unspecified	Unspecified	Unspecified
(Wan et al., 2010)	PSO	Continuous	Jensen	-
(Saavedra-Moreno et al., 2011)	GA-GHA	Discrete	Jensen	5.5Dx5.5D
(Chen & MacDonald, 2012)	GA	Discrete	Jensen	4Dx4D
(Rajper & Amin, 2012)	SS, GA	Discrete	Jensen	5Dx5D
(Eroğlu & Ulusam Seçkiner, 2012)	ACSA	Continuous	Jensen	-
(Chowdhury et al., 2012)	PSO	Continuous	Frandsen	-
(Wan et al., 2012)	GPSO	Continuous	Jensen	-
(Du Pont & Cagan, 2012)	EPS	Continuous	Jensen	-
(Kwong et al., 2012)	NSGA-II	Continuous	Jensen	-
(Chowdhury et al., 2013)	MDPSO	Continuous	Frandsen	-
(Y. Chen et al., 2013)	GA	Continuous	Jensen	-
(K. Chen et al., 2013)	GGA	Continuous	Jensen	-
(Pookpunt & Ongsakul, 2013)	BPSO	Continuous	Jensen	-
(Chen, 2013)	MOGA	Continuous	Jensen	4Dx4D
(Gonzalez et al., 2013)	GA	Discrete	Frandsen	variable

Table 2.1 (continued)

(Pérez et al., 2013)	HM-GBO	Discrete	Jensen	4Dx4D
(Couto et al., 2013)	GA	Discrete	Jensen	5Dx5D
(Duan et al., 2014)	MGA	Discrete	Jensen	4Dx4D
(Rahbari et al., 2014)	GA-QAP	Continuous	Frandsen	-
(Turner et al., 2014)	MILQO	Continuous	Jensen	-
(Gao et al., 2014)	MPGA	Both	Jensen	variable
(Salcedo-Sanz et al., 2014)	CRO	Discrete	*Open Wind*	5Dx5D
(Shakoor et al., 2015)	GA	Discrete	Jensen	5Dx5D
(Hou et al., 2015)	PSO	Continuous	Jensen	-
(Park & Law, 2015)	SCP	Continuous	Jensen	-
(Feng & Shen, 2015)	RS	Continuous	Jensen	-
(Wang et al., 2015)	GA	Discrete	Jensen	2.5Dx2.5D
(DuPont et al., 2016)	EPS-MAS	Continuous	Jensen	-
(Pookpunt & Ongsakul, 2016)	BPSO-TVAC	Discrete	Jensen	4-8Dx4-8D
(Shakoor et al., 2016)	DPS	Discrete	Jensen	5Dx5D
(Kuo et al., 2016)	CFD-MIP	Discrete	CFD	1.75Dx1.75D
(Hou et al., 2016)	PSO-MAM	Continuous	Jensen	-

Table 2.1 (continued)

(Abdulrahman & Wood, 2017)	GA	Continuous	Jensen	-
(Tang et al., 2017)	GA	Discrete	Jensen	4Dx4D
(Feng & Shen, 2017)	MDPSO	Continuous	Jensen	-
(Serrano González et al., 2017)	IBA	Unspecified	Jensen	Unspecified
(Song et al., 2018)	GPSO	Continuous	Jensen	-
(Tang et al., 2018)	GA-PSO	Continuous	Jensen	-
(Wang et al., 2018)	GA	Continuous	Jensen	-
(Gualtieri, 2019)	SOM	Continuous	Jensen	-
(Stanley & Ning, 2019)	GBO	Continuous	FLORIS	-
(Sun et al., 2019)	MPGA	Continuous	Jensen	-
(Ju & Liu, 2019)	AGA-SIGA	Discrete	Jensen	4Dx4D
(Park et al., 2019)	GA	Discrete	Jensen	~3Dx3D
(Wu et al., 2020)	GA	Discrete	Jensen	5Dx5D
(Reddy & Roy, 2020)	GA	Discrete	Jensen	5Dx3D
(Huang et al., 2020)	HS-NSGA-II	Continuous	Jensen	-

CHAPTER 3

METHODOLOGY

In this chapter, the methodology used in this thesis to solve WFLOP using GA is defined. GA and its operators are explained in following subsections.

3.1 Problem definition

The problem in this study is to create a wind farm layout by minimizing the cost while maximizing the generated power.

3.1.1 Objective function

The objective function can simply be defined as a function that is determined depending on the decision variables in the optimization problem and that ultimately maximizes or minimizes the decision variables (Mirzaei, 2014). There are many variables such as AEP, COE, net present value (NPV), energy efficiency, robustness of power production, degree of visual impact which can be selected as decision variables as objective function for solving WFLOP (Brogna et al., 2020). However, as the number of considered decision variables increases, the objective function gets more complex. In combinatorial optimization problems, simple objective function selection speeds up reaching the solution of the problem. However, it may give results that are not close to the accurate solution. On the other hand, selection of complex objective function gives more accurate and reliable results but the solution time increases significantly (Elkinton et al., 2008). Therefore, an objective function providing a balance between these two ends and aiming to minimize COE is chosen for this thesis, and the formulation is given below:

$$Objective\ function\ = min\ COE = min \frac{Cost}{P_{total}} \quad (1)$$

where P_{total} is the total power generated by the wind farm in this thesis. The details of cost calculations are explained in Section 4.2.

Wind farm dimensions, turbine number (fixed or variable), turbine characteristics and wind characteristics must be defined to restrict the domain before determination of the algorithm to solve the WFLOP.

3.1.2 Definition of GA

In this subsection, the structure and operators of the GA are explained.

The GA approach, the basis of which was first developed by Holland (1975), is one of the EAs based on the theory of evolution modeled by Darwin. As in nature, individuals in a population pass on their genes to the next generation according to their fitness for survival (Hinçal et al., 2011). Moreover, while adapting to their environment, these individuals go through some evolutionary processes such as selection, recombination (crossover), and mutation (Pohlheim, 2005). GA for WFLOP is an algorithm that aims to reach the optimum result by following natural selection and an iterative method that repeats continuously until reaching the result (Elkinton et al., 2008). Also, GA is very prone to avoid local optimum solutions since it generates random individuals in the solution (Pohlheim, 1999). In WFLOPs, each layout variation is defined as “individual” and from now on each layout will be referred to as “individual”.

In GA, as a first step, the genetic makeup of individuals is determined. For WFLOPs, the genetic structure consists of 0s and 1s. Each element indicates if there is a turbine in that location or not. If there is no turbine in that location, it is expressed as 0, if there is 1.

A flowchart for GA followed in this thesis is presented in Figure 3.1

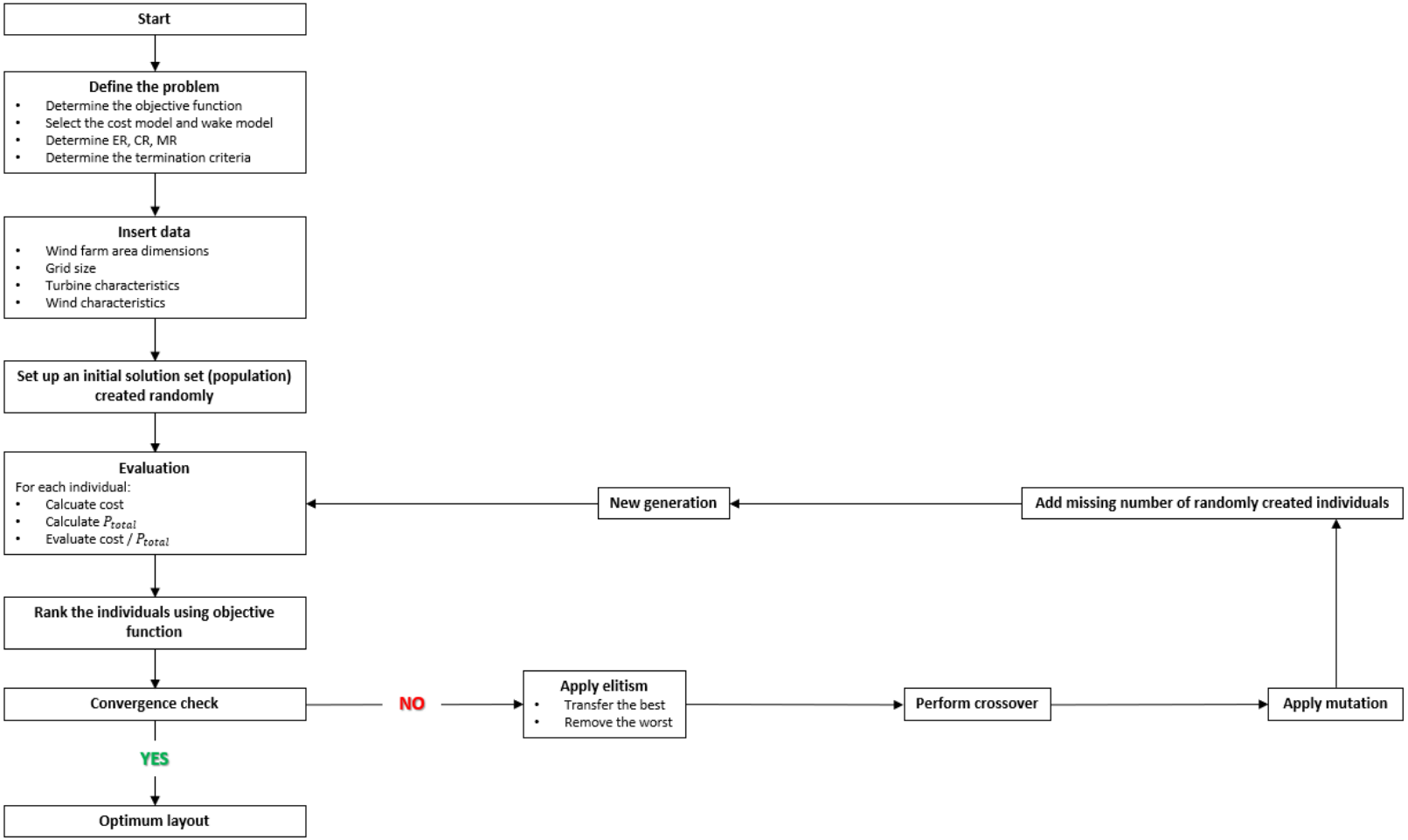

Figure 3.1 GA flowchart used in this thesis

Steps followed in GA and operators of GA are explained in the following.

3.1.2.1 Initial solution

After determination of the genetics of the problem, an initial solution set consisting of a certain number (populations size) of randomly generated individuals is created (Pohlheim, 2005).

3.1.2.2 Evaluation and ranking

The suitability of the individuals selected from the solution set is evaluated and each individual is ranked according to their suitability (or fitness) which is calculated according to the objective function (Pohlheim, 2005).

Fitness shows how fit an individual is to pass on his genes to the next generation, in other words, to survive. In most studies, the fitness value is expressed by the objective function value (Mathew, 2012). Therefore, the fitness value of each individual is calculated by using the objective function.

3.1.2.3 Elitism

For a more appropriate solution, individuals progress through elitism until they reach the most appropriate result by transferring their genes to the next generations (Elkinton et al., 2008). At this step, the most fit individuals of the current generation is transferred to the next generation, and the same number of the worst individuals are removed from the solution set. After the remaining individuals complete their evolutionary processes (crossover and mutation), they are transferred to the next generation (Sharp & DuPont, 2018).

3.1.2.4 Crossover

The crossover operator is the function of two parents to pass their genes to their children, hence to the next generations. After the crossover is performed, two new individuals, namely children, are created. For crossover operation, the number of crossover points must be determined, which is usually 1. However, another positive integer can also be selected, but as this number increases, it will cause an increase in computation time. Another requirement is that the crossover rate (CR) must be selected to determine the number of parents to which this crossover operation will be applied in the current solution set (Elkinton et al., 2008; Pohlheim, 2005). Sivanandam & Deepa (2008) recommended that CR be a value between 0.6-0.9.

In performing the crossover operator, randomly selected parents are mated, and the children with their parents' genes are inherited to the next generation. In this way, parent genes are transferred to other generations by evolution, not exactly as they were. The process of performing crossover using 1 crossover point, which is selected randomly, is illustrated in Figure 3.2.

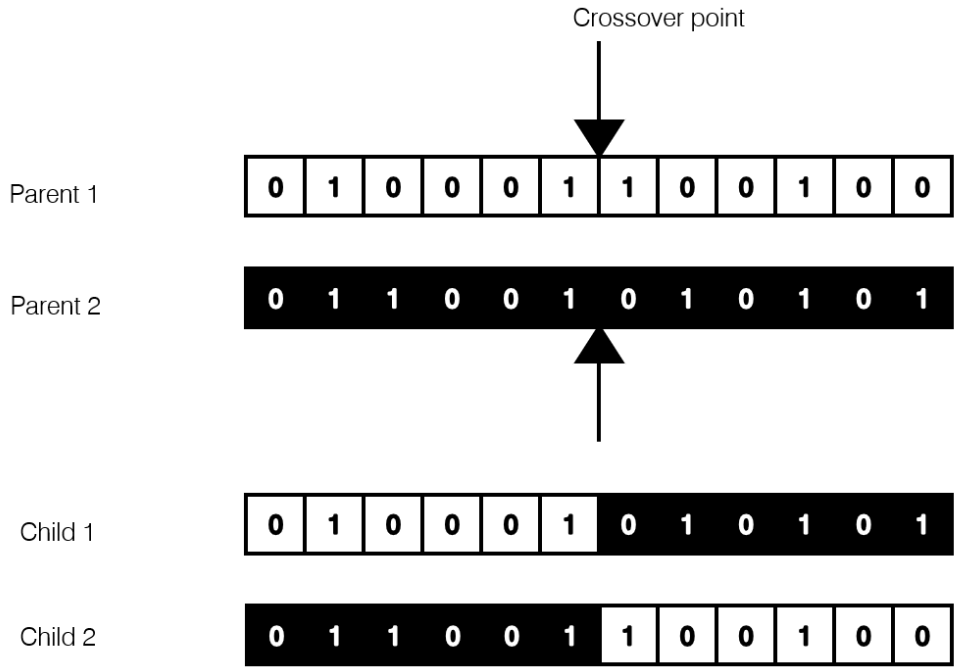

Figure 3.2 The crossover process for a variable number of turbines with 1 crossover point, modified from (Elkinton et al., 2008)

Sharp & DuPont (2018) performed crossover by randomly exchanging the equal number of wave converters to ensure that the number of converters remains constant (see Figure 3.3). This type of crossover can be performed also in WFLOP since both are layout problems. The only difference is that having different types of converters.

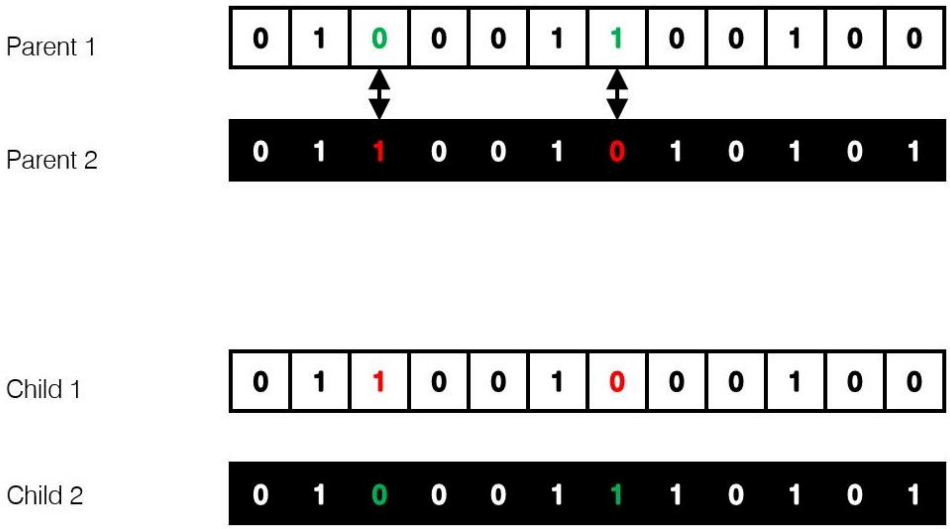

Figure 3.3 The crossover process for a fixed number of converters, modified from (Sharp & DuPont, 2018)

3.1.2.5 Mutation

The evolution created by the mutation operator is also random due to the structure of GA. The main function of this operator is to empty or fill a grid cell (see Figure 3.4). The children born after operating the crossover will have one or more of the genes mutated. The number of gene will be mutated is controlled by the mutation rate (MR) which was recommended by Sivanandam & Deepa (2008) as between 0.01-0.1. As a result of the mutation, the value of that number of gene is reversed (i.e., 0→1 or vice versa). Thus, the small changes caused by the mutation weaken the probability of the generations to repeat each other (Elkinton et al., 2008).

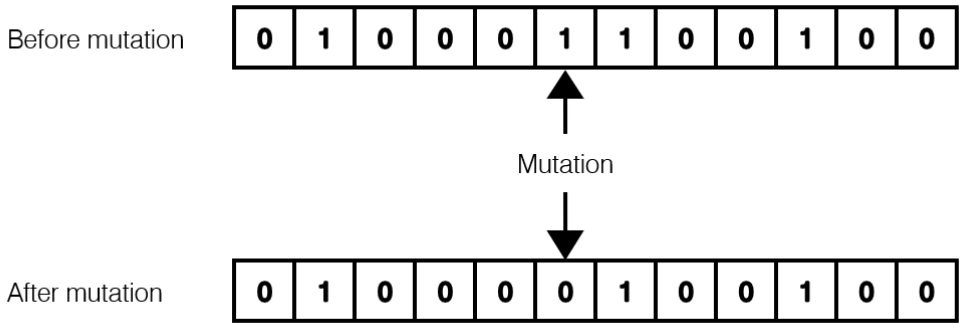

Figure 3.4 Mutation for a variable number of turbines, modified from (Elkinton et al., 2008)

For a fixed number of wind turbines, the turbine number must be kept constant by applying mutation for a child for 2 times. But changing genes must be reverse of each other. In other words, applying mutation for a fixed number of wind turbines means relocating one of the turbines as illustrated in Figure 3.5 (Sharp & DuPont, 2018).

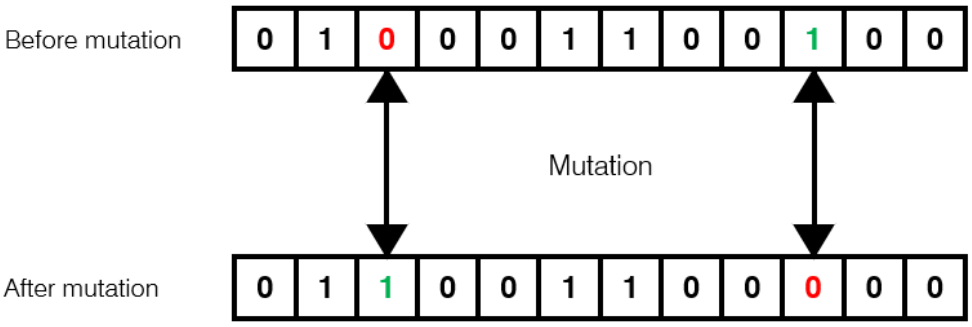

Figure 3.5 Mutation for a fixed number of turbines, modified from (Sharp & DuPont, 2018)

In order to complete the new generation formed after the elitism is completed, the solution set is filled with randomly created individuals as much as the missing number if needed (Sharp & DuPont, 2018).

3.1.2.6 Termination criteria

The efficiency (eff) of a wind farm is defined by Mosetti (1994) as the ratio of the generated power of the layout and the total generated power of the same number of stand-alone turbines in the layout (Equation 2).

$$eff = \frac{P_{total}\ of\ the\ layout}{\sum P_{total}\ of\ the\ same\ number\ of\ stand-alone\ turbines\ in\ the\ layout} \quad (2)$$

In this thesis, the only termination criterion is 100% efficiency; however, in general, wind farms do not generate power with full efficiency since the generated power of a layout is most probably smaller than the summation of the total generated power by same number of stand-alone turbines in that layout. The reason behind that is the wake losses created by the turbines on each other due to shading effect. Therefore, the algorithm will most probably not stop working until the defined generation number is reached.

The main aim of all WFLO studies is to create a layout that maximizes the total power generation. On the other hand, in order to make WFLO feasible, the cost should be considered at the same time. The formulations used in this thesis to calculate power generation of a wind turbine are explained in Section 4.1.

Following these, it is explained which cost model and wake model are used in this thesis, and what should be the minimum spacing distance between turbines for both to prevent damages and to prevent wakes overflowing into adjacent columns. Also, GA application for the WFLO model developed for this thesis is explained in Chapter 4.

CHAPTER 4

MODELLING

In this thesis, two models were developed considering: (a) variable turbine number, and (b) fixed turbine number. The aim of developing model (a) is to obtain a wind farm layout which generates maximum energy with minimum cost. There are two reasons to develop model (b): (i) to find out an optimum layout which generates maximum energy for fixed turbine number, and (ii) to improve the layout obtained from model (a). The first reason why there is a need to create two different models in this thesis is that using larger number of grids in the problem may result in optimum turbine number but may not result in optimum layout. Another reason of developing two models is that the crossover and mutation operators are operated differently in terms of allowing variable or fixed turbine number selection, as explained in subsections 3.1.2.4 and 3.1.2.5. In this study, due to difference in applications of crossover and mutation for variable and fixed turbine number, two codes are developed using Python programming language in PyCharm software.

The formulations used to calculate power generation in this thesis are presented in the following. Also, cost and wake calculations used in this thesis and adaptation of grid size depending on wind characteristics are given. Following these, application of GA in this study is explained.

4.1 Power generation of a wind turbine

The power generation of a wind turbine can be expressed in Watt (W) as (Carrillo et al., 2013):

$$P = \frac{1}{2} C_P A \rho V^3 \tag{3}$$

where C_P is the power coefficient that is specified by the manufacturer, A is the rotor area in m^2, ρ is the air density (1.225 kg/m^3 in general (International Electrotechnical Commission, 2005)) and V is the wind speed in m/s. Theoretically, the maximum value of the power coefficient, known as Betz limit (Betz, 1920), is specified as 0.593 (16/27). However, it is not possible to achieve this theoretical limit in practice, it can be about 0.5 in general because of losses in generation, like wake, due to aerodynamics (Carrillo et al., 2013).

There is a relation between the power generated by a wind turbine and the wind speed depending on the turbine characteristics, as expressed in the following (Lydia et al., 2014):

$$P(V) = \begin{cases} 0 & V < V_{ci} \; or \; V_{co} < V \\ 0.5 C_P A \rho V^3 & V_{ci} \leq V \leq V_r \\ P_r & V_r < V \leq V_{co} \end{cases} \quad (4)$$

where V_{ci} is the cut-in wind speed, V_r is the rated wind speed, and V_{co} is the cut-out wind speed which vary depending on the turbine characteristics. If the turbine characteristics are known, the turbine's power generation can be calculated. The power curve according to the characteristics of the turbine (see Table 4.1) Mosetti et al. (1994) used in their study is plotted in Figure 4.1. Also, the values in Table 4.1 would be required for wake calculations. As can be seen from Equation 4, turbine blades do not generate power even though they rotate until the wind reaches a certain speed (V_{ci}). After reaching V_{ci}, the generated power increases exponentially with the cubic power of the wind speed as the wind speed increases. However, after reaching V_r, the power generation does not increase and remains constant up to a certain speed (V_{co}). In fact, after V_{co}, the turbine shuts itself down, so the power generation is cut off in order to prevent the risk of possible rotor damage due to the high turbulence effects (Deep et al., 2020).

Table 4.1 Parameters and turbine characteristics used in (Mosetti et al., 1994)

Parameter (unit)	Value
V_{ci} (m/s)	2
V_r (m/s)	12.8
V_{co} (m/s)	18
C_P (-)	0.389
z (m)	60
C_T (-)	0.88
z_0 (m)	0.3
D (m)	40

Although in offshore the surface roughness (z_0) is much smaller than in onshore, it was taken as 0.3 in wake calculations in order to be in same conditions used by Mosetti et al. (1994) since the results would be compared to them. Also, z_0 is related to site conditions, not turbine characteristics.

According to the values in Table 4.1, the power expression (P) yields the following (Mosetti et al., 1994):

$$P = \sum_{i}^{N} 0.3V^3 \tag{5}$$

where N stands for the turbine number in the wind farm.

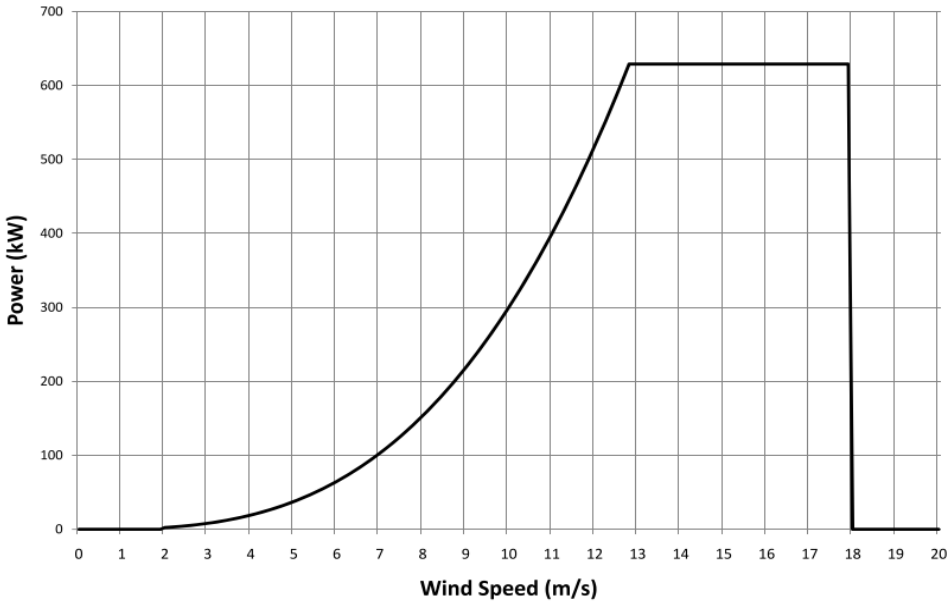

Figure 4.1 Power curve of the turbine used by Mosetti et al. (1994)

In this thesis, the power generation of a wind turbine is calculated using Equation 4. The main aim of this study is to obtain a wind farm layout maximizing the power generation capacity. Due to wake effects as explained in Section 3.1.2.6, the power generation of the whole wind farm cannot be calculated considering number of turbines and stand-alone turbines' power generation capacity. Considering wake effects for each turbine, the power generation should be calculated individually. Thus, algebraic sum of generation capacity of each turbine gives the total power generation of the layout.

4.2 Cost model

The cost of a wind farm changes depending on some parameters such as its capacity, number of turbines. Therefore, there is no fixed cost model for different wind farms (Wang et al., 2015). Mosetti's (1994) cost model has been used in most of the WFLOP studies (Herbert-Acero et al., 2014). Assuming the purchase cost of a single wind turbine as 1, Mosetti et al. (1994) stated that if many wind turbines are purchased, this cost can be reduced by a maximum of one third:

$$cost = N\left[\frac{2}{3} + \frac{1}{3}e^{-0.00174N^2}\right] \quad (6)$$

Chen (2013) developed a cost function using the real cost data of all wind farms installed in Texas, USA. However, in a comparison study (Wang et al., 2015), it was concluded that the Mosetti's cost model became more accurate as the number of turbines increases. In this thesis, Mosetti's cost model was used in calculations due to its widespread use, simplicity in application and accuracy for large turbine numbers.

4.3 Jensen's wake model

Jensen (1983) modelled the wake effects, as can be seen in Figure 4.2, resulting from the interaction of wind turbines for the first time, and the model was furtherly developed by Katic et al. (1987). Jensen formulated the wind behind a turbine upstream by expressing the conservation of momentum law for wind speed. Comparing the calculations using Jensen's wake model and actual measurements by Vermeulen (1979), it was observed that computed and experimentally measured values were very compatible with each other. The results using Jensen's wake model was also compared with the measurements from Nibe-wake project (Swift-Hook et al., 1984), and again the results were satisfactorily close to each other (see Table 4.2).

Table 4.2 Comparison of measured and calculated wind speed in the wake (Højstrup, 1983; Jensen, 1983)

Downwind distance (m)	Measured (m/s)	Computed (m/s)
40	3.95	4.35
100	5.03	5.70

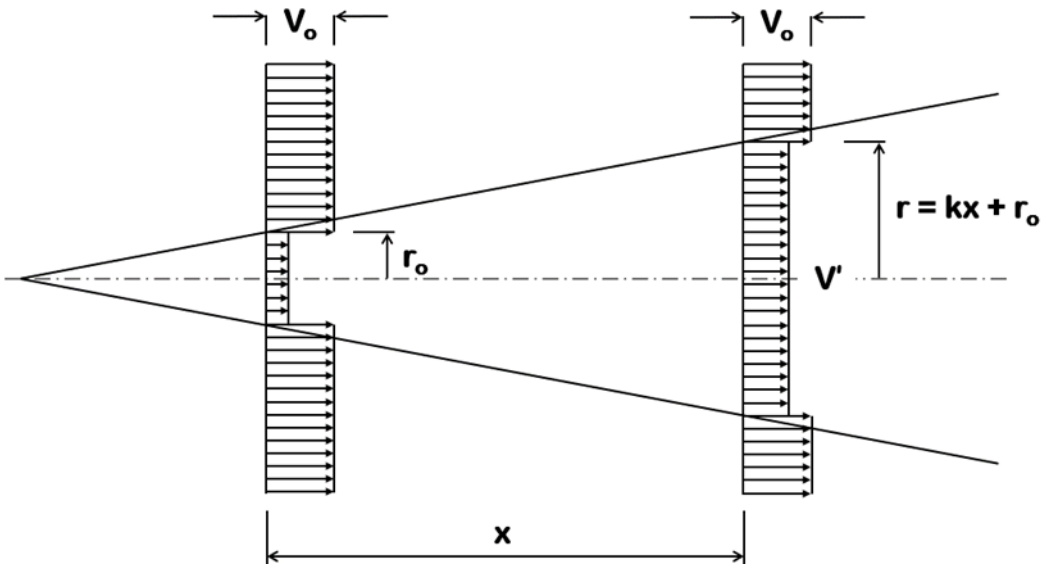

Figure 4.2 Schematic Jensen wake model for a single wind turbine, modified from (Jensen, 1983)

$$V' = V_0\left[1 - 2a\left(\frac{r_0}{r_0 + kx}\right)^2\right] \tag{7}$$

where a is the axial induction factor, x is the distance behind an upstream turbine, r_0 is the upstream turbine rotor radius, k is the entrainment/wake decay constant, V_0 is the free stream wind speed and V' is the wind speed on downstream turbine (see Figure 4.2). The axial induction factor, a, is associated with the thrust coefficient, C_T, and r is related with r_0 as can be determined from the expressions below:

$$C_T = 4a(1 - a) \tag{8}$$

$$r_0 = r\sqrt{\frac{1 - a}{1 - 2a}} \tag{9}$$

The entrainment/wake decay constant k is empirically expressed as:

$$k = \frac{0.5}{ln\left(\frac{z}{z_0}\right)} \tag{10}$$

where z is the hub height of the wind turbine and z_0 is the surface roughness of the site. All these parameters are related with the turbine, wind, and site characteristics.

The entrainment/wake decay constant k is empirically declared as 0.04 for offshore systems (Beaucage et al., 2012; Rudion, 2008) while 0.075 for onshore (Mortensen et al., 2001).

In this study, the wind is assumed to be blowing from the same direction with a constant average speed of 12 m/s in the free stream, as in (Mosetti et al., 1994).

Figure 4.3 shows wind speed along a single wind turbine following Equation 7, and it is obvious that free stream wind speed recovers later for offshore compared to onshore due to the lower entrainment constant. On the other hand, as k decreases, the wake width in the direction of the crosswind direction gets narrower (see Figure 4.4).

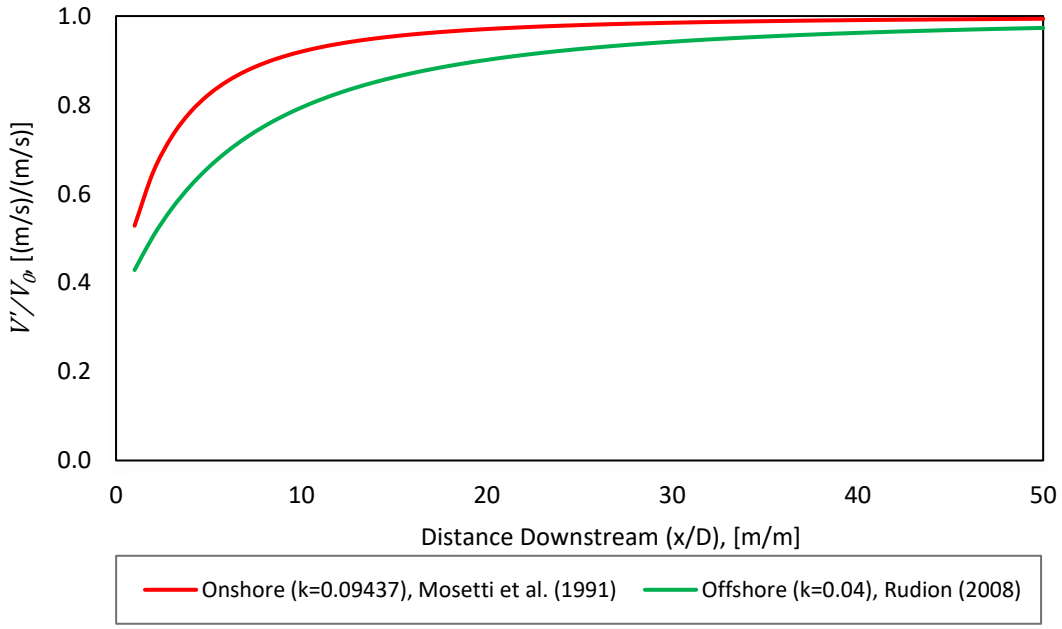

Figure 4.3 Wind speed along a single turbine wake

4.4 Turbine spacing

As described in literature review, turbines should be located at safe distance intervals in order to prevent the negative effects of turbulence created by the turbines on each other due to the wake. In discrete approach, locating the turbines into the middle of the grids ensures that the turbines cannot be located closer to each other than a safe distance. The wake width expands linearly (see Equation 7) according to Jensen's wake model used in this thesis.

Turbines should be spaced minimum as the half of the wake width in crosswind direction to be not affected from each other's wake in crosswind direction. For onshore wind farm area with the dimensions of 50Dx50D used in (Mosetti et al., 1994), the half of the wake width never expands 3D in crosswind direction so 3D is adequate for turbine spacing in crosswind direction (see Figure 4.4). On the other hand, while the same area used in Mosetti et al.'s study is considered as in offshore, the half of the wake width never expands 1.5D in crosswind direction. Moreover, the wake effect is almost disappeared after 40D downstream distance (see Figure 4.3) so the maximum wake width expansion will be smaller. Thus, 2D turbine spacing in crosswind direction is safe for constant wind direction in offshore. An example to support this, only for a hypothetical condition that the wind speed and direction remain constant, Şişbot et al. (2010) argued that the area can be divided into rectangular grid cells of 8Dx2D instead of squared grid cells for offshore, also in accordance with rule of thumb. For turbine spacing in prevailing wind direction, 4D has been widely used in the literature (see Table 2.1), it does not depend on whether the wind farm is in onshore or offshore.

As a summary of Section 4.4, in this thesis, the grid sizes of 4Dx3D for onshore and 4Dx2D for offshore provide safety in terms of preventing the negative effects of turbulence created by the turbines on each other due to the wake.

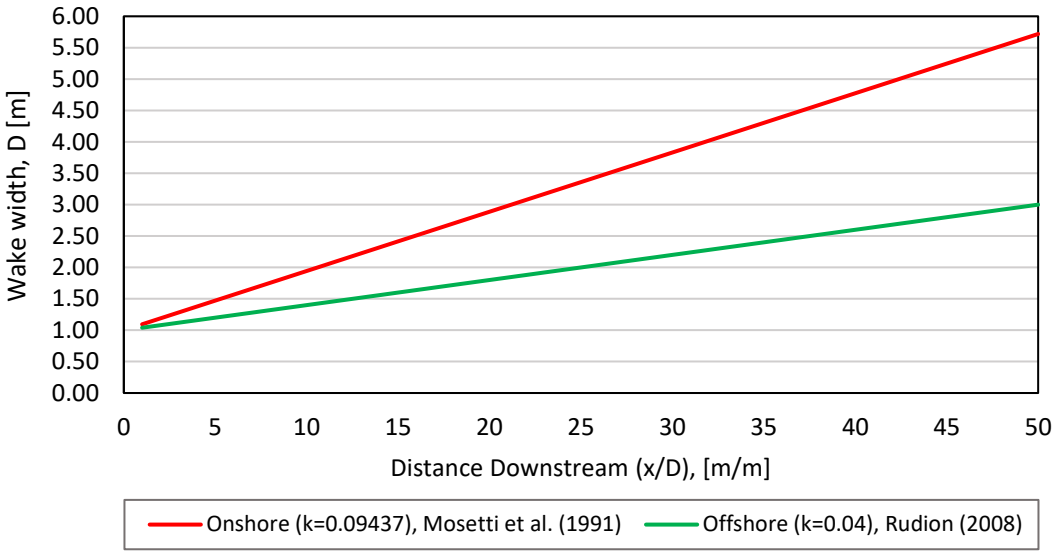

Figure 4.4 Wake width along a single wind turbine

4.5 Application of GA

The flowchart of GA used in this thesis is presented in Figure 3.1 in methodology part, and also summary of steps followed in application of GA is presented in Figure 4.5.

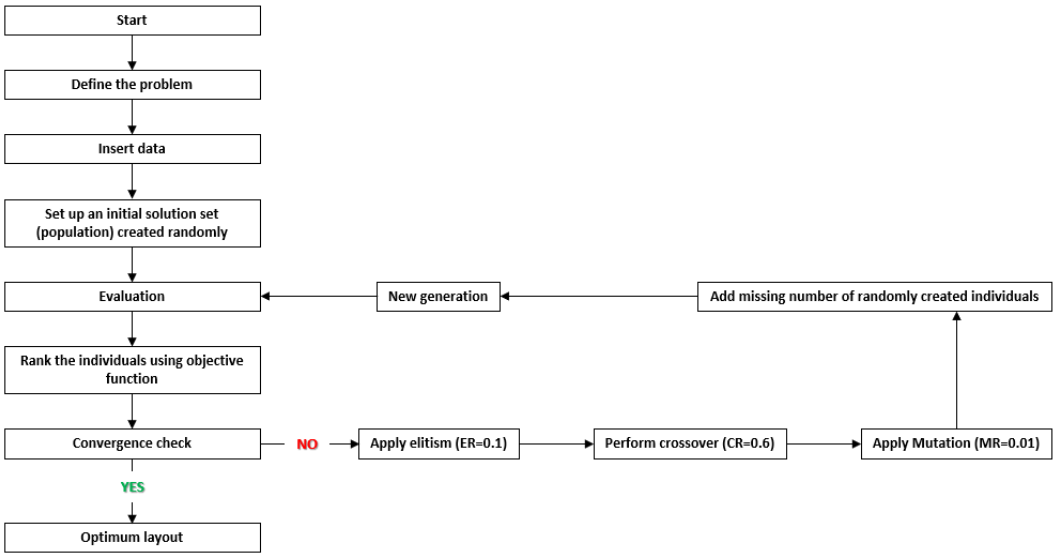

Figure 4.5 GA flowchart applied in this thesis

First in GA, the initial solution set is created using a certain number of individuals that are consisting of random numbers of 0s and 1s or certain number of 0s and 1s, for variable or fixed number of turbines respectively. For each individual, a fitness value is calculated using the objective function which is cost per unit power. Since the aim of optimization is to minimize the objective function, the individuals are ranked by their fitness values from smallest to biggest. After ranking, the upper percentage (10%), determined by ER, of the ranked solution set is transferred directly to the next generation, and the same percentage (10%) of lower is removed from the solution set. After elitism was applied, the parent solution pairs are selected randomly for crossover. Crossover is performed for the upper percentage of the ranked solution set including the transferred part in elitism. However, this time the percentage (60%) is determined by CR. The pairs of individuals (parents) mated randomly, and the resulting individuals (children) are created by crossover. After crossover, mutation is performed for resulting children. For mutation, MR determines the number of genes reversed. The resulting children after mutation are transferred to the next generation. After all operators are performed, if the next generation lacks individual, the missing number of randomly created individuals is added to the next generation so that the next generation will have the same number of individuals as the current one. This cycle is repeated for the specified number of generations. At the end of cycle, it is checked whether the solution has converged to an optimum or not. If it has converged, the process stops working; if not, it continues. Another option is to set a termination criterion, such as stop working if the efficiency is equal to or more than a certain percentage. However, in this study, no termination criterion is used in order to ensure that the optimum is reached. Rather, the process stops working if and only if the efficiency is 100%.

The parameters and operators' rates chosen for application of GA modelled for this study is presented in Table 4.3.

Table 4.3 Selected GA parameters

Parameter	Value
Individual number	1,000
Elitism Rate (ER)	0.1
Crossover Rate (CR)	0.6
Mutation Rate (MR)	0.01
Generation number	3,000

The number of individuals and generations used in this thesis were determined to be at least the same as the previous studies (Grady et al., 2005; Mosetti et al., 1994) to be compared.

Following these, the comparison of the developed models with Mosetti et al. (1994) and Grady et al. (2005), and the results of the models for application in Turkey with different grid sizes are presented and discussed in Chapter 5.

CHAPTER 5

RESULTS AND DISCUSSION

In this chapter, model (a) developed in this thesis was verified by comparing the results with previous studies (Grady et al., 2005; Mosetti et al., 1994). For this purpose, the wind farm area and the parameters such as turbine characteristics, wind conditions and grid size (5Dx5D) used by Mosetti et al. (1994) and Grady et al. (2005) were used to verify model (a). After that, the area used in verification was also optimized for a smaller grid size, 4Dx3D. The results for 4Dx3D grid size were compared to that of 5Dx5D grid size to evaluate if there is any improvement or not. Lastly, an optimum layout was suggested for a potential offshore wind farm area predetermined for Turkey by using model (a) and model (b). After all applications of model (a), model (b) was also applied to evaluate whether any improvement was obtained. All of the codes developed for model (a) and model (b) were run using a computer which has a 11^{th} Gen Intel(R) Core(TM) i5-1135G7 @ 2.40 GHz processor with 8 GB RAM.

5.1 Verification of the model

The wind farm area used in previous studies (Grady et al., 2005; Mosetti et al., 1994), 2 km x 2 km, was optimized using model (a) to obtain a layout having maximum energy at minimum cost. For this purpose, the parameters in Table 4.1 such as grid size, wind conditions, turbine characteristics and properties were used to be able to make a comparison with the previous studies. The code was run 3 times to evaluate whether model (a) is reliable in terms of giving same results and all runs showed same results. After applying model (a), model (b) was applied to the same area using same parameters for the turbine number obtained from model (a). However, no improvement was observed. That means the layout obtained from model (a) is the

optimum layout for 5Dx5D grid size. Figure 5.1 illustrates the optimum layouts for 5Dx5D grid size, both obtained in this thesis and obtained in the previous studies.

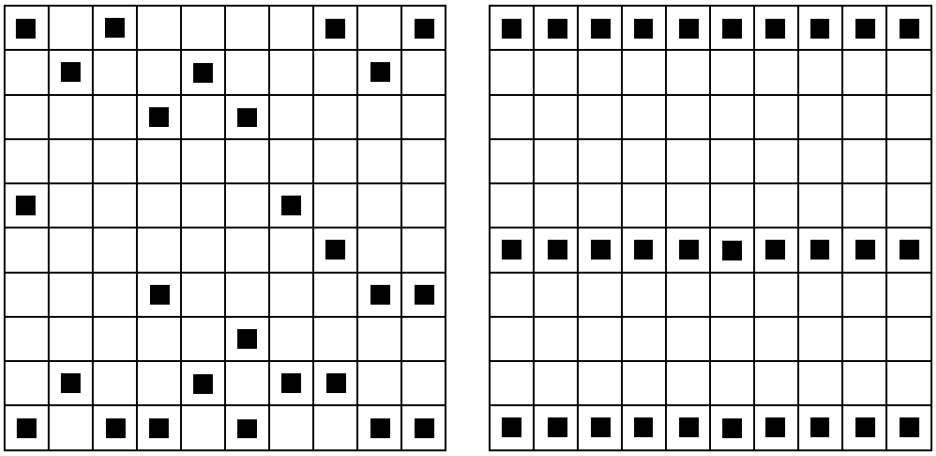

(i) (ii)

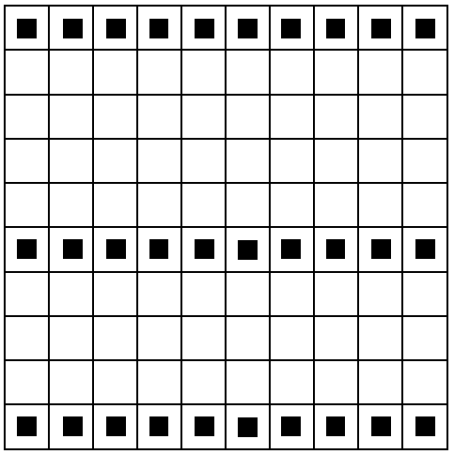

(iii)

Figure 5.1 Optimum layouts for: (i) Mosetti et al. (1994), (ii) Grady et al. (2005) and (iii) model (a) and model (b)

Table 5.1 includes the results for 5Dx5D grid size, both obtained in this thesis and obtained in the previous studies.

Table 5.1 Comparison of results for - (i) (Mosetti et al., 1994), (ii) (Grady et al., 2005), (iii) model (a) and (iv) model (b)

Parameter (unit)	(i)	(ii)	(iii)	(iv)
Fitness value (-)	0.0016197	0.0015436	0.0014824	0.0014824
Turbine number (N)	26	30	30	30
Total power (kW)	12,352	14,310	14,901	14,901
Efficiency (%)	91.645	92,015	93.336	93.336
Cost (-)	20.006	22.089	22.089	22.089
Wake loss (%)	8.355	7.985	6.664	6.664

The results of model (a) have the same number of turbines (see Table 5.1) and the same layout (see Figure 5.1) as those of Grady et al. (2005). Moreover, the fitness value of the optimum layout obtained from model (a) is lower compared to the layout obtained in (Grady et al., 2005). Therefore, as expected, efficieny is higher and wake effect is lower for model (a). In this way, it was verified that the model (a) developed for this thesis is suitable to solve WFLOP. As can be seen in Figure 5.1 and Table 5.1, optimum layout obtained by Mosetti et al. (1994) is different than the others. It is possible that the number of individuals and generations used by Mosetti et al. (1994) does not allow to converge the global optimum layout, as described in Section 2.2.

Grady et al. (2005) applied the optimization method in a different way in terms of using columns seperately. They optimized a single column and copied the layout of this column to the other columns. However, this creates an error in cost calculation since the cost of three wind turbines in a single column is not one tenth of the cost of thirty wind turbines, which is the total number of turbines in all columns. Also, Equation 3 was used to approximate $P = 0.3V^3$ in the previous studies (Grady et al., 2005; Mosetti et al., 1994). However, as Biswas et al. (2017) calculated, the actual coefficient is not 0.3 but 0.307976.

In this thesis, all columns in the wind farm were considered together, and power calculations were performed following Biswas et al. (2017) so the actual coefficient was taken as 0.307976. As can be seen in Figure 5.1, same layout obatined by Grady et al. (2005) was obtained in this study. Also, as it is clearly seen in Table 5.1, model (a) gave better results than that of Grady et al. (2005) due to the difference in application in terms of considering all colums in the wind farm together and the difference in power generation formula using actual coefficient value as 0.307976.

As can be seen from Figure 5.2, the fitness value has not been improved any more after about 900th generations. This means that the optimum layout was reached for 5Dx5D grid size. Although the optimum layout was reached at 900th generation when the execution time of running the code was approximately 13 minutes, the total execution time of running the code was approximately 40 minutes for 3,000 generations.

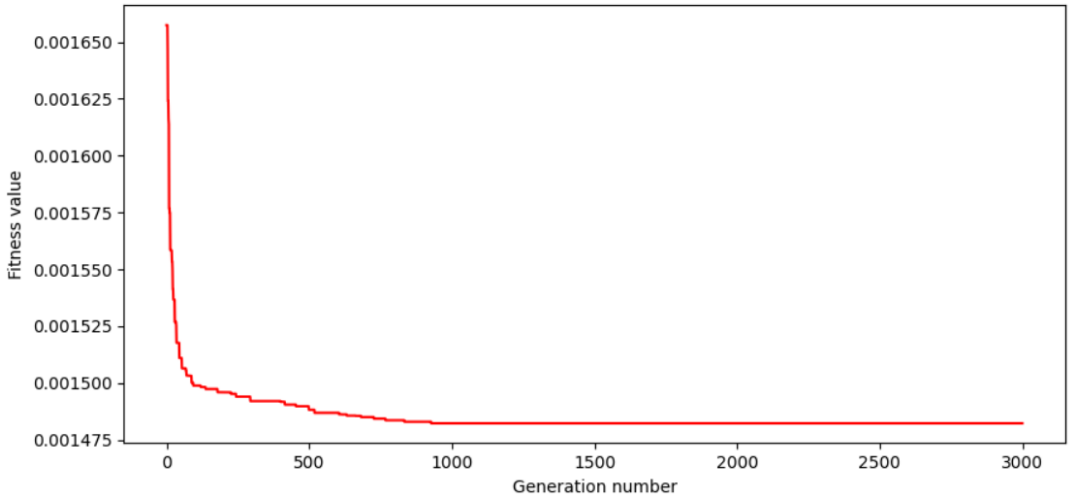

Figure 5.2 The evolution of the fitness value for model (a) using 5Dx5D grid size

5.2 4Dx3D grid size

The same area used for verification was also used for optimization using model (a) for a smaller grid size (4Dx3D) to evaluate whether the results are improved or not in terms of efficiency and fitness value. Except for grid size, all parameters such as

wind conditions, turbine characteristics were the same as those used for the 5Dx5D grid size. Similar to verification process (see Section 5.1), the code was run 3 times to evaluate whether model (a) is reliable in terms of giving same results; however, it did not show the same layout. The only difference in these layouts was the layout of the intermediate raw which is illustrated in a red box in Figure 5.3. However, this difference did not cause any other difference in fitness value, turbine number and efficiency. Because total wake in the wind farm remained the same, and the distance between the intermediate raw and the bottom row (y) was kept constant, as can be seen in Figure 5.3. After applying model (a), model (b) was applied to the same area using same parameters for the turbine number obtained from model (a). However, no improvement was observed. That means the layout obtained from model (a) is the optimum layout for 4Dx3D grid size. Figure 5.3 illustrates the optimum layouts obtained in this thesis for 5Dx5D grid size and 4Dx3D grid size.

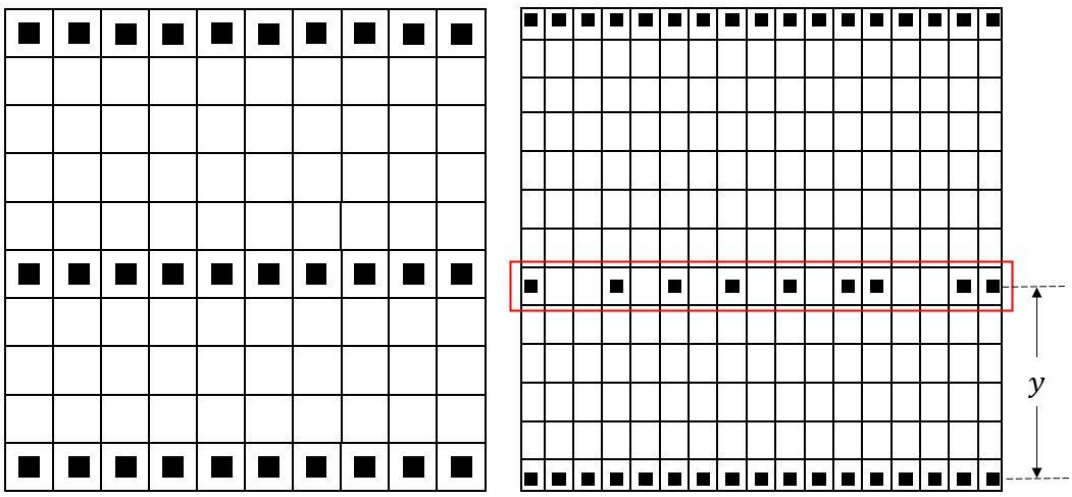

Figure 5.3 (i) Optimum layout for: (i) 5Dx5D grid size using model (a) and model (b) and (ii) 4Dx3D grid size using model (a) and model (b)

The top and bottom rows are filled with turbines, but the intermediate row is not filled for 4Dx3D grid size as shown in Figure 5.3 because placing another turbine on that row increases the fitness value. The reason for this increase in the fitness value

is that the additional cost of placing one more turbine does not compensate for the wake added to the system.

The grid cells at the edge of the area do not fit the area exactly, they overflow a little since the ratio of the edge dimensions (50D) of the wind farm area to the grid dimensions (4D and 3D) is not an integer (see Figure 5.4). Therefore, the grids on the edges of the wind farm area were trimmed to fit the area, so the grids on the edges are finer, and even the grids on the corners are even finer. Wind turbines at the edges of the wind farm area were not placed in the middle of the trimmed grid, but in the middle of the untrimmed grid. Because if they were placed in the middle of the trimmed grid, the wake effect would increase as the wind turbines would be closer to each other. This is illustrated in Figure 5.4.

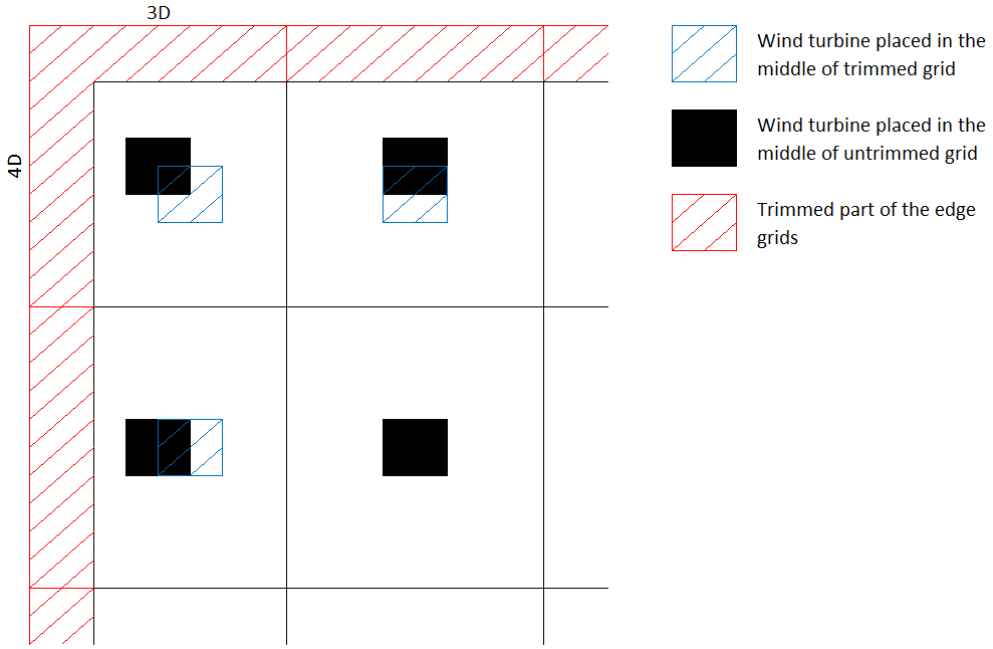

Figure 5.4 Illustration of trimmed and untrimmed grids and placement of turbines

All results obtained for 5Dx5D grid size and 4Dx3D grid size are presented in Table 5.2.

Table 5.2 Comparison of the results for: (i) 5Dx5D grid size using model (a) and model (b), (ii) 4Dx3D grid size using model (a) and (iii) 4Dx3D grid size using model (b)

Parameter (unit)	(i)	(ii)	(iii)
Fitness value (-)	0.0014824	0.0013330	0.0013330
Turbine number (N)	30	43	43
Total power (kW)	14,901	21,935	21,935
Efficiency (%)	93.336	95.857	95.857
Cost (-)	22.089	29.2409	29.2409
Wake loss (%)	6.664	4.143	4.143

As can be seen in Table 5.2, the results indicated that dividing the area into finer grids improved the solution by allowing placement of more turbines with a less fitness value. Although the number of turbines were increased for 4Dx3D grid size, wake effect was reduced, which results in an increase in efficiency. Also, moving the turbines located at the upper and bottom rows to the boundaries of the wind farm area improved the results by 0.26% reduce in wake loss.

Even if it can not be seen from Figure 5.5 due to the very small change in the fitness value, it was observed from the results that the fitness value reached the minimum value of 0.00133 at the 1,681st generation and has not been improved anymore, remained constant. That means the optimum layout was reached at the 1,681st generation. In this thesis, when the results for 4Dx3D grid size were examined, it was observed that allowing 3,000 generations is sufficient to reach the optimum layout for this problem. That might seem to indicate that allowing the generation number of 3,000 were unnecessary since the optimum layout was reached at the 1,681st generation. However, 3,000 generations may be insufficient to reach the optimum result depending on the complexity of the problem and the abundance of possible solutions. Therefore, the allowed number of generations may be increased depending on the requirements of the problem.

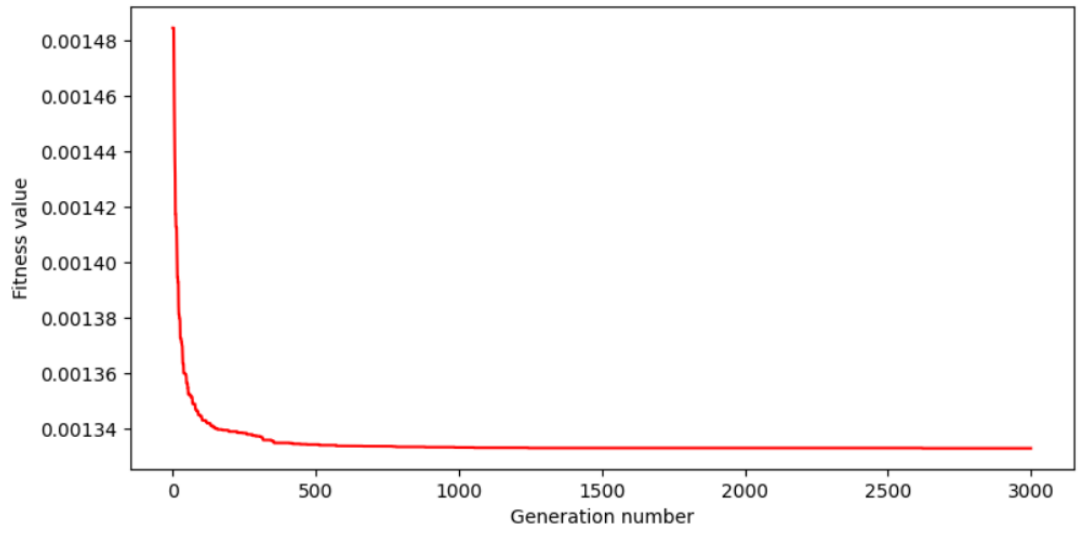

Figure 5.5 The evolution of the fitness value for model (a) using 4Dx3D grid size

Up to this point, results obtained using developed codes in this thesis were presented and discussed. Developed codes to solve WFLOP were also applied for a potential site in Turkey, and the results of the case study are presented in the following.

5.3 A case study: Investigation of optimum layout for a potential offshore wind farm in Turkey

Considering high wind potential, the region of Bozcaada coast has been technically found suitable for offshore wind farm deployment. Yıldız (2021) selected five areas for offshore wind farm installations (see Figure 5.6), the boundaries of which were determined by considering territorial waters, military areas, port existance, shipping routes, shipwrecks, seismic activities, bird migration routes, visual impacts, pipelines and so on.

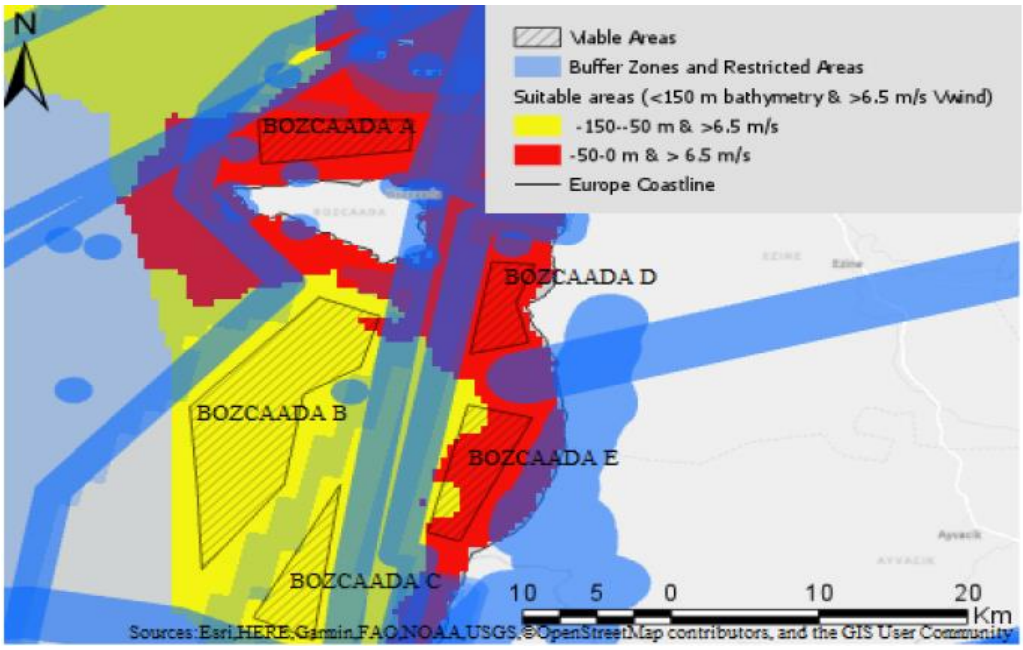

Figure 5.6 Buffer zones and restricted areas for Bozcaada and selected potential wind farm areas (Yıldız, 2021)

In this thesis, the models were constructed for rectangular and square-shaped areas. Therefore, only two of the selected areas, Bozcaada A and Bozcaada E, may be suitable for this thesis in terms of area shape. However, Yıldız (2021) stated that except for Bozcaada A, all areas selected in Bozcaada are located in military protection zone. Morevoer, as can be seen in Figure 5.7, Bozcaada A area is very suitable to install offshore wind turbines using bottom-fixed support structures considering the water depth (0-50 m).

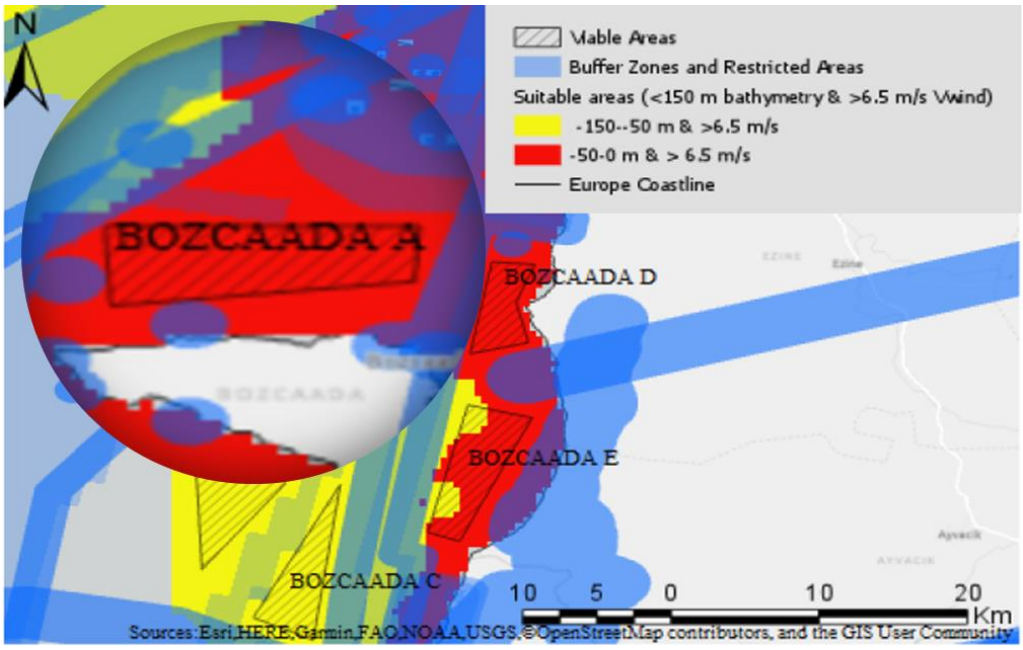

Figure 5.7 Bozcaada A, modified from (Yıldız, 2021)

Since the hypothetical nature of the area allows, its shape is converged to a rectangle in order to be applicable in this thesis (see Figure 5.8).

The area predetermined for a potential offshore wind farm installation was firstly optimized using model (a) to determine the feasible number of wind turbine for this area. Then, model (b) was used to improve the results obtained from model (a). However, the layout and the results remained same. 4Dx2D grid size, which is appropriate as mentioned in Section 4.4, was used for this offshore wind farm area. The properties of the Bozcaada A area such as wind conditions and dimensions are given in Table 5.3.

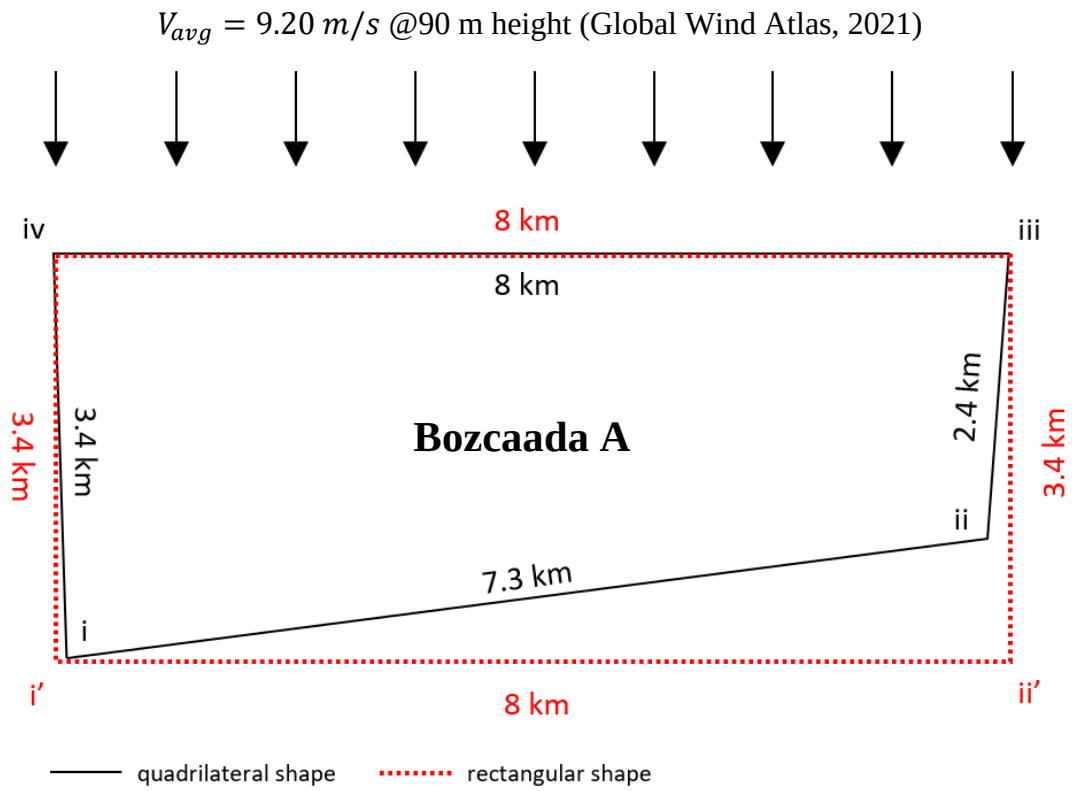

Figure 5.8 Original (quadrilateral) and converged (rectangular) shape of selected wind farm area

Table 5.3 The properties of Bozcaada A (Global Wind Atlas, 2021; Yıldız, 2021)

Parameter (unit)	Value
width (km)	3.40
length (km)	8.00
k for offshore (-)	0.04
V_{avg} (m/s)	~9.20
Wind direction (-)	30° NE

The average wind speed (V_{avg}) at hub height should be taken into account in power calculations. Therefore, the average wind speed at 90 m was calculated for both the original area and the converged area using linear interpolation relative to the average

speeds at 50 m height (Figure 5.9 and Figure 5.11) and at 100 m height (Figure 5.10 and Figure 5.12). The average wind speed at 90 m height is same for both original and converged area. Therefore, slightly expanding the original area to converge its shape to a rectangle does not cause any error in power generation calculations.

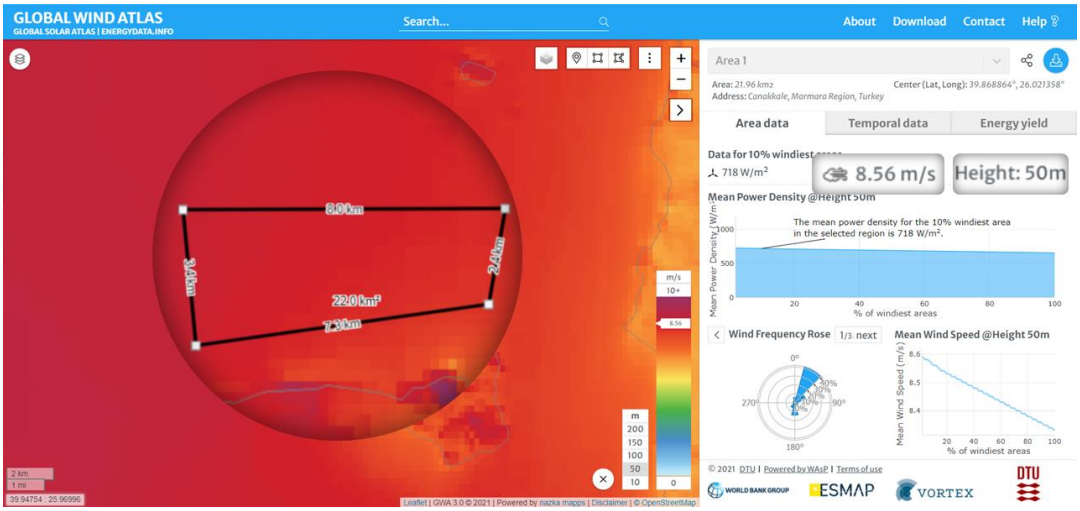

Figure 5.9 Average wind speed at 50 m height for the original area (Global Wind Atlas, 2021)

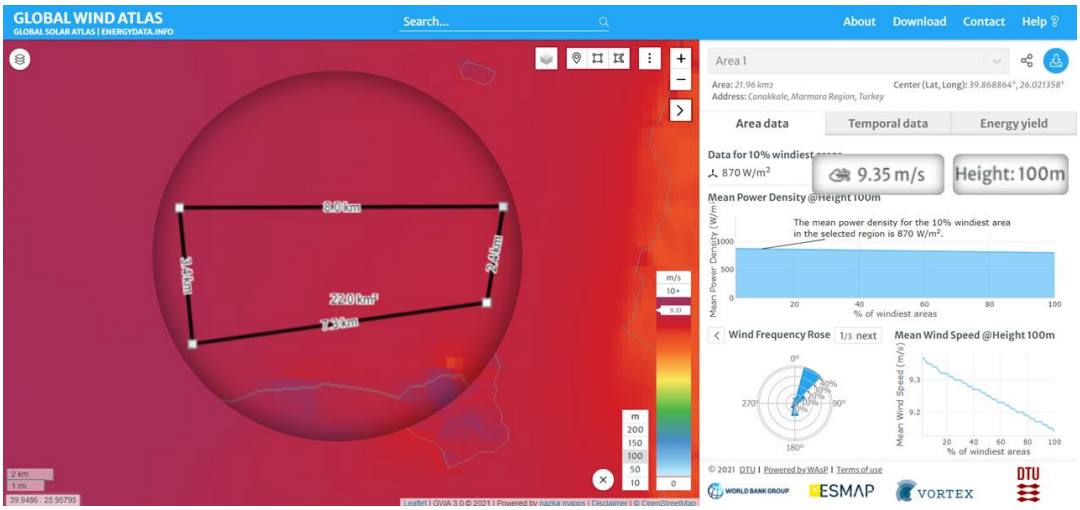

Figure 5.10 Average wind speed at 100 m height for the original area (Global Wind Atlas, 2021)

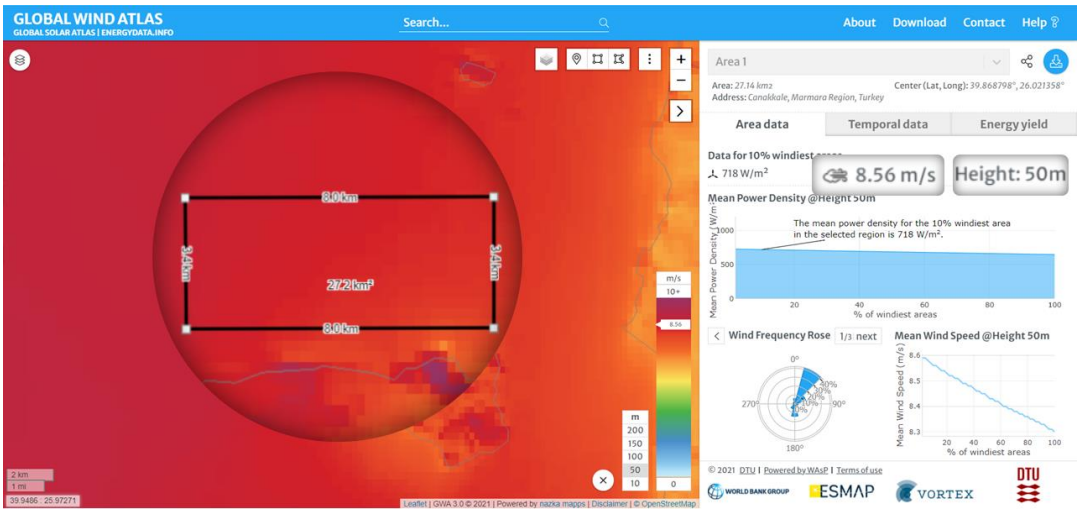

Figure 5.11 Average wind speed at 50 m height for the converged area (Global Wind Atlas, 2021)

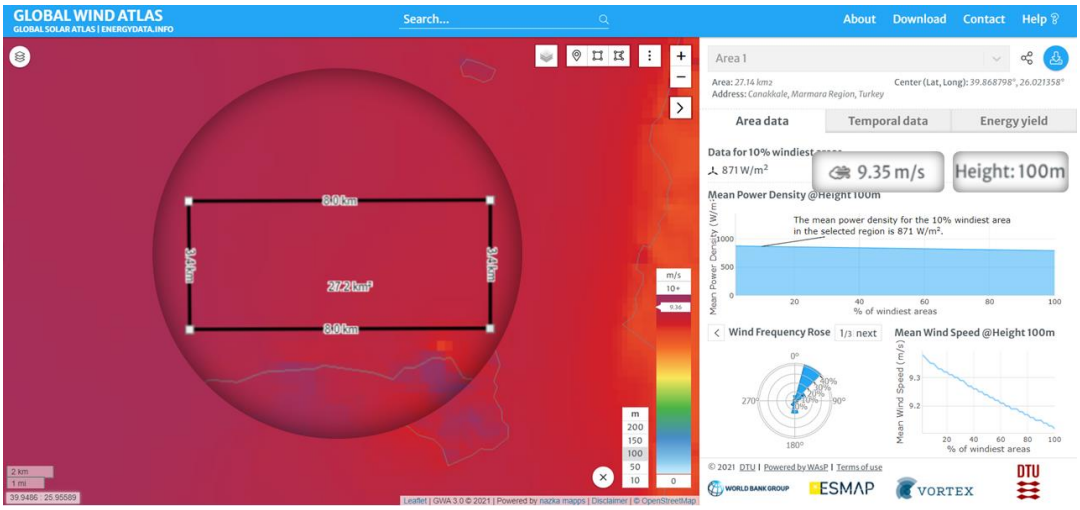

Figure 5.12 Average wind speed at 100 m height for the converged area (Global Wind Atlas, 2021)

C_P and C_T vary depending on wind speed; however, they are assumed to be constant, and V_r (11.4 m/s) for C_P and V_{avg} (9.2 m/s) for C_T has been taken into consideration by using the technical report of NREL 5-MW (Jonkman et al., 2009). The turbine characteristics of NREL 5-MW is given in Table 5.4.

Table 5.4 Parameters and turbine characteristics of NREL 5-MW (Jonkman et al., 2009)

Parameter (unit)	Value
V_{ci} (m/s)	5.00
V_r (m/s)	11.40
V_{co} (m/s)	25.00
C_P for V_r (-)	0.442
z (m)	90.00
C_T for V_{avg} (-)	0.65
D (m)	126.00

For the selected area in Turkey, optimum turbine number was obtained applying model (a) using NREL 5-MW turbines. For 4Dx2D grid size, 45 was found as optimum turbine number for this area. The same area was optimized using model (a) for 2Dx2D and 1Dx2D grid sizes to evaluate whether the optimum turbine number changes or not. 46 was found as optimum turbine number for both 2Dx2D and 1Dx2D, so these smaller grid sizes allow only locating one more turbine. For these grid sizes, model (b) was also applied after application of model (a), but no improvement was observed. The results for these three grid sizes are given in Table 5.5.

Table 5.5 The results of different grid sizes: (i) 4Dx2D, (ii) 2Dx2D and (iii) 1Dx2D

Parameter (unit)	(i)	(ii)	(iii)
Fitness value (-)	0.0002678	0.0002669	0.0002669
N (-)	45	46	46
Total power (MW)	113.6	116.4	116.4
Efficiency (%)	96.04	96.24	96.24
Cost (-)	30.442	31.052	31.052
Wake loss (%)	3.96	3.76	3.76

The optimum layouts for these three grid sizes are shown in Figure 5.13. For each case, the turbines are located in the first row until it is full of turbines, then the rest of the turbines are located randomly to the grids in the last raw. The only difference among these layouts using different grid sizes is the turbine number. Both 2D and 1D grid size in prevailing wind direction allow 46 turbines while 4D grid size in prevailing wind direction allows 45. Thus, the results of 4Dx2D size were improved a little for 2Dx2D and 1Dx2D grid sizes.

All results obtained using different grid sizes in this chapter showed that using finer grids allow locating same or a greater number of turbines for the same area. This means that as the grid size gets smaller, the probability of obtaining a more optimal layout for the same area increases. However, the minimum spacing distance between turbines should be ensured for 4D in prevailing wind direction and 2D in crosswind direction.

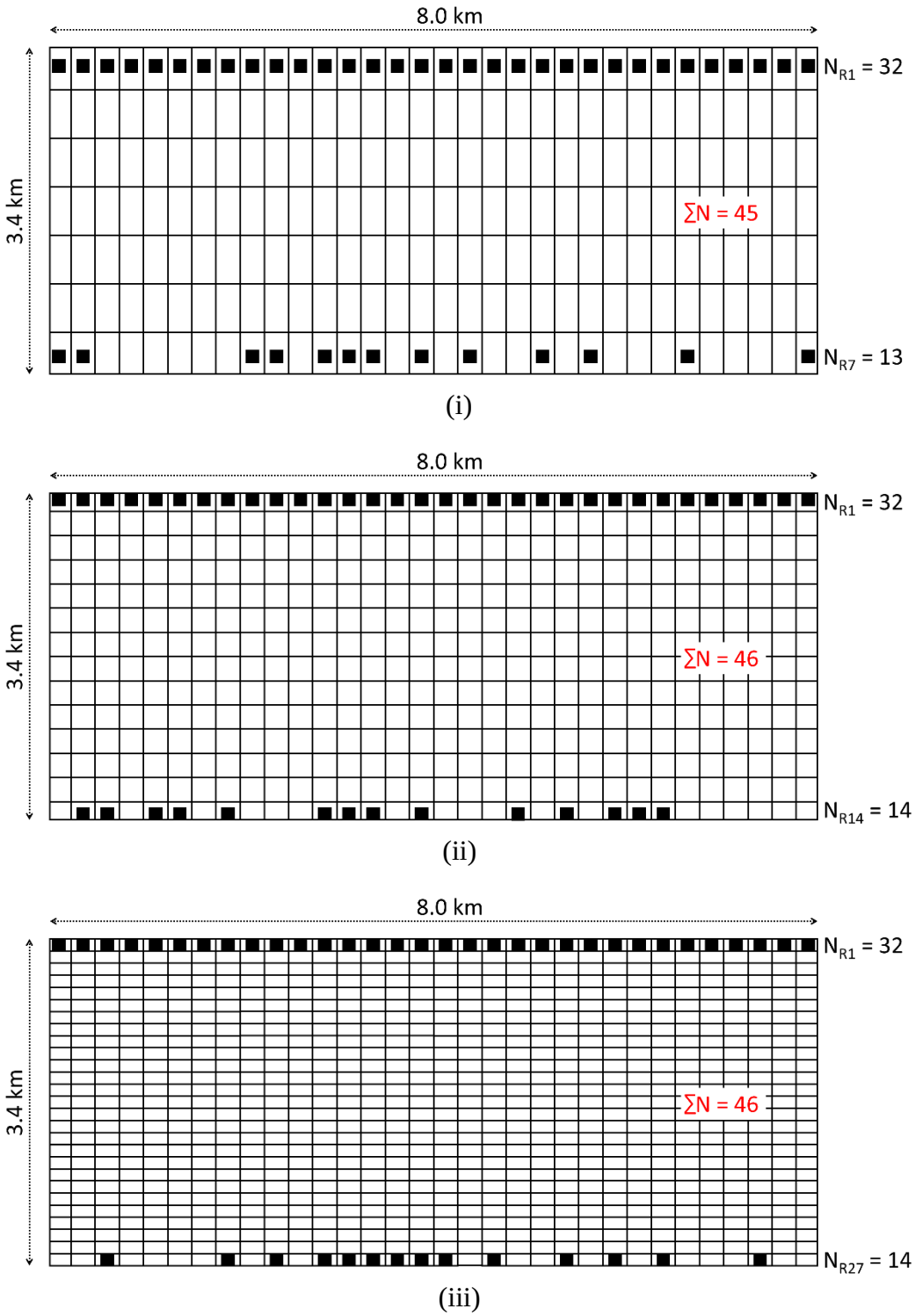

Figure 5.13 The optimum layouts using different grid sizes: (i) 4Dx2D, (ii) 2Dx2D and (iii) 1Dx2D

5.4 Comparison of different grid sizes

After obtaining all the results for grid sizes of 4Dx2D, 2Dx2D and 1Dx2D, the generation number in which the optimum solution was reached, are presented in Table 5.6. The results showed that as the number of grids increases, the number of generations in which the optimum solution is reached also increases. It can be said that the number of generations increases in proportional to the square of the grid number for those cases, but it will not be realistic to make such a definite inference by comparing only three cases. Similarly, the computation time also increased with the increasing grid number. It can definitely be said that the computation time increases in proportional to the grid number.

Table 5.6 Comparison of different grid sizes

Grid size	Number of grids	N	Computation time	Generation number
4Dx2D	224	45	~30 min	172nd
2Dx2D	448	46	~55 min	532nd
1Dx2D	964	46	~100 min	2,121st

If a grid size is shorter than minimum spacing distance between two turbines was used in the prevailing wind direction, it should be checked whether there is at least minimum spacing distance between turbines in the prevailing wind direction. For layouts obtained for 2Dx2D and 1Dx2D grid sizes, the minimum spacing distance in prevailing wind direction condition is provided as can be seen in Figure 5.13. Following these, conclusion of this thesis is presented.

CHAPTER 6

CONCLUSION

In this thesis, two models were developed using GA to solve WFLOP for: (a) variable turbine number and (b) fixed turbine number. Jensen wake model and Mosetti's cost model were used to calculate the wake of a wind farm and the cost of a wind farm respectively. Computational domain was considered using discrete approach. Model (a) aims to obtain a wind farm layout generating maximum energy at minimum cost. Model (b) aims to obtain a wind farm layout generating maximum energy for a fixed number of turbines, thus fixed cost. Also, model (b) aims to improve the results obtained from model (a). Two codes were developed using Python programming language to perform model (a) and model (b). Two codes were required since there are differences in application of crossover and mutation operators of GA for variable and fixed turbine numbers. In this thesis, a population consisting of 1,000 individuals was allowed to evolve over 3,000 generations, which was determined to reach optimum layout.

This thesis mainly focuses on investigating the performance of different grid sizes. For this purpose, model (a) was verified using 5Dx5D grid size by comparing the results with those of Mosetti et al. (1994) and Grady et al. (2005). Then, model (a) was applied to the same area used in previous studies using same parameters for 4Dx3D grid size. Using 4Dx3D grid size improved the results of model (a) using 5Dx5D, by decreasing the wake loss by 2.5% and increasing the efficiency of the wind farm by 2.5%.

Another aim of this thesis was to propose a preliminary wind farm layout for a region in Turkey having high offshore wind potential. For this purpose, model (a) was applied to an offshore wind farm area in Bozcaada which is the most suitable for this thesis. Three grid sizes were used: (i) 4Dx2D, (ii) 2Dx2D and (iii) 1Dx2D. It was

observed that (ii) and (iii) give the same results, but slightly improve the results of (i). Throughout this thesis, model (b) was also applied after each application of model (a). However, no improvement was observed in this thesis.

The main contribution of this study is to develop a code which helps to obtain better results using smaller grid sizes than that of Grady et al. (2005) who improved the results of the benchmark study (Mosetti et al., 1994). Considering the recent strategic cooperations between Turkey and the leading European countries in offshore industry (Germany, Denmark and the UK), Turkey may have the first offshore wind farm in near future. Therefore, it is critical to be able to carry out preliminary analysis for a potential offshore wind farm area in Turkey. The novelty of this work is to propose a preliminary layout for an offshore wind farm area in Turkey by applying the codes developed in this thesis.

In conclusion, acquired contributions and inferences of this thesis can be summarized as follows:

- Two accurate models were developed for both variable and fixed turbine numbers.
- The grid size used in discrete approach can be adapted depending on the wind conditions such as wind directions and related parameters.
- The grid sizes in prevailing wind direction and crosswind direction should be considered separately due to varying continuity of the wake which depends on the wind direction.
- Consideration of a smaller grid size may improve the results in terms of higher energy with higher efficiency, lower wake effect, etc.
- The generation number that is required to reach optimum layout is proportional to the number of grids which depends on the grid size.

In this thesis, wind speed and wind direction were assumed constant for simplification of WFLOP due to the limited time in MSc study. Moreover, the

developed models are only able to optimize the rectangular-shaped wind farm areas. However, the wind farm area might not always be in regular shape, and the wind direction is variable in real environment. Also, in this study, only the purchase cost of the turbine was considered for cost calculations. Following issues should be further investigated in future studies:

- A more detailed study should be carried out to obtain more comprehensive optimization models by considering the costs of construction, maintenance and repair, operation, support structure, cable, etc.
- A more specific solution can be obtained by adding constraints such as limited purchase budget and limited cable length.
- Using different types of wind turbines with different hub heights might be an alternative option to reduce wake effects.
- The operators of GA may be modified to reach the optimum result faster by eliminating unfeasible solutions.

LIST OF REFERENCES

Abdulrahman, M., & Wood, D. (2017). Investigating the Power-COE trade-off for wind farm layout optimization considering commercial turbine selection and hub height variation. *Renewable Energy*, *102*, 267–278. https://doi.org/10.1016/j.renene.2016.10.038

AFAD Online Earthquake Catalog. (2021). *AFAD Online Earthquake Catalog*. R.T. Ministry of Interıor, Disaster and Management Presidency, Department of Earthquake, Turkish Accelerometric Database and Analysis System. https://deprem.afad.gov.tr/ddakatalogu

Ammara, I., Leclerc, C., & Masson, C. (2002). A viscous three-dimensional differential/actuator-disk method for the aerodynamic analysis of wind farms. *Journal of Solar Energy Engineering, Transactions of the ASME*, *124*(4), 345–356. https://doi.org/10.1115/1.1510870

Archer, C. L., Vasel-Be-Hagh, A., Yan, C., Wu, S., Pan, Y., Brodie, J. F., & Maguire, A. E. (2018). Review and evaluation of wake loss models for wind energy applications. *Applied Energy*, *226*(February 2018), 1187–1207. https://doi.org/10.1016/j.apenergy.2018.05.085

Argin, M., Yerci, V., Erdogan, N., Kucuksari, S., & Cali, U. (2019). Exploring the offshore wind energy potential of Turkey based on multi-criteria site selection. *Energy Strategy Reviews*, *23*, 33–46. https://doi.org/10.1016/j.esr.2018.12.005

Bansal, R. C., Bhatti, T. S., & Kothari, D. P. (2002). On some of the design aspects of wind energy conversion systems. *Energy Conversion and Management*, *43*(16), 2175–2187. https://doi.org/10.1016/S0196-8904(01)00166-2

Barthelmie, R. J. (1998). A Brief Review of Offshore Wind Energy Activity in the 1990s. *Wind Engineering*, *22*(6), 265–273.

Beaucage, P., Brower, M., Robinson, N., & Alonge, C. (2012). Overview of six commercial and research wake models for large offshore wind farms. *European Wind Energy Conference and Exhibition 2012, EWEC 2012*, *1*, 213–222.

Betz, A. (1920). Das Maximum der theoretisch möglichen Ausnutzung des Windes durch Windmotoren. *Zeitschrift Fur Das Gesamte Turbinenwesten*.

Bilgili, M., Yasar, A., & Simsek, E. (2011). Offshore wind power development in Europe and its comparison with onshore counterpart. *Renewable and Sustainable Energy Reviews*, *15*(2), 905–915. https://doi.org/10.1016/j.rser.2010.11.006

Bingöl, F. (n.d.). *Ege Denizi Rüzgar Atlası ve Deniz Üstü Rüzgar Ölçümleri*.

Biswas, P. P., Suganthan, P. N., & Amaratunga, G. A. J. (2017). Optimization of wind turbine rotor diameters and hub heights in a windfarm using differential evolution algorithm. In *Advances in Intelligent Systems and Computing* (Vol. 547, Issue April, pp. 131–141). https://doi.org/10.1007/978-981-10-3325-4_13

Bölük, G. (2013). Renewable energy: Policy issues and economic implications in Turkey. *International Journal of Energy Economics and Policy*, *3*(2), 153–167.

Breton, S., & Moe, G. (2009). Status, plans and technologies for offshore wind turbines in Europe and North America. *Renewable Energy*, *34*(3), 646–654. https://doi.org/10.1016/j.renene.2008.05.040

Brogna, R., Feng, J., Sørensen, J. N., Shen, W. Z., & Porté-Agel, F. (2020). A new wake model and comparison of eight algorithms for layout optimization of wind farms in complex terrain. *Applied Energy*, *259*(November 2019), 114189. https://doi.org/10.1016/j.apenergy.2019.114189

Byrne, B. W., McAdam, R., Burd, H. J., Houlsby, G. T., Martin, C. M., Zdravković, L., Taborda, D. M. G., Potts, D. M., Jardine, R. J., Sideri, M., Schroeder, F. C., Gavin, K., Doherty, P., Igoe, D., Wood, A. M., Kallehave, D., & Skov Gretlund, J. (2015). New design methods for large diameter piles under lateral loading for offshore wind applications. *3rd International Symposium on Frontiers in Offshore Geotechnics (ISFOG 2015), Oslo, Norway*, 10–12. https://doi.org/10.1201/b18442-96

Carrillo, C., Obando Montaño, A. F., Cidrás, J., & Díaz-Dorado, E. (2013). Review of power curve modelling for windturbines. *Renewable and Sustainable Energy Reviews*, *21*, 572–581. https://doi.org/10.1016/j.rser.2013.01.012

Castro Mora, J., Calero Barón, J. M., Riquelme Santos, J. M., & Burgos Payán, M. (2007). An evolutive algorithm for wind farm optimal design. *Neurocomputing*, *70*(16–18), 2651–2658. https://doi.org/10.1016/j.neucom.2006.05.017

Chen, J. (2011). Development of offshore wind power in China. *Renewable and Sustainable Energy Reviews*, *15*(9), 5013–5020. https://doi.org/10.1016/j.rser.2011.07.053

Chen, K., Song, M. X., & Zhang, X. (2013). The investigation of tower height matching optimization for wind turbine positioning in the wind farm. *Journal of Wind Engineering and Industrial Aerodynamics*, *114*, 83–95. https://doi.org/10.1016/j.jweia.2012.12.010

Chen, L., & MacDonald, E. (2012). Considering landowner participation in wind farm layout optimization. *Journal of Mechanical Design, Transactions of the ASME*, *134*(8), 4–9. https://doi.org/10.1115/1.4006999

Chen, Y. (2013). *Commercial wind farm layout design and optimization* [Texas A&M University-Kingsville]. https://search.proquest.com/openview/2c59415b7826790123149f70ba0d9efc/1?pq-origsite=gscholar&cbl=18750

Chen, Y., Li, H., Jin, K., & Song, Q. (2013). Wind farm layout optimization using genetic algorithm with different hub height wind turbines. *Energy Conversion and Management*, *70*, 56–65. https://doi.org/10.1016/j.enconman.2013.02.007

Chowdhury, S., Zhang, J., Messac, A., & Castillo, L. (2012). Unrestricted wind farm layout optimization (UWFLO): Investigating key factors influencing the maximum power generation. *Renewable Energy*, *38*(1), 16–30. https://doi.org/10.1016/j.renene.2011.06.033

Chowdhury, S., Zhang, J., Messac, A., & Castillo, L. (2013). Optimizing the arrangement and the selection of turbines for wind farms subject to varying wind conditions. *Renewable Energy*, *52*, 273–282. https://doi.org/10.1016/j.renene.2012.10.017

Couto, T. G. do, Farias, B., Diniz, A. C. G. C., & Morais, M. V. G. De. (2013). Optimization of Wind Farm Layout Using Genetic Algorithm. *10th World Congress on Structural and Multidisciplinary Optimization*, 1–10.

Da, Z., Xiliang, Z., Jiankun, H., & Qimin, C. (2011). Offshore wind energy development in China : Current status and future perspective. *Renewable and Sustainable Energy Reviews*, *15*(9), 4673–4684. https://doi.org/10.1016/j.rser.2011.07.084

De Risi, R., Bhattacharya, S., & Goda, K. (2018). Seismic performance assessment of monopile-supported offshore wind turbines using unscaled natural earthquake records. *Soil Dynamics and Earthquake Engineering*, *109*, 154–172. https://doi.org/10.1016/j.soildyn.2018.03.015

Deb, K., Pratap, A., Agarwal, S., & Meyarivan, T. (2002). A fast and elitist multiobjective genetic algorithm: NSGA-II. *IEEE Transactions on Evolutionary Computation*, *6*(2), 182–197. https://doi.org/10.1109/4235.996017

deCastro, M., Salvador, S., Gómez-Gesteira, M., Costoya, X., Carvalho, D., Sanz-Larruga, F. J., & Gimeno, L. (2019). Europe, China and the United States: Three different approaches to the development of offshore wind energy. *Renewable and Sustainable Energy Reviews*, *109*(November 2018), 55–70. https://doi.org/10.1016/j.rser.2019.04.025

Deep, S., Sarkar, A., Ghawat, M., & Rajak, M. K. (2020). Estimation of the wind energy potential for coastal locations in India using the Weibull model. *Renewable Energy*, *161*, 319–339. https://doi.org/10.1016/j.renene.2020.07.054

Du Pont, B. L., & Cagan, J. (2012). An extended pattern search approach to wind farm layout optimization. *Journal of Mechanical Design, Transactions of the ASME*, *134*(8), 1–18. https://doi.org/10.1115/1.4006997

Duan, B., Wang, J., & Gu, H. (2014). Modified genetic algorithm for layout optimization of multi-type wind turbines. *Proceedings of the American Control Conference*, 3633–3638. https://doi.org/10.1109/ACC.2014.6859416

DuPont, B., Cagan, J., & Moriarty, P. (2016). An advanced modeling system for optimization of wind farm layout and wind turbine sizing using a multi-level extended pattern search algorithm. *Energy*, *106*, 802–814. https://doi.org/10.1016/j.energy.2015.12.033

Elkinton, C. N., Manwell, J. F., & Mcgowan, J. G. (2008). Algorithms for offshore wind farm layout optimization. *Wind Engineering*, *32*(1), 67–83.

Emami, A., & Noghreh, P. (2010). New approach on optimization in placement of wind turbines within wind farm by genetic algorithms. *Renewable Energy*, *35*(7), 1559–1564. https://doi.org/10.1016/j.renene.2009.11.026

Eroğlu, Y., & Ulusam Seçkiner, S. (2012). Design of wind farm layout using ant colony algorithm. *Renewable Energy*, *44*, 53–62. https://doi.org/10.1016/j.renene.2011.12.013

Eroğlu, Y., & Ulusam Seçkiner, S. (2013). Wind farm layout optimization using particle filtering approach. *Renewable Energy*, *58*, 95–107. https://doi.org/10.1016/j.renene.2013.02.019

European Environment Agency (EEA). (2009). *Europe's onshore and offshore wind energy potential an assessment of environmental and economic constraints*.

Fagerfjäll, P. (2010). *Optimizing wind farm layout – more bang for the buck using mixed integer linear programming* [Chalmers University of Technology & Gothenburg University]. http://www.math.chalmers.se/Math/Research/Optimization/reports/masters/Fagerfjall-final.pdf

Falkner R. (2016). The Paris Agreement and the new logic of international climate politics. *International Affairs*, *92*(5), 1107–1125.

Feng, J., & Shen, W. Z. (2015). Solving the wind farm layout optimization problem using random search algorithm. *Renewable Energy*, *78*, 182–192. https://doi.org/10.1016/j.renene.2015.01.005

Feng, J., & Shen, W. Z. (2017). Design optimization of offshore wind farms with multiple types of wind turbines. *Applied Energy*, *205*(September), 1283–1297. https://doi.org/10.1016/j.apenergy.2017.08.107

Feng, Y., Tavner, P. J., & Long, H. (2010). Early experiences with UK round 1 offshore wind farms. *Proceedings of Institution of Civil Engineers: Energy*, *163*(4), 167–181. https://doi.org/10.1680/ener.2010.163.4.167

Gao, X., Yang, H., & Lu, L. (2014). Investigation into the optimal wind turbine layout patterns for a Hong Kong offshore wind farm. *Energy*, *73*, 430–442. https://doi.org/10.1016/j.energy.2014.06.033

Global Wind Atlas. (2021). *Wind Map*. https://globalwindatlas.info/

Goldberg, M., Sinclair, K., & Milligan, M. (2004). Job and Economic Development Impact (JEDI) Model: A User-Friendly Tool to Calculate Economic Impacts from Electricity Projects. In *National Renewable Energy Laboratory (NREL)*.

Gonzalez, J. S., Payan, M. B., & Santos, J. R. (2013). A new and efficient method for optimal design of large offshore wind power plants. *IEEE Transactions on Power Systems*, *28*(3), 3075–3084. https://doi.org/10.1109/TPWRS.2013.2251014

Google Earth. (2022). *Google Earth*. https://earth.google.com/web/data=Mj8KPQo7CiExTndFMjJOcU56c2JUM1c5SjV0U3hsempueU1ZVDVTSEgSFgoUMDQzOTE5NjU3NDFGODQ2RjEzOUI

GOV.UK. (2021). *Contracts for Difference*. https://www.gov.uk/government/publications/contracts-for-difference/contract-for-difference

GOV.UK. (2022). *Department of Trade and Industry*. https://www.gov.uk/government/organisations/department-of-trade-and-industry

Grady, S. A., Hussaini, M. Y., & Abdullah, M. M. (2005). Placement of wind turbines using genetic algorithms. *Renewable Energy*, *30*(2), 259–270. https://doi.org/10.1016/j.renene.2004.05.007

Gualtieri, G. (2019). A novel method for wind farm layout optimization based on wind turbine selection. *Energy Conversion and Management*, *193*(April), 106–123. https://doi.org/10.1016/j.enconman.2019.04.059

Hattam, C., Hooper, T., & Papathanasopoulou, E. (2017). A well-being framework for impact evaluation: The case of the UK offshore wind industry. *Marine Policy*, *78*(January), 122–131. https://doi.org/10.1016/j.marpol.2016.10.024

Henderson, A. R., Morgan, C., Smith, B., Sørensen, H. C., Barthelmie, R. J., & Boesmans, B. (2003). Offshore Wind Energy in Europe - A Review of the State-of-the-Art. *Wind Energy*, *6*(1), 35–52. https://doi.org/10.1002/we.82

Herbert-Acero, J.-F., Franco-Acevedo, J.-R., Valenzuela-Rendón, M., & Probst-Oleszewski, O. (2009). *Linear Wind Farm Layout Optimization through Computational Intelligence*. 692–703. https://doi.org/10.1007/978-3-642-05258-3_61

Herbert-Acero, J. F., Probst, O., Réthoré, P. E., Larsen, G. C., & Castillo-Villar, K. K. (2014). A review of methodological approaches for the design and optimization of wind farms. *Energies*, *7*(11), 6930–7016. https://doi.org/10.3390/en7116930

Hevia-Koch, P., & Klinge Jacobsen, H. (2019). Comparing offshore and onshore wind development considering acceptance costs. *Energy Policy*, *125*(October 2018), 9–19. https://doi.org/10.1016/j.enpol.2018.10.019

Higgins, P., & Foley, A. (2014). The evolution of offshore wind power in the United Kingdom. *Renewable and Sustainable Energy Reviews*, *37*, 599–612. https://doi.org/10.1016/j.rser.2014.05.058

Higgins, P., & Foley, A. M. (2013). Review of Offshore Wind Power Development in the United Kingdom. *2013 12th International Conference on Environment and Electrical Engineering*, 589–593. https://doi.org/10.1109/EEEIC.2013.6549584

Hinçal, O., Altan-Sakarya, A. B., & Ger, A. M. (2011). Optimization of Multireservoir Systems by Genetic Algorithm. *Water Resources Management*, *25*(5), 1465–1487. https://doi.org/10.1007/s11269-010-9755-0

Hines, E. M., & White, W. H. (2014). Offshore wind in the Northeast. *Structures Congress 2014 - Proceedings of the 2014 Structures Congress*, 1652–1663. https://doi.org/10.1061/9780784413357.145

Højstrup, J. (1983). Nibe Wake, part one. *International Technical Report, Risø*.

Holland, J. H. (1975). *Adaptation in Natural and Artificial Systems*. University of Michigan Press, Ann Arbor.

Hou, P., Hu, W., Chen, C., Soltani, M., & Chen, Z. (2016). Optimization of offshore wind farm layout in restricted zones. *Energy*, *113*, 487–496. https://doi.org/10.1016/j.energy.2016.07.062

Hou, P., Hu, W., Soltani, M., & Chen, Z. (2015). Optimized Placement of Wind Turbines in Large-Scale Offshore Wind Farm Using Particle Swarm Optimization Algorithm. *IEEE Transactions on Sustainable Energy*, *6*(4), 1272–1282. https://doi.org/10.1109/TSTE.2015.2429912

Huang, H. S. (2007). Distributed genetic algorithm for optimization of wind farm annual profits. *2007 International Conference on Intelligent Systems Applications to Power Systems, ISAP*, 1–6. https://doi.org/10.1109/ISAP.2007.4441654

Huang, L., Tang, H., Zhang, K., Fu, Y., & Liu, Y. (2020). 3-D Layout Optimization of Wind Turbines Considering Fatigue Distribution. *IEEE Transactions on Sustainable Energy*, *11*(1), 126–135. https://doi.org/10.1109/TSTE.2018.2885946

Ilhan, A., & Bilgili, M. (2016). An Overview of Turkey ' s Offshore Wind Energy Potential Evaluations. *Turkish Journal of Scientific Reviews*, *9*(2), 55–58.

Ilkiliç, C., & Aydin, H. (2015). Wind power potential and usage in the coastal regions of Turkey. *Renewable and Sustainable Energy Reviews*, *44*, 78–86. https://doi.org/10.1016/j.rser.2014.12.010

International Electrotechnical Commission. (2005). Wind turbines—Part 12-1: power performance measurements of electricity producing wind turbines. *IEC 61400-12-1*.

Jensen, N. O. (1983). A Note on Wind Generator Interaction. *RISØ-M-2411*.

Jonkman, J., Butterfield, S., Musial, W., & Scott, G. (2009). Definition of a 5-MW reference wind turbine for offshore system development (No. NREL/TP-500-38060). In *National Renewable Energy Lab.(NREL)*. https://doi.org/10.1115/1.4038580

Ju, X., & Liu, F. (2019). Wind farm layout optimization using self-informed genetic algorithm with information guided exploitation. *Applied Energy*, *248*(April), 429–445. https://doi.org/10.1016/j.apenergy.2019.04.084

Kallehave, D., Byrne, B. W., LeBlanc Thilsted, C., & Mikkelsen, K. K. (2015). Optimization of monopiles for offshore wind turbines. *Philosophical Transactions of the Royal Society A: Mathematical, Physical and Engineering Sciences*, *373*(2035). https://doi.org/10.1098/rsta.2014.0100

Katic, I., Højstrup, J., & Jensen, N. O. (1987). A Simple Model for Cluster Efficiency. *EWEC'86 Proceedings*, *1*, 407–410.

Kaya, B., & Oğuz, E. (2019). Tekil Kazik Temelli Açık Deniz Rüzgar Türbinlerinin Avrupa'daki Gelişimi. *5. İzmir Rüzgâr Sempozyumu // 3-5 Ekim 2019 // İzmir*, 175–195.

Köroğlu, M. Ö., & Ülgen, K. (2018). Offshore Wind Energy Plant : A Case study of Çanakkale. *Güç Sistemleri Konferansı 15-16 Kasım 2018 Ankara*, 160–165. https://doi.org/10.5281/zenodo.1482655

Kumar, Y., Ringenberg, J., Depuru, S. S., Devabhaktuni, V. K., Lee, J. W., Nikolaidis, E., Andersen, B., & Afjeh, A. (2016). Wind energy: Trends and enabling technologies. *Renewable and Sustainable Energy Reviews*, *53*, 209–224. https://doi.org/10.1016/j.rser.2015.07.200

Kuo, J. Y. J., Romero, D. A., Beck, J. C., & Amon, C. H. (2016). Wind farm layout optimization on complex terrains – Integrating a CFD wake model with mixed-integer programming. *Applied Energy*, *178*, 404–414. https://doi.org/10.1016/j.apenergy.2016.06.085

Kusiak, A., & Song, Z. (2010). Design of wind farm layout for maximum wind energy capture. *Renewable Energy*, *35*(3), 685–694. https://doi.org/10.1016/j.renene.2009.08.019

Kwong, W. Y., Zhang, P. Y., Morgenroth, M., Romero, D., Amon, C., & Moran, J. (2012). Wind farm layout optimization considering energy generation and noise propagation. *Proceeding of the ASME 2021 International Design Engineering Technical Conferences & Computers and Information in Engineering Conference, Chicago, IL, USA*, 1–10.

Lackner, M. A., & Elkinton, C. N. (2007). An analytical framework for offshore wind farm layout optimization. *Wind Engineering*, *31*(1), 17–31. https://doi.org/10.1260/030952407780811401

Ladenburg, J., & Dubgaard, A. (2007). Willingness to pay for reduced visual disamenities from offshore wind farms in Denmark. *Energy Policy*, *35*, 4059–4071. https://doi.org/10.1016/j.enpol.2007.01.023

Lee, J., & Zhao, F. (2020). GWEC | GLOBAL WIND REPORT 2019. In *GWEC*.

Lee, J., & Zhao, F. (2021). GWEC | Global Wind Report 2021. In *Global Wind Energy Council*. http://www.gwec.net/global-figures/wind-energy-global-status/

Lefebvre, S., & Collu, M. (2012). Preliminary design of a floating support structure for a 5 MW offshore wind turbine. *Ocean Engineering*, *40*, 15–26. https://doi.org/10.1016/j.oceaneng.2011.12.009

Lloyd, G., & Hassan, G. (1994). Study of offshore wind energy in the EC. *Verlag Natürliche Energie JOUR*, *72*.

Lombardi, D., Bhattacharya, S., & Wood, D. M. (2013). Dynamic soil-structure interaction of monopile supported wind turbines in cohesive soil. *Soil Dynamics and Earthquake Engineering*, *49*, 165–180. https://doi.org/10.1016/j.soildyn.2013.01.015

Lydia, M., Kumar, S. S., Selvakumar, A. I., & Prem Kumar, G. E. (2014). A comprehensive review on wind turbine power curve modeling techniques. *Renewable and Sustainable Energy Reviews*, *30*, 452–460. https://doi.org/10.1016/j.rser.2013.10.030

Ma, Y., Yang, H., Zhou, X., Li, J., & Wen, H. (2009). The dynamic modeling of wind farms considering wake effects and its optimal distribution. *WNWEC 2009 - 2009 World Non-Grid-Connected Wind Power and Energy Conference*, 134–137. https://doi.org/10.1109/WNWEC.2009.5335828

Malhotra, S. (2011). Selection, Design and Construction of Offshore Wind Turbine Foundations. In I. H. Al-Bahadly (Ed.), *Wind Turbines* (pp. 231–264). https://doi.org/10.5772/32009

Malkoc, Y. (2007). The Role of Wind energy in Turkish Electric Energy Supply. *The Chamber of Electrical Engineer of Turkey Energy Journal*, *3*, 45–50.

Marmidis, G., Lazarou, S., & Pyrgioti, E. (2008). Optimal placement of wind turbines in a wind park using Monte Carlo simulation. *Renewable Energy*, *33*(7), 1455–1460. https://doi.org/10.1016/j.renene.2007.09.004

Mathew, T. V. (2012). Genetic algorithm. In *Indian Institute of Technology, Bombay*. https://doi.org/10.1007/s12539-011-0108-3

Micelli, F. (2012). *Offshore wind turbines foundation types | Wind farms construction*.

Mirzaei, S. (2014). Defining a Business-Driven Optimization Problem. In *Encyclopedia of Business Analytics and Optimization* (pp. 708–715).

Mittal, A. (2010). Optimization of the Layout of Large Wind Farms Using a Genetic Algorithm. In *Department of Mechanical and Aerospace Engineering, Case Western Reverse University*.

Mortensen, N. G., Heathfield, D. N., Landberg, L., Rathmann, O., Troen, I., & Lundtang Petersen, E. (2001). Wind Atlas Analysis and Application Program: WAsP 7 Help Facility. *Roskilde: Risø National Laboratory*.

Mosetti, G., Poloni, C., & Diviacco, B. (1994). Optimization of wind turbine positioning in large windfarms by means of a genetic algorithm. *Journal of Wind Engineering and Industrial Aerodynamics*, *51*(1), 105–116.

Nikolaos, N. (2004). *Deep water offshore wind technologies*. Thesis of Master in Science, University of Strathclyde Department of Mechanical Engineering.

O'Kelly, B. C., & Arshad, M. (2016). Offshore wind turbine foundations - analysis and design. In *Offshore Wind Farms: Technologies, Design and Operation*. Elsevier Ltd. https://doi.org/10.1016/B978-0-08-100779-2.00020-9

O'Sullivan, R. (2021). Offshore wind in Europe - Key trends and statistics 2020. In *WindEurope*.

Oh, K. Y., Nam, W., Ryu, M. S., Kim, J. Y., & Epureanu, B. I. (2018). A review of foundations of offshore wind energy convertors: Current status and future perspectives. *Renewable and Sustainable Energy Reviews*, *88*(February 2017), 16–36. https://doi.org/10.1016/j.rser.2018.02.005

Ozturk, U. A., & Norman, B. A. (2004). Heuristic methods for wind energy conversion system positioning. *Electric Power Systems Research*, *70*(3), 179–185. https://doi.org/10.1016/j.epsr.2003.12.006

Park, J., & Law, K. H. (2015). Layout optimization for maximizing wind farm power production using sequential convex programming. *Applied Energy*, *151*, 320–334. https://doi.org/10.1016/j.apenergy.2015.03.139

Park, J. W., An, B. S., Lee, Y. S., Jung, H., & Lee, I. (2019). Wind farm layout optimization using genetic algorithm and its application to Daegwallyeong wind farm. *JMST Advances*, *1*(4), 249–257. https://doi.org/10.1007/s42791-019-00026-z

Patel, M. R. (1999). Wind and power solar systems. *Boca Raton, FL: CRC Press*.

Pérez, B., Mínguez, R., & Guanche, R. (2013). Offshore wind farm layout optimization using mathematical programming techniques. *Renewable Energy*, *53*, 389–399. https://doi.org/10.1016/j.renene.2012.12.007

Pohlheim, H. (1999). *GEATbx: genetic and evolutionary algorithm toolbox for use with Matlab*. *95*(August).

Pohlheim, H. (2005). Evolutionary Algorithms: Overview, Methods and Operators. In *Documentation for genetic evalutionary algorithm toolbox for use with Matlab version 3.7*. https://doi.org/10.1016/B978-008044910-4.00525-3

Pookpunt, S., & Ongsakul, W. (2013). Optimal placement of wind turbines within wind farm using binary particle swarm optimization with time-varying acceleration coefficients. *Renewable Energy*, *55*, 266–276. https://doi.org/10.1016/j.renene.2012.12.005

Pookpunt, S., & Ongsakul, W. (2016). Design of optimal wind farm configuration using a binary particle swarm optimization at Huasai district, Southern Thailand. *Energy Conversion and Management*, *108*, 160–180. https://doi.org/10.1016/j.enconman.2015.11.002

POWER TECHNOLOGY. (2021). *Vineyard Wind 1 Offshore Wind Farm, Massachusetts*. https://www.power-technology.com/projects/vineyard-wind-1-offshore-wind-farm-massachusetts/

Rahbari, O., Vafaeipour, M., Fazelpour, F., Feidt, M., & Rosen, M. A. (2014). Towards realistic designs of wind farm layouts: Application of a novel placement selector approach. *Energy Conversion and Management*, *81*, 242–254. https://doi.org/10.1016/j.enconman.2014.02.010

Rahmani, R., Khairuddin, A., Cherati, S. M., & Mahmoud Pesaran, H. A. (2010). A novel method for optimal placing wind turbines in a wind farm using particle swarm optimization (PSO). *2010 9th International Power and Energy Conference, IPEC 2010*, 134–139. https://doi.org/10.1109/IPECON.2010.5697144

Rajper, S., & Amin, I. J. (2012). Optimization of wind turbine micrositing: A comparative study. *Renewable and Sustainable Energy Reviews*, *16*(8), 5485–5492. https://doi.org/10.1016/j.rser.2012.06.014

Reddy, K. N., & Roy, S. B. (2020). Layout optimization for a large offshore wind farm using Genetic Algorithm. *EGU General Assembly 2020, Online, 4-8 May 2020*. https://doi.org/https://doi.org/10.5194/egusphere-egu2020-12654

Rivas, R. A., Clausen, J., Hansen, K. S., & Jensen, L. E. (2009). Solving the turbine positioning problem for large offshore wind farms by simulated annealing. *Wind Engineering*, *33*(3), 287–298. https://doi.org/10.1260/0309-524x.33.3.287

Rudion, K. (2008). Aggregated modelling of wind farms. *Otto-von-Guericke Universität*.

Saavedra-Moreno, B., Salcedo-Sanz, S., Paniagua-Tineo, A., Prieto, L., & Portilla-Figueras, A. (2011). Seeding evolutionary algorithms with heuristics for optimal wind turbines positioning in wind farms. *Renewable Energy*, *36*(11), 2838–2844. https://doi.org/10.1016/j.renene.2011.04.018

Salcedo-Sanz, S., Gallo-Marazuela, D., Pastor-Sánchez, A., Carro-Calvo, L., Portilla-Figueras, A., & Prieto, L. (2014). Offshore wind farm design with the Coral Reefs Optimization algorithm. *Renewable Energy*, *63*, 109–115. https://doi.org/10.1016/j.renene.2013.09.004

Satir, M., Murphy, F., & Mcdonnell, K. (2018). Feasibility study of an offshore wind farm in the Aegean Sea, Turkey. *Renewable and Sustainable Energy Reviews*, *81*, 2552–2562. https://doi.org/10.1016/j.rser.2017.06.063

Sawyer, S., Shukla, S., & Fichaux, N. (2013). *30 Years of Policies for Wind Energy: Lessons from 12 Wind Energy Markets*.

Şengül, E. (2019). *Strengthened Danish-Turkish relations on offshore wind energy*. Anadolu Agency Energy. https://www.aa.com.tr/en/energy/invesments/turkey-denmark-work-closely-for-offshore-wind-growth/27361

Serrano González, J., Trigo García, Á. L., Burgos Payán, M., Riquelme Santos, J., & González Rodríguez, Á. G. (2017). Optimal wind-turbine micro-siting of offshore wind farms: A grid-like layout approach. *Applied Energy*, *200*, 28–38. https://doi.org/10.1016/j.apenergy.2017.05.071

Sezer-Uzol, N., & Uzol, O. (2013). Effect of steady and transient wind shear on the wake structure and performance of a horizontal axis wind turbine rotor. *Wind Energy*, *16*, 1–17. https://doi.org/10.1002/we

Shakoor, R., Hassan, M. Y., Raheem, A., & Rasheed, N. (2015). The modelling of wind farm layout optimization for the reduction of wake losses. *Indian Journal of Science and Technology*, *8*(17). https://doi.org/10.17485/ijst/2015/v8i17/69817

Shakoor, R., Hassan, M. Y., Raheem, A., & Rasheed, N. (2016). Wind farm layout optimization using area dimensions and definite point selection techniques. *Renewable Energy*, *88*, 154–163. https://doi.org/10.1016/j.renene.2015.11.021

Shakoor, R., Hassan, M. Y., Raheem, A., & Wu, Y. K. (2016). Wake effect modeling: A review of wind farm layout optimization using Jensen's model. *Renewable and Sustainable Energy Reviews*, *58*, 1048–1059. https://doi.org/10.1016/j.rser.2015.12.229

Sharp, C., & DuPont, B. (2018). Wave energy converter array optimization: A genetic algorithm approach and minimum separation distance study. *Ocean Engineering*, *163*(June), 148–156. https://doi.org/10.1016/j.oceaneng.2018.05.071

Şişbot, S., Turgut, Ö., Tunç, M., & Çamdalı, Ü. (2010). Optimal positioning of wind turbines on Gökçeada using multi-objective genetic algorithm. *Wind Energy*, *13*(April 2009), 297–306. https://doi.org/10.1002/we

Sivanandam, S. N., & Deepa, S. N. (2008). Introduction to genetic algorithms. In *Introduction to Genetic Algorithms*. https://doi.org/10.1007/978-3-540-73190-0

Song, M. X., Chen, K., & Wang, J. (2018). Three-dimensional wind turbine positioning using Gaussian particle swarm optimization with differential evolution. *Journal of Wind Engineering and Industrial Aerodynamics*, *172*(November 2017), 317–324. https://doi.org/10.1016/j.jweia.2017.10.032

Sørensen, T., Nielsen, P., & Thøgersen, M. L. (2006). Recalibrating wind turbine wake model parameters - Validating the wake model performance for Large offshore Wind Farms. *European Wind Energy Conference and Exhibition 2006*, *2*, 1660–1665.

Stanley, A. P. J., & Ning, A. (2019). Coupled wind turbine design and layout optimization with nonhomogeneous wind turbines. *Wind Energy Science*, *4*(1), 99–114. https://doi.org/10.5194/wes-4-99-2019

Sun, H., Yang, H., & Gao, X. (2019). Investigation into spacing restriction and layout optimization of wind farm with multiple types of wind turbines. *Energy*, *168*(2019), 637–650. https://doi.org/10.1016/j.energy.2018.11.073

Swift-Hook, D. T., Hojstrup, J., McIntosch, D. N., Millborrow, D. J., & Taylor, G. J. (1984). Nibe wake measurements project in Denmark. *European Wind Energy Conference 22-28 Octber*, 47–55.

Tang, X., Shen, Y., Li, S., Yang, Q., & Sun, Y. (2017). Mixed installation to optimize the position and type selection of turbines for wind farms. *International Conference on Neural Information Processing*, 307–315. https://doi.org/10.1007/978-3-319-70136-3

Tang, X., Yang, Q., Wang, K., Stoevesandt, B., & Sun, Y. (2018). Optimisation of wind farm layout in complex terrain via mixed-installation of different types of turbines. *IET Renewable Power Generation*, *12*(9), 1065–1073. https://doi.org/10.1049/iet-rpg.2017.0787

Timmons, D., Harris, J. M., & Roach, B. (2014). *The Economics of Renewable Energy A GDAE Teaching Module on Social and Environmental Issues in Economics*. 53.

Turner, S. D. O., Romero, D. A., Zhang, P. Y., Amon, C. H., & Chan, T. C. Y. (2014). A new mathematical programming approach to optimize wind farm layouts. *Renewable Energy*, *63*, 674–680. https://doi.org/10.1016/j.renene.2013.10.023

TWEA. (2020). *Turkish Wind Energy Statistic Report - January 2020*.

TWEA. (2021). *Turkish Wind Energy Statistic Report - July 2021*.

Uğurlu, A., & Gokcol, C. (2017). An overview of Turkey's renewable energy trend. *Journal of Energy Systems*, *1*(4), 148–158. https://doi.org/10.30521/jes.361920

UNFCCC. (2022). *About the secreteriat | UNFCCC*. https://unfccc.int/about-us/about-the-secretariat

United Nations Climate Change. (2019). *What is the Kyoto Ptorocol? | UNFCCC*.

Van Oord. (2022). *Gemini: Social, environmental and economic spin-off*. https://www.vanoord.com/en/sustainability/cases/gemini-social-environmental-and-economic-spin/

Vermeulen, P. E. J., Builtjes, P., Dekker, J., & Lammerts van Bueren, G. (1979). *An experimental study of the wake behind a full scale vertical-axis wind turbine*.

Vis, I. F. A., & Ursavas, E. (2016). Assessment approaches to logistics for offshore wind energy installation. *Sustainable Energy Technologies and Assessments*, *14*, 80–91. https://doi.org/10.1016/j.seta.2016.02.001

Wan, C., Wang, J., Yang, G., Gu, H., & Zhang, X. (2012). Wind farm micro-siting by Gaussian particle swarm optimization with local search strategy. *Renewable Energy*, *48*, 276–286. https://doi.org/10.1016/j.renene.2012.04.052

Wan, C., Wang, J., Yang, G., Li, X., & Zhang, X. (2009). Optimal micro-siting of wind turbines using real-coded genetic algorithms based on improved wind and turbine models. *Joint 48th IEEE Conference on Decision and Control and 28th Chinese Control Conference Shanghai, P.R. China*, 5092–5096.

Wan, C., Wang, J., Yang, G., & Zhang, X. (2010). Optimal micro-siting of wind farms by particle swarm optimization. *Advances in Swarm Intelligence, First International Conference, ICSI 2010, Beijing, China, June 12-15, 2010, Proceedings, Part I*, 198–205.

Wan, C., Wang, J., Yang, G., & Zhang, X. (2009). Optimal siting of wind turbines using real-coded genetic algorithms. *Proceedings of European Wind Energy Association Conference and Exhibition. Marseille, France*, 1–6.

Wang, L., Cholette, M. E., Fu, Y., Yuan, J., Zhou, Y., & Tan, A. C. C. (2018). Combined optimization of continuous wind turbine placement and variable hub height. *Journal of Wind Engineering and Industrial Aerodynamics*, *180*(June), 136–147. https://doi.org/10.1016/j.jweia.2018.07.016

Wang, L., Cholette, M. E., Zhou, Y., Yuan, J., Tan, A. C. C., & Gu, Y. (2018). Effectiveness of optimized control strategy and different hub height turbines on a real wind farm optimization. *Renewable Energy*, *126*, 819–829. https://doi.org/10.1016/j.renene.2018.04.004

Wang, L., Tan, A. C. C., & Gu, Y. (2015). Comparative study on optimizing the wind farm layout using different design methods and cost models. *Journal of Wind Engineering and Industrial Aerodynamics*, *146*, 1–10. https://doi.org/10.1016/j.jweia.2015.07.009

Winter, P., & Zachariasen, M. (1997). Euclidean Steiner minimum trees: An improved exact algorithm. *Networks*, *30*(3), 149–166. https://doi.org/10.1002/(SICI)1097-0037(199710)30:3<149::AID-NET1>3.0.CO;2-L

Wu, X., Hu, Y., Li, Y., Yang, J., Duan, L., Wang, T., Adcock, T., Jiang, Z., Gao, Z., Lin, Z., Borthwick, A., & Liao, S. (2019). Foundations of offshore wind turbines : A review. *Renewable and Sustainable Energy Reviews*, *104*, 379–393. https://doi.org/10.1016/j.rser.2019.01.012

Wu, Y., Zhang, S., Wang, R., Wang, Y., & Feng, X. (2020). A design methodology for wind farm layout considering cable routing and economic benefit based on genetic algorithm and GeoSteiner. *Renewable Energy*, *146*, 687–698. https://doi.org/10.1016/j.renene.2019.07.002

Yildiz, B., Altan-Sakarya, A. B., & Ger, A. M. (2014). Optimum design of slurry pipelines by genetic algorithm. *Civil Engineering and Environmental Systems*, *31*(4), 311–330. https://doi.org/10.1080/10286608.2014.912638

Yıldız, H. K. (2021). *Offshore wind farm site selection for Aegean and Mediterranean Sea, Turkey*. Middle East Technical Unviersity.

Zaaijer, M. B., & Henderson, A. R. (2004). Review of current activities in offshore wind energy. *Proceedings of the International Offshore and Polar Engineering Conference*, *March*, 101–108.

APPENDICES

A. Python code of model (a)

```
# -*- coding: utf-8 -*-

import numpy as np
import copy
import random
import matplotlib.pyplot as plt
import math
import time
start_time = time.time()


population_size = 1000
generation_num = 3000
er = 0.1
cr = 0.6

rotor_diameter = 126
grid_size_ver = 4           # in diameter
grid_size_hor = 2           # in diameter

wind_farm_size_hor = 8000   # in m
wind_farm_size_ver = 3400   # in m

row_num = round(wind_farm_size_ver / (grid_size_ver *
rotor_diameter))
column_num = round(wind_farm_size_hor / (grid_size_hor *
rotor_diameter))
cell_num = row_num * column_num

entrainment_constant = 0.04
thrust_coefficient = 0.65
axial_ind_factor = 0.5 * (1 - (1 - thrust_coefficient) ** 0.5)

cut_power_coefficient = 0.99999
cut_in_wind_speed = 5       # in m/s
rated_wind_speed = 11.4     # in m/s
avg_wind_speed = 9.20       # in m/s
air_density = 1.225         # in kg/m3
power_coefficient = 0.442
turbine_power = 0.5 * power_coefficient * air_density * math.pi *
((rotor_diameter ** 2) / 4) * (avg_wind_speed ** 3) / 1000  # in kW


def print_list(listo):
    print("========")
    for i in listo:
        print(i)
    print("========")
```

```
def is_value_between(val, minn, maxx):
    return val <= minn or val >= maxx


def is_static_values_valid():
    warning_msg_list = []
    if population_size < 10:
        msg = "population_size, 10 dan küçük olamaz."
        warning_msg_list.append(msg)
    if population_size % 10 != 0:
        msg = "population_size, 10 nun katı olmalı."
        warning_msg_list.append(msg)
    if generation_num < 3:
        msg = "generation_num, 3 den küçük olamaz."
        warning_msg_list.append(msg)
    if is_value_between(cut_power_coefficient, 0, 1):
        msg = "cut_power_coefficient 0 ile 1 arasında olmalı."
        warning_msg_list.append(msg)
    if is_value_between(er, 0, 1):
        msg = "er 0 ile 1 arasında olmalı."
        warning_msg_list.append(msg)
    if is_value_between(cr, 0, 1):
        msg = "cr 0 ile 1 arasında olmalı."
        warning_msg_list.append(msg)
    if is_value_between(er + cr, 0, 1):
        msg = "er + cr 0 ile 1 arasında olmalı."
        warning_msg_list.append(msg)

    is_valid_values = len(warning_msg_list) == 0
    if not is_valid_values:
        print("----- WARNING -----")
        print_list(warning_msg_list)
        print("----- WARNING -----")
    return is_valid_values


def get_random_layout_raw_array():
    turbine_num = random.randint(1, cell_num - 1)
    raw_array = np.hstack((np.ones((turbine_num,), int),
np.zeros((cell_num - turbine_num,), int)))
    np.random.shuffle(raw_array)
    return raw_array


def get_column_divided_array_from_raw_array(raw_array):
    column_divided_array = []
    sub_array = []
    for cellIndex in range(len(raw_array)):
        sub_array.append(raw_array[cellIndex])
        if cellIndex % row_num == row_num - 1:
            column_divided_array.append(sub_array)
            sub_array = []
    return column_divided_array
```

```
def get_power_from_column_divided_array(column_divided_array):
    total_power = 0
    for column in column_divided_array:
        wind_speed = []
        for cellIndex in range(len(column)):
            counter = 1
            if column[cellIndex] == 1 and len(wind_speed) == 0:
                wind_speed.append(avg_wind_speed)
            elif column[cellIndex] == 1 and len(wind_speed) > 0:
                for row_number in range(cellIndex):
                    if cellIndex > 0 and column[cellIndex -
row_number - 1] == 1:
                        reduced_speed = wind_speed[len(wind_speed)-
1] * (1 - 2 * axial_ind_factor * ((rotor_diameter / 2) /
(rotor_diameter / 2 + entrainment_constant * grid_size_ver *
rotor_diameter * counter)) ** 2)
                        if reduced_speed < cut_in_wind_speed:
                            reduced_speed = 0
                        wind_speed.append(reduced_speed)
                        break
                    else:
                        counter += 1

        for i in range(len(wind_speed)):
            total_power = total_power + 0.5 * power_coefficient *
air_density * math.pi * ((rotor_diameter ** 2) / 4) *
(wind_speed[i] ** 3) / 1000
    return round(total_power, 4)


def get_layout_object_from_raw_array(raw_array):
    column_divided_array =
get_column_divided_array_from_raw_array(raw_array)
    dynamic_turbine_num = list(raw_array).count(1)
    layout_obj = {
        "raw_array": raw_array,
        "dynamic_turbine_num": dynamic_turbine_num,
        "column_divided_array": column_divided_array,
        "power":
get_power_from_column_divided_array(column_divided_array),
        "cost_power_ratio":
(get_cost(dynamic_turbine_num))/(get_power_from_column_divided_arra
y(column_divided_array)),
        "cost": get_cost(dynamic_turbine_num)
    }
    return layout_obj


def get_random_layouts(size):
    layouts = []
    for i in range(size):

layouts.append(get_layout_object_from_raw_array(get_random_layout_r
```

```
aw_array()))
    return layouts


def get_crossover_layouts(layouts):
    if len(layouts) % 2 != 0:
        return layouts
    else:
        ret_layouts = []
        for i in range(len(layouts)):
            if i % 2 == 1:
                raw_lay1 = layouts[i - 1]["raw_array"]
                raw_lay2 = layouts[i]["raw_array"]
                make_new_crossover(raw_lay1, raw_lay2)

ret_layouts.append(get_layout_object_from_raw_array(raw_lay1))

ret_layouts.append(get_layout_object_from_raw_array(raw_lay2))
        return get_mutated_layouts(ret_layouts)


def make_new_crossover(raw1, raw2):
    middle_index = math.floor(len(raw1)/2)
    swap_list = raw1[middle_index : len(raw1)]
    raw1[middle_index : len(raw1)] = raw2[middle_index : len(raw1)]
    raw2[middle_index : len(raw1)] = swap_list
    if list(raw1).count(1) == 0:
        make_new_mutation(raw1)
    if list(raw2).count(1) == 0:
        make_new_mutation(raw2)


def make_crossover(raw1, raw2):
    raw1_valid_zeros_indexes = []
    raw1_valid_ones_indexes = []
    for i in range(len(raw1)):
        if (raw1[i] == 0) and (raw2[i] == 1):
            raw1_valid_zeros_indexes.append(i)
        elif (raw1[i] == 1) and (raw2[i] == 0):
            raw1_valid_ones_indexes.append(i)
    if len(raw1_valid_zeros_indexes) > 0:
        raw1_give_zero_index =
random.choice(raw1_valid_zeros_indexes)
        raw1_give_one_index =
random.choice(raw1_valid_ones_indexes)
        raw1[raw1_give_zero_index] = 1
        raw1[raw1_give_one_index] = 0
        raw2[raw1_give_zero_index] = 0
        raw2[raw1_give_one_index] = 1
    else:

        pass


def get_mutated_layouts(layouts):
```

```
    ret_layouts = []
    for layout in layouts:
        raw_lay = layout["raw_array"]
        make_new_mutation(raw_lay)

ret_layouts.append(get_layout_object_from_raw_array(raw_lay))
    return ret_layouts


def make_new_mutation(raw):
    if list(raw).count(1) != 1:
        mutation_index = random.choice(range(len(raw)))
        raw[mutation_index] = 0 if raw[mutation_index] == 1 else 1


def make_mutation(raw):
    zeros_indexes = []
    ones_indexes = []
    for i in range(len(raw)):
        if raw[i] == 0:
            zeros_indexes.append(i)
        else:
            ones_indexes.append(i)
    toggle_zero_index = random.choice(zeros_indexes)
    toggle_one_index = random.choice(ones_indexes)
    raw[toggle_zero_index] = 1
    raw[toggle_one_index] = 0


def get_top_piece_generation(generation, rate):
    return copy.deepcopy(generation[0: int(population_size *
rate)])


def get_generation(prev_generation):
    generation = []
    if len(prev_generation) == 0:
        generation += get_random_layouts(population_size)
    else:
        generation += get_top_piece_generation(prev_generation, er)
        generation +=
get_crossover_layouts(get_top_piece_generation(prev_generation,
cr))
        generation += get_random_layouts(int(population_size * (1 -
er - cr)))

    generation = sorted(generation, key=lambda k:
k['cost_power_ratio'], reverse=False)
    return generation


def get_cost(turbine_number):
    return turbine_number * (2 / 3 + ((1 / 3) * math.exp(-0.00174 *
(turbine_number ** 2))))
```

```
def start_evolution():
    winner_layouts_powers_list = []
    active_generation = get_generation([])

winner_layouts_powers_list.append(active_generation[0]["cost_power_
ratio"])
    evolve_num = 0
    for i in range(generation_num):
        if active_generation[0].get("power") >
cut_power_coefficient *
active_generation[0].get("dynamic_turbine_num") * turbine_power:
            break
        active_generation = get_generation(active_generation)

winner_layouts_powers_list.append(active_generation[0]["cost_power_
ratio"])
        evolve_num += 1

    winner_lay = active_generation[0]
    execution_time = (time.time() - start_time)
    print("Execution time in sec: " + str(execution_time))
    print("-------------  Winner Layout  -------------")
    print("Evolve                : " + str(evolve_num) + " times")
    print("raw_array             : " + str(winner_lay["raw_array"]))
    print("column_divided_array : " +
str(winner_lay["column_divided_array"]))
    print("power                 : " + str(winner_lay["power"]))
    print("max power             : " +
str(winner_lay["dynamic_turbine_num"] * turbine_power))
    print("efficiency            : " + str(round(100 *
winner_lay["power"] / (winner_lay["dynamic_turbine_num"] *
turbine_power), 2)) + " %")
    print("TURBINE NUMBER        : " +
str(winner_lay["dynamic_turbine_num"]))
    print("WINNER COST           : " + str(winner_lay["cost"]))
    print("cutoff efficiency     : " +
str(round(cut_power_coefficient * 100, 2)) + " %")
    print("-------------  Winner Layout  -------------")
    print("-------------  Winners List  -------------")
    print(len(winner_layouts_powers_list))
    print(winner_layouts_powers_list)
    print("WINNER COST / POWER  : " +
str(winner_layouts_powers_list[-1]))
    print("-------------  Winners List  -------------")

    x = range(len(winner_layouts_powers_list))
    y = winner_layouts_powers_list
    plt.title("Line graph")
    plt.xlabel("Generation number")
    plt.ylabel("Fitness value")
    plt.plot(x, y, color="red")
    plt.show()
```

```
if __name__ == '__main__':
    if is_static_values_valid():
        start_evolution()
```

B. Python code of model (b)

```
# -*- coding: utf-8 -*-

import math
import numpy as np
import copy
import random
import matplotlib.pyplot as plt
import time
start_time = time.time()

population_size = 1000
generation_num = 3000
er = 0.1
cr = 0.6

rotor_diameter = 40
grid_size_ver = 4       # in diameter
grid_size_hor = 3       # in diameter
turbine_num = 43

wind_farm_size_hor = 2000
wind_farm_size_ver = 2000

row_num = math.ceil(wind_farm_size_ver / (grid_size_ver *
rotor_diameter))
column_num = math.ceil(wind_farm_size_hor / (grid_size_hor *
rotor_diameter))
cell_num = row_num * column_num

entrainment_constant = 0.09437
thrust_coefficient = 0.88
axial_ind_factor = 0.5 * (1 - (1 - thrust_coefficient) ** 0.5)

cut_power_coefficient = 0.99999
cut_in_wind_speed = 2       # in m/s
rated_wind_speed = 12.8     # in m/s
avg_wind_speed = 12         # in m/s
air_density = 1.2254        # in kg/m3
power_coefficient = 0.4
turbine_power = 0.5 * power_coefficient * air_density * math.pi *
((rotor_diameter ** 2) / 4) * (avg_wind_speed ** 3) / 1000  # in kW


def print_list(listo):
    print("========")
    for i in listo:
        print(i)
    print("========")


def is_value_between(val, minn, maxx):
```

```
    return val <= minn or val >= maxx


def is_static_values_valid():
    warning_msg_list = []
    if population_size < 10:
        msg = "population_size, 10 dan küçük olamaz."
        warning_msg_list.append(msg)
    if population_size % 10 != 0:
        msg = "population_size, 10 nun katı olmalı."
        warning_msg_list.append(msg)
    if generation_num < 3:
        msg = "generation_num, 3 den küçük olamaz."
        warning_msg_list.append(msg)
    if is_value_between(cut_power_coefficient, 0, 1):
        msg = "cut_power_coefficient 0 ile 1 arasında olmalı."
        warning_msg_list.append(msg)
    if is_value_between(er, 0, 1):
        msg = "er 0 ile 1 arasında olmalı."
        warning_msg_list.append(msg)
    if is_value_between(cr, 0, 1):
        msg = "cr 0 ile 1 arasında olmalı."
        warning_msg_list.append(msg)
    if is_value_between(er + cr, 0, 1):
        msg = "er + cr 0 ile 1 arasında olmalı."
        warning_msg_list.append(msg)
    if turbine_num > cell_num:
        msg = "turbine_num, cell_num dan büyük olamaz"
        warning_msg_list.append(msg)

    is_valid_values = len(warning_msg_list) == 0
    if not is_valid_values:
        print("----- WARNING -----")
        print_list(warning_msg_list)
        print("----- WARNING -----")
    return is_valid_values


def get_random_layout_raw_array():
    raw_array = np.hstack((np.ones((turbine_num,), int),
np.zeros((cell_num - turbine_num,), int)))
    np.random.shuffle(raw_array)
    return raw_array


def get_column_divided_array_from_raw_array(raw_array):
    column_divided_array = []
    sub_array = []
    for cellIndex in range(len(raw_array)):
        sub_array.append(raw_array[cellIndex])
        if cellIndex % row_num == row_num - 1:
            column_divided_array.append(sub_array)
            sub_array = []
    return column_divided_array
```

```
def get_power_from_column_divided_array(column_divided_array):
    total_power = 0
    for column in column_divided_array:
        wind_speed = []
        for cellIndex in range(len(column)):
            counter = 1
            if column[cellIndex] == 1 and len(wind_speed) == 0:
                wind_speed.append(avg_wind_speed)
            elif column[cellIndex] == 1 and len(wind_speed) > 0:
                for row_number in range(cellIndex):
                    if cellIndex > 0 and column[cellIndex -
row_number - 1] == 1:
                        reduced_speed = wind_speed[len(wind_speed)-
1] * (1 - 2 * axial_ind_factor * ((rotor_diameter / 2) /
(rotor_diameter / 2 + entrainment_constant * grid_size_ver *
rotor_diameter * counter)) ** 2)
                        if reduced_speed < cut_in_wind_speed:
                            reduced_speed = 0
                        wind_speed.append(reduced_speed)
                        break
                    else:
                        counter += 1

        for i in range(len(wind_speed)):
            total_power = total_power + 0.5 * power_coefficient *
air_density * math.pi * ((rotor_diameter ** 2) / 4) *
(wind_speed[i] ** 3) / 1000
    return round(total_power, 4)


def get_layout_object_from_raw_array(raw_array):
    column_divided_array =
get_column_divided_array_from_raw_array(raw_array)
    layout_obj = {
        "raw_array": raw_array,
        "column_divided_array": column_divided_array,
        "power":
get_power_from_column_divided_array(column_divided_array)
    }
    return layout_obj


def get_random_layouts(size):
    layouts = []
    for i in range(size):

layouts.append(get_layout_object_from_raw_array(get_random_layout_r
aw_array()))
    return layouts


def get_crossover_layouts(layouts):
    if len(layouts) % 2 != 0:
        return layouts
```

```
    else:
        ret_layouts = []
        for i in range(len(layouts)):
            if i % 2 == 1:
                raw_lay1 = layouts[i - 1]["raw_array"]
                raw_lay2 = layouts[i]["raw_array"]
                make_crossover(raw_lay1, raw_lay2)

ret_layouts.append(get_layout_object_from_raw_array(raw_lay1))

ret_layouts.append(get_layout_object_from_raw_array(raw_lay2))
        return get_mutated_layouts(ret_layouts)


def make_crossover(raw1, raw2):
    raw1_valid_zeros_indexes = []
    raw1_valid_ones_indexes = []
    for i in range(len(raw1)):
        if (raw1[i] == 0) and (raw2[i] == 1):
            raw1_valid_zeros_indexes.append(i)
        elif (raw1[i] == 1) and (raw2[i] == 0):
            raw1_valid_ones_indexes.append(i)
    if len(raw1_valid_zeros_indexes) > 0:
        raw1_give_zero_index =
random.choice(raw1_valid_zeros_indexes)
        raw1_give_one_index =
random.choice(raw1_valid_ones_indexes)
        raw1[raw1_give_zero_index] = 1
        raw1[raw1_give_one_index] = 0
        raw2[raw1_give_zero_index] = 0
        raw2[raw1_give_one_index] = 1
    else:

        pass


def get_mutated_layouts(layouts):
    ret_layouts = []
    for layout in layouts:
        raw_lay = layout["raw_array"]
        make_mutation(raw_lay)

ret_layouts.append(get_layout_object_from_raw_array(raw_lay))
    return ret_layouts


def make_mutation(raw):
    zeros_indexes = []
    ones_indexes = []
    for i in range(len(raw)):
        if raw[i] == 0:
            zeros_indexes.append(i)
        else:
            ones_indexes.append(i)
    toggle_zero_index = random.choice(zeros_indexes)
```

```
    toggle_one_index = random.choice(ones_indexes)
    raw[toggle_zero_index] = 1
    raw[toggle_one_index] = 0


def get_top_piece_generation(generation, rate):
    return copy.deepcopy(generation[0: int(population_size *
rate)])


def get_generation(prev_generation):
    generation = []
    if len(prev_generation) == 0:
        generation += get_random_layouts(population_size)
    else:
        generation += get_top_piece_generation(prev_generation, er)
        generation +=
get_crossover_layouts(get_top_piece_generation(prev_generation,
cr))
        generation += get_random_layouts(int(population_size * (1 -
er - cr)))

    generation = sorted(generation, key=lambda k: k['power'],
reverse=True)
    return generation


def start_evolution():
    winner_layouts_powers_list = []
    active_generation = get_generation([])

winner_layouts_powers_list.append(active_generation[0]["power"])
    evolve_num = 0
    for i in range(generation_num):
        if active_generation[0].get("power") >
cut_power_coefficient * turbine_num * turbine_power:
            break
        active_generation = get_generation(active_generation)

winner_layouts_powers_list.append(active_generation[0]["power"])
        evolve_num += 1

    winner_lay = active_generation[0]
    execution_time = (time.time() - start_time)
    print("Execution time in sec: " + str(execution_time))
    print("-------------  Winner Layout  -------------")
    print("Evolve                : " + str(evolve_num) + " times")
    print("raw_array             : " + str(winner_lay["raw_array"]))
    print("column_divided_array : " +
str(winner_lay["column_divided_array"]))
    print("power                 : " + str(winner_lay["power"]))
    print("max power             : " + str(turbine_num *
turbine_power))
    print("efficiency            : " + str(round(100 *
winner_lay["power"] / (turbine_num * turbine_power), 2)) + " %")
```

```
    print("cutoff efficiency    : " +
str(round(cut_power_coefficient * 100, 2)) + " %"
    print("-------------  Winner Layout  -------------")
    print("-------------  Winners List  -------------")
    print(len(winner_layouts_powers_list))
    print(winner_layouts_powers_list)
    print("-------------  Winners List  -------------")

    x = range(len(winner_layouts_powers_list))
    y = winner_layouts_powers_list
    plt.title("Line graph")
    plt.xlabel("X axis")
    plt.ylabel("Y axis")
    plt.plot(x, y, color="red")
    plt.show()


if __name__ == '__main__':
    if is_static_values_valid():
        start_evolution
```